



University
of Glasgow

<https://theses.gla.ac.uk/>

Theses Digitisation:

<https://www.gla.ac.uk/myglasgow/research/enlighten/theses/digitisation/>

This is a digitised version of the original print thesis.

Copyright and moral rights for this work are retained by the author

A copy can be downloaded for personal non-commercial research or study,
without prior permission or charge

This work cannot be reproduced or quoted extensively from without first
obtaining permission in writing from the author

The content must not be changed in any way or sold commercially in any
format or medium without the formal permission of the author

When referring to this work, full bibliographic details including the author,
title, awarding institution and date of the thesis must be given

Enlighten: Theses

<https://theses.gla.ac.uk/>
research-enlighten@glasgow.ac.uk

RADIOTRACER STUDIES OF THE NICKEL
CATALYSED HYDROGENATION OF ACETYLENE

THESIS
SUBMITTED FOR THE DEGREE
OF
DOCTOR OF PHILOSOPHY
OF THE
UNIVERSITY OF GLASGOW
BY
GWENDOLINE F. BERNDT, B.Sc.

OCTOBER, 1980

ProQuest Number: 10984318

All rights reserved

INFORMATION TO ALL USERS

The quality of this reproduction is dependent upon the quality of the copy submitted.

In the unlikely event that the author did not send a complete manuscript and there are missing pages, these will be noted. Also, if material had to be removed, a note will indicate the deletion.



ProQuest 10984318

Published by ProQuest LLC (2018). Copyright of the Dissertation is held by the Author.

All rights reserved.

This work is protected against unauthorized copying under Title 17, United States Code
Microform Edition © ProQuest LLC.

ProQuest LLC.
789 East Eisenhower Parkway
P.O. Box 1346
Ann Arbor, MI 48106 – 1346

ACKNOWLEDGMENTS

I would like to express my sincere thanks to Professor S.J. Thomson and Dr. G. Webb, my supervisors, for suggesting the topic which is the subject of this thesis, and for their advice and encouragement throughout the course of the work. I would also like to thank Dr. S.V. Norval, my industrial supervisor, for his interest and co-operation.

Thanks are also due to Dr. K.C. Campbell, Mr. T. Boyle, Mr. R. Wilson and my colleagues in the Surface Chemistry Group for their assistance and to the staff of the Glassblowing Workshop for the construction of the vacuum apparatus.

I gratefully acknowledge the award of a maintenance grant by the Science Research Council and I.C.I. Petrochemicals Division.

Finally, I would like to thank Miss E. Forbes, my typist, for her patient and skilful preparation of the typescript.

SUMMARY

The adsorption of acetylene on silica-supported nickel has been investigated using a [^{14}C]radiotracer technique. It has been found that the acetylene adsorption isotherms have two regions, a steep primary region and a linear secondary region. From the amount of ethane formed during the primary adsorption of acetylene, the average composition of the primary region has been calculated to be $\text{C}_2\text{H}_{1.9}$, indicating that the species adsorbed on the primary region are predominantly dissociatively adsorbed. Evidence has been obtained to show that the species involved in actual catalytic turnover during a hydrogenation reaction are located on the secondary region.

The adsorption of ethylene also occurs in two distinct stages, but the primary region is less steep than is found with acetylene.

Carbon monoxide adsorption shows only one adsorption region, as expected from Langmuir-type adsorption. Comparison of the acetylene adsorption isotherms with carbon monoxide isotherms suggests that the turning point observed in acetylene isotherms corresponds to monolayer coverage of the metal with hydrocarbon. Thus the onset of the secondary region only occurs when the monolayer is complete.

The hydrogenation of acetylene over Ni/SiO_2 has been found to occur in two distinct stages, the onset of the second stage being accompanied by a sharp increase in rate.

It has been observed that the rate of reaction progressively decreases in a series of consecutive reactions until a constant 'steady state' activity is achieved. From reaction to reaction there is a build-up on the surface of strongly retained hydrocarbon material. On a steady state catalyst the amount of carbon monoxide which can be adsorbed is substantially less than on a freshly reduced catalyst.

The experimental observations are interpreted in terms of a hydrogen transfer mechanism between dissociatively adsorbed C_2H_x species on the primary region and associatively adsorbed acetylene on the secondary region. Deactivation is thought to occur because of a surface polymerisation reaction, also involving C_2H_x species, which decreases the surface concentration of the latter.

When $[^{14}C]$ ethylene is added to an acetylene hydrogenation mixture, a small amount of ethylene hydrogenation is observed to occur independently of acetylene hydrogenation but the rate of hydrogenation is much slower than in the absence of acetylene. The effect is not due to competitive adsorption of acetylene and ethylene. It is proposed that the slow rate of ethylene hydrogenation under acetylene hydrogenation conditions is due to a hydrogen availability effect. From the added $[^{14}C]$ ethylene experiments the amount of ethane formed via a gas phase ethylene intermediate has been found to be small by comparison with the amount formed directly from acetylene. The major factor governing selectivity is therefore the ability, or otherwise, of the metal to catalyse

the direct hydrogenation of acetylene to ethane.

Pre-adsorption of carbon monoxide has been found to increase the selectivity for ethylene, while simultaneously decreasing the overall rate of hydrogenation. It is suggested that carbon monoxide and hydrogen compete for the same surface sites. When the system is hydrogen deficient the favoured pathway is the hydrogenation of acetylene to ethylene, resulting in an increase in the selectivity.

The effects of in situ catalyst pretreatment on the dehydrogenation of cyclohexane over $\text{Pt}/\gamma\text{-Al}_2\text{O}_3$ have also been investigated. It has been found that benzene and butadiene deactivate the catalyst but have no effect on the selectivity for cyclohexene production. Ethylene pretreatment increases the selectivity but also causes a decrease in catalyst activity.

CONTENTS

	Page
Acknowledgments	
Summary	
<u>Chapter One</u> <u>Introduction</u>	1
General Introduction	1
1.1 Metal-Catalysed Hydrogenation	4
1.2 The Adsorption of Acetylene and Ethylene at Metal Surfaces	9
1.3 The Hydrogenation of Acetylene	15
<u>Chapter Two</u> <u>Objectives of the Present Work</u>	28
<u>Chapter Three</u> <u>Experimental</u>	30
3.1 The Vacuum System	30
3.2 Volumes of the Apparatus	32
3.3 The Geiger-Müller System	34
3.4 The Pressure Transducer	38
3.5 The Gas Chromatography System	39
3.6 The Proportional Counter	42
3.7 Catalyst	45
3.8 Materials	46
3.9 Preparation of [^{14}C]Carbon Monoxide	47
3.10 Experimental Procedure	48

		Page
<u>Chapter Four</u>	<u>Results</u>	50
4.1	Catalyst Deactivation by C_2H_2/H_2 Mixtures	50
4.1.1	Pressure Fall-Time Curves	50
4.1.2	Deactivation	51
4.1.3	Regeneration	52
4.1.4	Effect of Catalyst Deactivation on Selectivity	52
4.2	$[^{14}C]$ Acetylene Adsorption	54
4.2.1	$[^{14}C]$ Acetylene Adsorption on Freshly Reduced Ni/SiO ₂	54
4.2.2	Reactivity of Species Adsorbed on Primary Region	55
4.2.3	Removal of Adsorbed Species by C_2H_2/H_2 Mixtures	56
4.2.4	$[^{14}C]$ Acetylene Adsorption on "Deactivated" Ni/SiO ₂	58
4.2.5	Permanent Retention During Adsorption Isotherm Experiments	60
4.2.6	$[^{14}C]$ Acetylene Adsorption on Steady State Ni/SiO ₂	60
4.3	$[^{14}C]$ Carbon Monoxide Adsorption	61
4.3.1	$[^{14}C]$ Carbon Monoxide Adsorption on Freshly Reduced Ni/SiO ₂	61
4.3.2	$[^{14}C]$ Carbon Monoxide Adsorption on Steady State Ni/SiO ₂	62

	Page
4.3.3	Poisoning of Acetylene Hydrogenation by Carbon Monoxide 63
4.4.	[^{14}C]Ethylene Adsorption 64
4.4.1	[^{14}C]Ethylene Adsorption on Freshly Reduced Ni/SiO ₂ 64
4.4.2	[^{14}C]Ethylene Adsorption on Steady State Ni/SiO ₂ 65
4.5	The Acetylene Hydrogenation Reaction 66
4.5.1	Product Distribution on Steady State Catalysts 66
4.5.2	Variation of Selectivity During a Steady State Reaction 67
4.5.3	[^{14}C]Ethylene Tracer Studies of Acetylene Hydrogenation 67
4.5.4	Permanent Retention of [^{14}C]Ethylene 71
4.6	The Effect of Variation of Hydrogen Pressure on the Acetylene Hydrogenation Reaction 72
4.6.1	Pressure Fall-Time Curves 72
4.6.2	Product Distribution 73
4.6.3	Selectivity for Ethylene 74
<u>Chapter Five</u>	<u>Discussion</u> 76
5.1	Introduction 76
5.2	Adsorption and Reactivity of Acetylene on Ni/SiO ₂ 78
5.3	Reaction Pathways and Selectivity in the Acetylene Hydrogenation Reaction 86

	Page
5.4	Formation of <u>n</u> -Butane 92
5.5	General Conclusions 94
<u>Chapter Six</u>	<u>Modification of Selectivity by</u> 96
	<u>Catalyst Pretreatment</u>
6.1	Introduction 96
6.2	Experimental 99
6.2.1	Catalyst 99
6.2.2	Materials 99
6.2.3	Apparatus 100
6.2.4	Experimental Procedure 102
6.3	Results 102
6.3.1	Standard Experiment 102
6.3.2	Treatment of Results 103
6.3.3	Benzene Pretreatment 104
6.3.4	Buta-1,3-diene Pretreatment I 104
6.3.5	Buta-1,3-diene Pretreatment II 105
6.3.6	Ethylene Pretreatment 105
6.4	Discussion 106
References	109

1. INTRODUCTION

General Introduction

For many years it has been recognized that certain substances, now known as catalysts, can, by their very presence, alter the rate of chemical reactions. Homogeneous catalytic processes have been used by mankind for thousands of years, for example in fermentation. Metallic catalysts were used in the laboratory before 1800 by Priestley and by the Dutch chemist Martinus van Marum, both of whom made observations regarding the dehydrogenation of alcohol on metals. However, it seems likely that these investigators regarded the metal merely as a source of heat.

During research which led to the miners' safety lamp, Davy(1) fixed a fine platinum wire above a coal-gas flame in a safety lamp. When additional coal-gas was introduced, the flame went out but the platinum wire remained hot for quite a time. Davy deduced that the oxygen and coal gas combined without flame when in contact with the hot wire, producing enough heat to keep the wire incandescent. Many other combustible vapours were found to produce the same effect when mixed with air. This was the first clear realisation that chemical reaction between two gaseous reactants can occur on a metal surface without the metal being chemically changed.

In 1822 Döbereiner discovered that platinum would enable hydrogen and oxygen to combine at room temperature. Dulong and Thénard showed that many other finely divided metals,

especially the noble metals could also produce this effect. Henry(2) made significant discoveries in the field of heterogeneous catalytic oxidation using either platinum sponge or moulded balls of china clay and spongy platinum. These catalytic balls were described earlier by Döbereiner to whom Henry refers. The two papers by Döbereiner and Henry were the first to describe the use of a supported platinum catalyst. By 1831 Phillips had patented the platinum catalytic process for commercial sulphuric acid manufacture. In an important paper in 1834 Faraday(3) proposed the idea of simultaneous adsorption of both reactants on a platinum surface.

Although these observations had been made there was no unifying theory until in 1836 Berzelius(4) coordinated a number of observations on both homogeneous and heterogeneous catalytic actions. He concluded 'It is then proved that several simple and compound bodies soluble and insoluble, have the property of exercising on other bodies an action very different from chemical affinity. By means of this action they produce, in these bodies, decompositions of their elements and different recombinations of these same elements to which they themselves remain indifferent'. Berzelius called these substances 'catalysts' and named the phenomenon 'catalysis'.

1836 is, therefore, taken as the beginning of the serious study of catalysis. The name appears to have been well chosen. It is derived from two Greek words 'kata'

meaning 'entirely' and 'lyo' meaning 'loose'. The implication is that a catalyst loosens the bonds of the reactant substances in such a way as to greatly alter the rate of reaction. Berzelius suggested that catalysis was due to some special 'catalytic force'. It is now generally recognized that the forces involved are probably those of ordinary chemical reactions. From these small beginnings vast industries based on catalysis have arisen and the subject continues to be an important field of research.

1.1 Metal-Catalysed Hydrogenation

An important class of reactions in organic chemistry is the addition of hydrogen across a double or triple carbon-carbon bond. Such processes are generally carried out in the presence of a catalyst. The nine Group VIII metals have been found to be the most efficient hydrogenation catalysts.

Metal catalysts can be used in various forms such as wires, foils, evaporated metal films, but probably the most important practical type is that in which the metal is supported on an inert material such as silica or alumina. The support can stabilize small metal particle sizes and thus a high metal surface to volume ratio can be obtained. This maximum utilization of the catalytically active metal makes supported catalysts very attractive for industrial use. They are also easy to handle and the majority of catalysts used in the chemical industry are indeed of this type.

The main disadvantage of supported catalysts is that they often exhibit variable activity, kinetics and activation energies. These observed differences may be due to method and conditions of preparation of the catalyst, resulting in variations in, for example, the particle size distribution, cleanliness, state of reduction of the surface and the degree of exposure of certain crystallographic planes.

Among the early systematic studies of catalytic hydrogenation were those of the metal-catalysed hydrogenation of acetylene carried out by Sheridan and co-workers (5-10), using pumice-supported Group VIII metals. Subsequently,

Bond and co-workers (11-22) investigated acetylene hydrogenation catalysed by both pumice- and alumina-supported metals. Various aspects of the reaction have been examined by other workers and the subject has been reviewed by Bond and Wells(23), by Wells(24), and by Webb(25).

Hydrogenation of an alkene or an alkyne is generally considered to be preceded by chemisorption on the catalyst surface. The process of chemisorption may be regarded as the saturation, by the adsorbate, of free valencies on the metal surface, which exist because an atom at the surface of a solid has a smaller coordination number than an atom in the bulk. The resulting adsorbate-metal bonds are of similar strength to those formed between atoms in molecules. The strength of adsorption is critical if a metal is to act as a catalyst. If a reactant is too strongly adsorbed, it will be difficult to remove and it may then act as a poison, if it is too weakly adsorbed, it may not remain on the surface long enough to react. It has generally been thought that when a surface is covered by a chemisorbed layer, further adsorption is unlikely, that is, chemisorption is limited to a monolayer: this assumption may not be valid (26).

Investigations of adsorption processes can provide information about the number of surface sites required for adsorption of one reactant molecule and the chemical nature of the adsorbed species. The mechanism of hydrogenation will depend on the nature of the adsorbed state and the way in which the adsorbed species interact with the hydrogen-

containing species. A major problem in investigations of adsorption is to decide whether the species actually observed are relevant to catalysis. Often, a kinetic study of a particular catalytic reaction leads to the postulation of a certain adsorbed species as reaction intermediate, whereas the corresponding adsorption study leads to the identification of a different surface species. It is possible that the surface species observed in adsorption studies are particularly stable and are not necessarily the active intermediates involved in catalytic processes.

Direct observation of an active species chemisorbed on a surface can be accomplished using a radiotracer technique first developed by Thomson and Wishlade(27) for metal films, and subsequently by Cormack, Thomson and Webb(28) for supported metals. Carbon-14, widely used in surface studies, emits a low energy β^- particle ($E_{\max} = 155 \text{ keV}$) with half-thickness for adsorption 2.4 mg cm^{-2} . Its penetrating power is therefore limited. If, however, the detector (commonly a Geiger-Müller tube) is mounted inside a vacuum system, few difficulties are encountered when working between 760 torr and 10^{-6} torr in the temperature range 0° to 60°C . Operation at higher temperatures with Geiger-Müller counters is difficult because of the limits to their temperature range for satisfactory operation - typically up to 60°C .

Suitably mounted detectors can be used to monitor directly surfaces and changes occurring on them. This makes possible the observation of the arrival, departure or

displacement of molecules or atoms, without interference with the system for conventional analysis.

Tritium, another widely used isotope in catalytic investigations, emits a β^- particle with a very low E_{\max} of only 18.6 keV. Consequently, it cannot be detected by end-window Geiger-Müller counting because of window absorption. Furthermore, its use in applications requiring direct observation of the surface is not practicable because of severe self-absorption problems.

The advantage of radiotracer methods for catalytic investigations is the sensitivity of detection of small numbers of atoms or molecules when these are radioactive. Typically 1 cm^2 of a surface might expose only 10^{15} sites whereon adsorption, displacement, oxidation, diffusion or catalysis may occur. However, if labelled with radioactivity of specific activity 1 mCi/mM, 10^{15} adsorbed molecules or atoms would produce a count rate of 200 cpm in a Geiger-Müller tube of 5% overall efficiency and changes in surface concentrations, below those required for monolayer adsorption, may be readily detected.

Although the radiotracer technique allows the direct observation of species chemisorbed on a surface under reaction conditions, it provides no information about the chemical identity of these species. Such information requires the application of techniques such as FEM, LEED, SIMS, ESCA and infrared spectroscopy.

Infrared spectroscopy has been the most widely used

technique for investigating the adsorption of hydrocarbons on supported metal catalysts, although there are limitations to its use. Infrared spectra arise from two main sources, one due to the bonds within the adsorbate molecule itself, the other due to the metal-adsorbate bonds. For catalysts supported on materials such as silica or alumina, the support material obscures the spectral region below 1300 cm^{-1} , which is the region where metal-carbon stretching frequencies would be expected. Spectra obtained therefore show only bands due to the adsorbate molecule itself. The interpretation of these spectra is frequently carried out by making comparisons with model compounds and in many cases this has led to difficulties because of the lack of suitable transition metal-hydrocarbon compounds.

Another limitation of the technique concerns the intensities of the expected bands. Sheppard(29) has suggested that surface intermediates may not be detected if the appropriate band intensities are weak, whilst Avery(30) has postulated that C-H bands associated with carbon atoms bonded directly to the metal are too weak to be observed. In consequence, bands which appear in the infrared spectra arise either from terminal C-H groups or C-H groups neighbouring the adsorbed carbon atoms. More recently, Pearce and Sheppard(31) have indicated the possible importance of a metal-surface selection rule such that only vibrations which give dipole changes perpendicular to the metal surface are infrared active.

Surface physics techniques have also been used to identify adsorbed species. Some of these, such as LEED and AES, are only suitable for use with single crystal metal catalysts and there is always the question as to whether species adsorbed on single crystals are those which are present on typical working catalysts. Dalmai-Imelik and Massardier(32) have examined the applicability of results obtained with single crystals to supported metal catalysts. Even with methods, such as SIMS, which are suitable for examination of supported catalysts, care has to be taken to ensure that the ions detected truly represent surface species and are not produced by fragmentation in the ionising beam during analysis.

Despite these limitations, much information has been obtained for hydrocarbons adsorbed on metals. Most of the studies have been concerned with ethylene. Information is also available for acetylene, but relatively few studies of higher hydrocarbons have been reported.

1.2 The Adsorption of Acetylene and Ethylene at Metal Surfaces

It is generally considered that, before undergoing hydrogenation, an unsaturated hydrocarbon must be adsorbed on to the metal surface. It is relevant therefore to examine the nature of the adsorbed states before attempting to discuss reaction mechanisms.

[^{14}C]Tracer studies of acetylene adsorption on silica-supported palladium, rhodium and iridium and alumina-supported palladium (33) have shown the co-existence of at least two adsorbed states, a dissociatively adsorbed species, which was retained on the surface during catalysis, and an associatively adsorbed species, which was reactive. Inoue and Yasumori(34) have shown the existence of four types of adsorbed acetylene on palladium; type A, which underwent desorption on evacuation, type B which was removed from the surface during hydrogenation, type C, which was not removed during hydrogenation but could be removed by treatment with hydrogen at 150°C , and type D which was retained even after reduction at 150°C .

Erkelens and Wösten(35) have suggested that the adsorption of acetylene leads to the formation of an associatively bonded (structure A), or a dissociatively adsorbed (structure B) species



and that, in addition to these species, part of the acetylene undergoes complete dissociation into carbon atoms, which penetrate into the bulk nickel, and into hydrogen atoms, which either desorb or remain adsorbed on the surface.

From U.V. photoemission spectroscopy Demuth(36) has

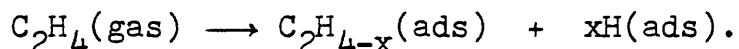
concluded that at temperatures below 180K acetylene is adsorbed on Pd(111), Pt(111) and Ni(111) surfaces as a π -bonded complex, but on warming a new surface species is formed which is similar to the species resulting from exposure of the clean surface to acetylene at room temperature. With both Pd(111) and Pt(111), this new surface species yields spectra characteristic of an 'olefinic' acetylene species (a di- σ -adsorbed species), but with Ni(111) dissociation to form C-C, C-H, CH_2 or C_2H radicals appears to occur.

Sheppard and Ward(37) have examined the adsorption of acetylene on 'bare' Ni/SiO₂ and on 'hydrogen-covered' Ni/SiO₂ using infrared spectroscopy. The infrared spectra showed bands ascribable to olefinic species (structure A) and to surface alkyl groups. Addition of hydrogen resulted in an intensification of the spectra and the appearance of new bands corresponding to surface alkyl groups of average structure $\text{CH}_3(\text{CH}_2)_3$. The results suggest that some degree of polymerisation occurs before hydrogenation. This is in contrast with the view that polymerisation occurs only through partially hydrogenated species such as $\text{MCH}=\text{CH}_2$ or $\text{MCH}=\text{CHM}$. Addition of premixed acetylene and hydrogen in the ratio of 1:1 to a 'bare' catalyst resulted in no detectable formation of ethylene or ethane, even after addition of more hydrogen to give an acetylene to hydrogen ratio of 1:50. However, identical experiments with a 'hydrogen-covered' catalyst did produce a mixture of ethane and ethylene. No polymerisation products were detected in the gas phase, but the authors

point out that the sensitivity of the infrared method for detecting these is not high.

Ethylene is an intermediate product of acetylene hydrogenation and, in the early stages of the reaction, may be the major product. The further hydrogenation of ethylene to ethane becomes important in the second stage of the reaction, when all the acetylene has reacted. The literature concerning the adsorbed states of ethylene on transition metals is extensive. As with acetylene, both dissociative and associative adsorption are thought to take place.

Evidence for dissociative chemisorption comes from the observation that, when ethylene is adsorbed on supported metal catalysts, self-hydrogenation to ethane is observed (38, 39),

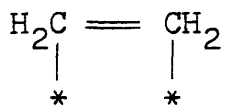


The hydrogen atoms liberated may then react with associatively adsorbed ethylene to form ethane (33). Volumetric (40, 41) and magnetic susceptibility measurements (42) suggest that the extent of dissociation is dependent upon the temperature and varies from metal to metal.

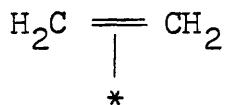
From the changes in magnetic susceptibility of Ni/SiO₂ during ethylene adsorption at room temperature, Selwood(42) has concluded that ethylene exists both as an associatively and a dissociatively adsorbed species. Infrared results have indicated that the chemical identity of the adsorbed olefin is critically dependent on the availability of surface hydrogen (43). On 'bare' Ni/SiO₂ at room temperature

associatively and dissociatively adsorbed species were observed. Admission of hydrogen caused an intensification of the spectrum and bands resulting from predominantly saturated species, formed by the hydrogenation of associatively adsorbed ethylene, were observed. Surface n-butyl groups appeared even at room temperature, formed perhaps from random polymerisation of dissociatively adsorbed ethylene residues.

Proposed structures of the associatively bonded species involve di- σ -bonding (structure C) (44), involving two metal atoms at a suitable distance apart, or π -bonding (structure D) (45) to one metal atom, though the molecule may cause other metal atoms to be obscured.



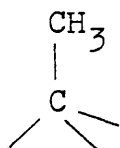
structure C



structure D

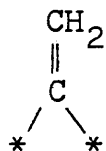
Prentice et al.(46), using infrared interferometry, have found evidence for both di- σ -bonded and π -bonded species on hydrogen-precovered Pd/SiO₂ and Pt/SiO₂. Both species can be easily hydrogenated, although the π -complex is more reactive.

Kesmodel et al.(47), using LEED, have examined the adsorption of ethylene on Pt(111) in the temperature range 300-350K. They have found evidence for a species coordinated to a threefold surface site (structure E) with the C-C axis normal to the surface.



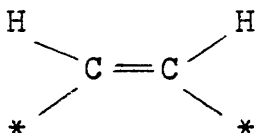
structure E

By comparison with reported reaction mechanisms on related transition metal clusters, they have suggested that structure F may be an intermediate in the formation of structure E.

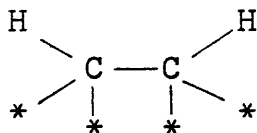


structure F

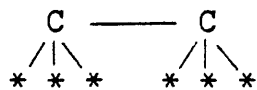
A variety of other dissociatively adsorbed species (structures G - J) have been proposed for ethylene adsorption on supported rhodium catalysts (48).



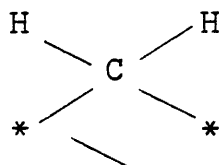
G



H



I



J

It has generally been assumed that the olefin species active in catalytic hydrogenation is associatively bonded, although the exact nature of the bonding is still the subject of debate. Thomson and Webb(26) have suggested that one or more of the dissociative species may have a role to play as the hydrogen transfer media in hydrogenation reactions.

1.3 The Hydrogenation of Acetylene

The mechanism of acetylene hydrogenation has been the subject of debate in the literature. Information about reaction mechanisms can readily be obtained using radioactive and stable tracer techniques. Carbon-14 and deuterium have been the most frequently used isotopes. The work to be described in this thesis involves the use of carbon-14 radiotracers and, therefore, it is pertinent to discuss the radiotracer technique in some detail.

The application of radioactive tracer techniques to mechanistic studies is, in principle, the same as their application to homogeneous systems. Gas chromatographic separation of the reaction products and immediate radioactive assay of the separate components yields information about the chemical identity of radioactive products and gives a quantitative measure of the degree of incorporation of the radioactive label. Hence reaction mechanisms can be elucidated.

Carbon-14 present as a constituent of a gaseous compound in a gas stream can be counted by end-window β^- detectors with low efficiency or counted, with efficiencies approaching absolute values, in proportional or scintillation counters. Gaseous compounds of tritium can be measured in ionisation chambers, proportional counters or in an internal mode in Geiger-Müller counters. Proportional counters and ionisation chambers have the advantage of being operable up to 200-250°C. However, care is required in considering whether

the chemical form of the labelled species will cause interference with the counting characteristics. Some gases, particularly halogenated compounds, may quench the electron multiplication process. Gordon et al.(49) have investigated this phenomenon for proportional counters.

A fundamental assumption in tracer chemistry is that the radioactive and stable isotopes of the same element have identical chemical properties and are chemically inseparable. For most cases this assumption is valid. In some systems, however, the difference in zero point energy of the radioactive and stable isotopes, arising from differences in mass of the two species, can lead to changes in equilibrium constants, rates of reaction and bond strengths. This effect would be most evident with tritium, where the relative isotopic mass difference is greatest. Due care has, therefore, to be taken when interpreting the results of tracer experiments.

[^{14}C]labelled hydrocarbons have been used extensively to investigate the mechanism of acetylene hydrogenation. In general, the reaction takes place in two stages, the onset of the second stage being accompanied by a sharp increase in rate. In the initial stages of the reaction ethylene is formed as an intermediate product along with ethane. Often, in addition to ethylene and ethane, hydrocarbons containing more than two carbon atoms are observed as products. The extent of polymerisation appears to be greater with the first row transition metals, iron, cobalt, nickel and copper, than

with the second and third row Group VIII metals. With alumina-supported metals the polymerisation products are almost exclusively C_4 -hydrocarbons (18, 19, 20). Several mechanisms for the hydropolymerisation of acetylene have been proposed (6, 7, 18, 19, 20, 50).

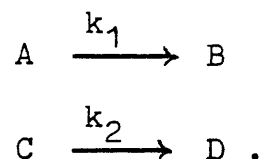
In a reaction, such as acetylene hydrogenation, where more than one product is formed, the preference for the formation of a desired product can be expressed numerically as the yield of desired product divided by the total product yield. This ratio is termed the selectivity, S. For formation of ethylene from acetylene,

$$S = \frac{P_{C_2H_4}}{P_{C_2H_4} + P_{C_2H_6}}$$

where P denotes partial pressure. Defined in this way S may take values between zero and unity.

Wheeler (51) has considered the kinetic factors which influence selectivity. He has distinguished three situations.

Type I selectivity involves the relative rates of reaction of two different types of compound on the same catalyst. This may be defined by the reaction scheme



Assuming that both reactions are first order and that the rate constants k_1 and k_2 refer to unit surface area, the rate

equations are

$$-\frac{dA}{dt} = k_1 A \quad \text{----- (1)}$$

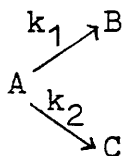
$$-\frac{dC}{dt} = k_2 C \quad \text{----- (2).}$$

Dividing (1) by (2) and integrating yields the equation

$$\alpha_A = 1 - (1 - \alpha_C)^\sigma \quad \text{----- (3)}$$

where α_A and α_B are the fractions of A and C reacted and σ is the ratio k_1/k_2 . Thus the amount of A reacted at a given conversion of C depends only on the value of σ .

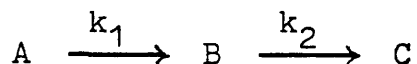
Type II selectivity occurs when a reactant species undergoes two simultaneous reaction paths. Here the reactant molecule A can be converted into either the desired product B or an undesired product C



Defining σ as before yields

$$\alpha_B = \sigma \alpha_C$$

Type III selectivity arises when the desired product B can undergo further reaction to an undesired product C.



High selectivity therefore depends on the rate constant k_1 being much larger than k_2 . For first order kinetics the rate equations are

$$-\frac{dA}{dt} = k_1 A \quad \text{----- (4)}$$

$$\frac{dB}{dt} = k_1 A - k_2 B \quad \text{----- (5)}.$$

Dividing (5) by (4)

$$-\frac{dB}{dA} = 1 - \frac{1}{\sigma} \frac{B}{A}$$

where

$$\sigma = \frac{k_1}{k_2}$$

Integration of this gives the conversion to B as a function of the amount of A reacted.

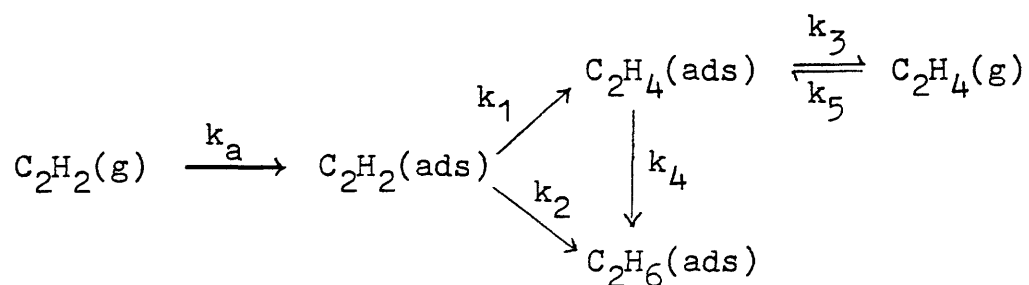
$$\alpha_B = \frac{\sigma}{\sigma-1} (1 - \alpha_A) \left[(1 - \alpha_A)^{\left(\frac{1-\sigma}{\sigma}\right)} - 1 \right] \quad \text{--- (6)}$$

Where α_B is the fraction of initial A converted to B and α_A is the fraction of A reacted. The yield of B, that is, the moles of B formed per mole of A reacted, is (α_B/α_A) and hence is obtained by dividing (5) by α_A .

Type III selectivity can usually be clearly distinguished from type II since, in the former, the yield of desired intermediate B decreases markedly with amount of A reacted, while in type II selectivity the yield of B is independent of the amount of A reacted.

An empirical method of determining the most favoured conditions for the production of a desired product B from a reactant A, at the expense of an undesired product C, has been discussed by Waterman and co-workers (52).

All three types of selectivity are relevant to catalytic hydrogenation and in some circumstances may all be operative simultaneously. This is the case in acetylene hydrogenation where the following reaction scheme can be considered:-



The selectivity for ethylene depends upon the relative amounts of ethylene and ethane produced. Three cases can be considered. (1) If k_4 and k_5 approach zero then the selectivity for ethylene will depend upon the ratio (k_1/k_2). Since this is purely mechanistic in nature, this type of selectivity has been termed mechanistic selectivity (15). (2) If k_2 and k_5 approach zero then the selectivity will be dependent upon the ratio (k_3/k_4). (3) If $k_2 \approx 0$ then selectivity will depend upon the ratio (k_3/k_5). If ethylene and acetylene adsorb on the same sites then, once ethylene is produced in the gas phase, the system contains another potential adsorbate and selectivity will depend upon the ratio (k_a/k_5). It has been suggested that this should be

termed thermodynamic selectivity (15, 24) on the basis that the surface coverages of acetylene (θ_x) and ethylene (θ_y) are given by

$$\theta_x = \frac{b_x P_x}{(1 + b_x P_x + b_y P_y)}$$

and

$$\theta_y = \frac{b_y P_y}{(1 + b_x P_x + b_y P_y)}$$

Thus

$$\frac{\theta_x}{\theta_y} = \frac{b_x P_x}{b_y P_y} = \frac{P_x}{P_y} \exp \left(- \frac{\sigma \Delta G}{RT} \right)$$

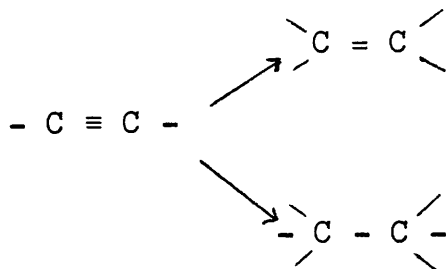
where $\sigma \Delta G$ is the difference in free energies of adsorption of X and Y. If $\sigma \Delta G$ is so large that one reactant is effectively excluded from the surface then it will not react, even although it may react rapidly in the absence of the more strongly adsorbed species. In general, therefore, the selectivity for ethylene formation will depend upon the ratios (k_1/k_2), (k_3/k_4) and (k_3/k_5).

Early interpretations of observed kinetics and product distributions for the acetylene reaction suggested that, in the first stage of the reaction, the major process was the hydrogenation of acetylene to ethylene. Because acetylene was adsorbed much more strongly than ethylene, the re-adsorption and further hydrogenation of ethylene was prevented, until the concentration of acetylene was almost zero. Near the acceleration point, ethylene could compete

for the surface and be hydrogenated to ethane. Thus selectivity for ethylene was thought to be governed by the ratio of ($\theta_{C_2H_2}/\theta_{C_2H_4}$), the thermodynamic factor, and the ratio (k_3/k_4), the mechanistic factor.

The derivation of the concept of thermodynamic selectivity makes the assumption that the potential adsorbates are competing for the same surface sites. Recent work by Al-Ammar and Webb(38) has indicated that the adsorption of [^{14}C]ethylene in the presence and absence of acetylene, on silica-supported rhodium, iridium and palladium and alumina-supported palladium, is similar. This suggests that ethylene and acetylene are adsorbed on different sites. From these studies it was also concluded that acetylene and ethylene underwent hydrogenation independently of each other. A general reaction scheme for acetylene hydrogenation was proposed (figure 1.1). Type I sites are active for the hydrogenation of acetylene to ethylene; type II are active for the direct conversion of acetylene to ethane, but inactive for ethylene hydrogenation, type III are active for ethylene hydrogenation, but inactive for acetylene hydrogenation.

The reaction scheme shown in figure 1.1 allows for the possibility of a direct pathway from acetylene to ethylene without involving gas phase ethylene. Such a pathway has also been suggested by Gucci et al. (53). They concluded that initially the reactions taking place on the surface were:-



and, only after the acetylene partial pressure had diminished substantially, was it possible for ethylene to be hydrogenated to ethane. Thus, the selectivity for ethylene will be governed by the ability, or otherwise, of the metal to catalyse the direct hydrogenation of acetylene to ethane.

McGown et al. (54), who investigated the hydrogenation of mixtures containing 2% [^{13}C]acetylene in ethylene over palladium-alumina, have postulated that two types of surface site exist; type X which can hydrogenate both acetylene and ethylene (equivalent to type I + type II above), and type Y which can hydrogenate ethylene even in the presence of acetylene (equivalent to type III). This latter study also showed that the presence of carbon monoxide increased the selectivity for ethylene formation. As with many selective poisons, carbon monoxide deactivated the catalyst in an absolute sense, the rate of production of ethylene falling to a lesser extent than the rate of ethane formation. The authors suggested that the enhanced selectivity was due to carbon monoxide either adsorbing in preference to ethylene on type Y sites, or reducing the amount of ethylene which formed α -diadsorbed species.

An understanding of the use of carbon monoxide to increase selectivity for ethylene formation requires a knowledge of the adsorbed states of carbon monoxide on metal surfaces. There is a considerable literature, reviewed by Ford(55), concerning the adsorption of carbon monoxide on transition metals. Adsorption on supported Group VIII metals has been studied in most detail by infrared spectroscopy and has been the subject of a recent review by Sheppard and Nguyen(56). Laser Raman Spectroscopy has begun to make contributions to the study of adsorbed species, but because finely divided metal catalysts are highly coloured, or more often black, there can be major problems from sample heating and adsorbate decomposition in the laser beam.

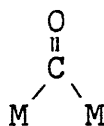
The infrared absorption bands associated with the carbon-oxygen bond stretching modes are very strong and readily measured. However, the particle size distribution and the extent of reduction of the metal particles determines the spectra obtained. Also, when a support is used, this may have an effect on the electronic environment of the metal crystallites. Thus, for example, the positions and intensities of the bands in the spectra of carbon monoxide adsorbed on platinum/Cabosil have been shown to have marked differences from those obtained with platinum/ α -alumina (43).

Carbon monoxide adsorbed on the transition metals gives an intense absorption band in the region between 2100 and 1700 cm^{-1} arising from the stretching vibration of the carbon-oxygen bond. This lowering from the observed value

of 2143 cm^{-1} for gaseous carbon monoxide is similar to that observed with metal carbonyls. Early work by Eischens and colleagues (43) assigned bands by analogy with metal carbonyl complexes. In $\text{Fe}(\text{CO})_5$ and $\text{Ni}(\text{CO})_4$, which contain only linear metal-carbon-oxygen structures, the principal carbon-oxygen stretching frequencies occur above 2000 cm^{-1} , whereas in $\text{Fe}(\text{CO})_9$, known from the crystal structure (57) to have three bridging carbon monoxide ligands, there is an additional strong band at 1828 cm^{-1} (58). From data such as this Eischens et al. assigned bands in the $2100 - 1950\text{ cm}^{-1}$ region to linear species (structure K) and those in the $1900 - 1800\text{ cm}^{-1}$ region to bridged species (structure L).



structure K



structure L

Many of the absorptions fell in the intermediate $2000 - 1900\text{ cm}^{-1}$ range, but were assigned to bridged species, because of the strong overlap with bands in the $1900 - 1800\text{ cm}^{-1}$ region.

Blyholder (59) suggested that some linear CO groups could give rise to carbon-oxygen stretching frequencies down to 1800 cm^{-1} . Using a technique (60) of evaporating nickel on to an oil film, previously deposited on to the salt windows of an infrared cell, he was able to prepare samples which were transparent down to 300 cm^{-1} (normally the spectral range is limited to $5000 - 1350\text{ cm}^{-1}$ because of the presence of the oxide support). For the bridged structure

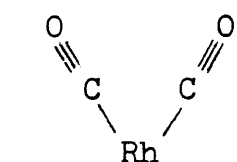
an asymmetric stretch would be expected in the region 1000 - 700 cm^{-1} but none was observed. A broad band was observed at 435 cm^{-1} and, by analogy with $\text{Ni}(\text{CO})_4$, which has a metal-carbon stretching frequency at 422 cm^{-1} and a Ni-C-O bending frequency at 461 cm^{-1} , this was assumed to be the Ni-C stretching frequency for carbon monoxide.

Later work by Primet et al. (61) has indicated that bridged species do exist ($\nu_{\text{CO}} \sim 1935 \text{ cm}^{-1}$) but that there is also evidence for species bonded to three or four metal atoms ($\nu_{\text{CO}} = 1935 - 1800 \text{ cm}^{-1}$), for example, in the centre of triangles of three metal atoms on (111) planes.

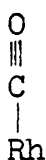
One of the major questions about carbon monoxide adsorption is why, on platinum, carbon monoxide adsorbs mainly in the linear form, whilst on palladium the bridged form predominates and on nickel both forms are found in approximately equal amounts. Recent theoretical studies by Politzer and Kasten(62) and by Blyholder(63) suggest that, when both linear and bridged sites are available, bridged sites are likely to be more stable for the bonding of carbon monoxide to a nickel surface. Variation of the bridged to linear ratio with metal content and surface coverage has been found with nickel-alumina catalysts (64). At higher carbon monoxide pressures, bridged species appeared between adjacent nickel atoms already bearing linear species.

Tunneling spectroscopy measurements (65) on rhodium-alumina have indicated the presence of two types of

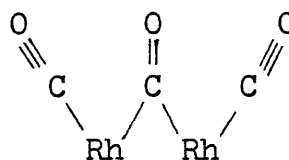
linearly bonded carbon monoxide molecules with nonequivalent metal-carbon bond strengths. These results are in good agreement with those obtained by Yang and Garland(66), who proposed a species consisting of two linear CO molecules bonded to a single rhodium atom (structure M), a linear species with one CO per rhodium atom (structure N), and a bridged species consisting of a CO bonded to two rhodium atoms, each of which also had a single linear CO (structure O)



structure M



structure N



structure O.

The amounts of (M) and (O) increased relative to (N) with increasing surface coverage.

Adsorption of other gases after adsorption of carbon monoxide can lead to changes in the frequencies of the bands corresponding to the carbon-oxygen stretching modes. Wojtczak et al. (67) found that additions of ethylene or propylene to nickel films carrying preadsorbed carbon monoxide produced shifts to lower frequencies of the bands at 2035 and 1890 cm^{-1} and a weakening of the band intensities. They concluded that the olefins were easily chemisorbed and could replace some, though not all, of the adsorbed carbon monoxide species.

CHAPTER 2

2. OBJECTIVES OF THE PRESENT WORK

The work contained in Chapters 1-5 of this thesis is a detailed investigation of the nickel catalysed hydrogenation of acetylene using radiotracer techniques. The aims of the work were:-

- (a) To investigate the build-up of carbonaceous deposits on the catalyst surface, to obtain information about the chemical identity of these species, and to determine what part, if any, they play in catalytic hydrogenation.
- (b) To investigate the adsorption characteristics of [^{14}C]acetylene and [^{14}C]acetylene/hydrogen mixtures.
- (c) To determine the extent to which bare metal exists on working catalysts.
- (d) To examine the effect of added [^{14}C]ethylene on the hydrogenation of acetylene.

From such studies it was intended to obtain further information regarding (i) the nature of the adsorbed species which are catalytically active in acetylene hydrogenation, (ii) the importance of permanently adsorbed hydrocarbon species, and (iii) the effect of catalyst deactivation on the reaction kinetics and selectivity for ethylene formation.

By use of [^{14}C]ethylene, as a tracer, it was intended to elucidate the various reaction pathways in the hydrogenation of acetylene to ethylene and ethane and hence gain an understanding of the factors which influence the behaviour of metal catalysts in selective hydrogenation.

The research described in Chapters 1-5 was complemented by an investigation of the effects of in situ catalyst pretreatment on the dehydrogenation of cyclohexane over $\text{Pt}/\gamma\text{-Al}_2\text{O}_3$. These investigations were carried out at ICI Petrochemicals Division Laboratories. The purpose of this work was to examine the effect, on the selectivity and rate of reaction, of pretreating the catalyst with various hydrocarbons, with the ultimate aim of finding a suitable catalyst pretreatment which would enhance the selectivity for a desired product.

CHAPTER 3

3. EXPERIMENTAL

3.1 The Vacuum System

The apparatus consisted of a conventional high vacuum system maintained at a pressure of 10^{-5} torr or better by a mercury-diffusion pump backed by a rotary oil pump. Gases were stored in four 1 litre storage bulbs. These were connected to the secondary manifold via 4 mm taps to allow ease of filling or evacuation. They were also connected via two 2 mm taps to a portion of the line close to the reaction vessel. One of the 1 litre storage vessels had a side-arm, on to which radioactive ampoules could be sealed. A 250 ml bulb was used to store [^{14}C]carbon monoxide. This had a side-arm for attachment of a [^{14}C]carbon dioxide to [^{14}C]carbon monoxide converter (section 3.9). A 500 ml mixing vessel was used for preparing and storing mixtures of acetylene and hydrogen for hydrogenation experiments.

In the vacuum line pressures between 1 torr and 760 torr were measured by a mercury manometer. In the reaction vessel pressures were monitored by a differential pressure transducer (section 3.4), rather than by use of a mercury manometer, to prevent any possible poisoning of the catalyst by mercury vapour and also to allow small pressure changes to be determined more accurately.

The reaction vessel (volume 418 cm^3) (figure 3.1) was similar to that used by Al-Ammar(68), with a few minor modifications. Two intercalibrated Geiger-Müller tubes,

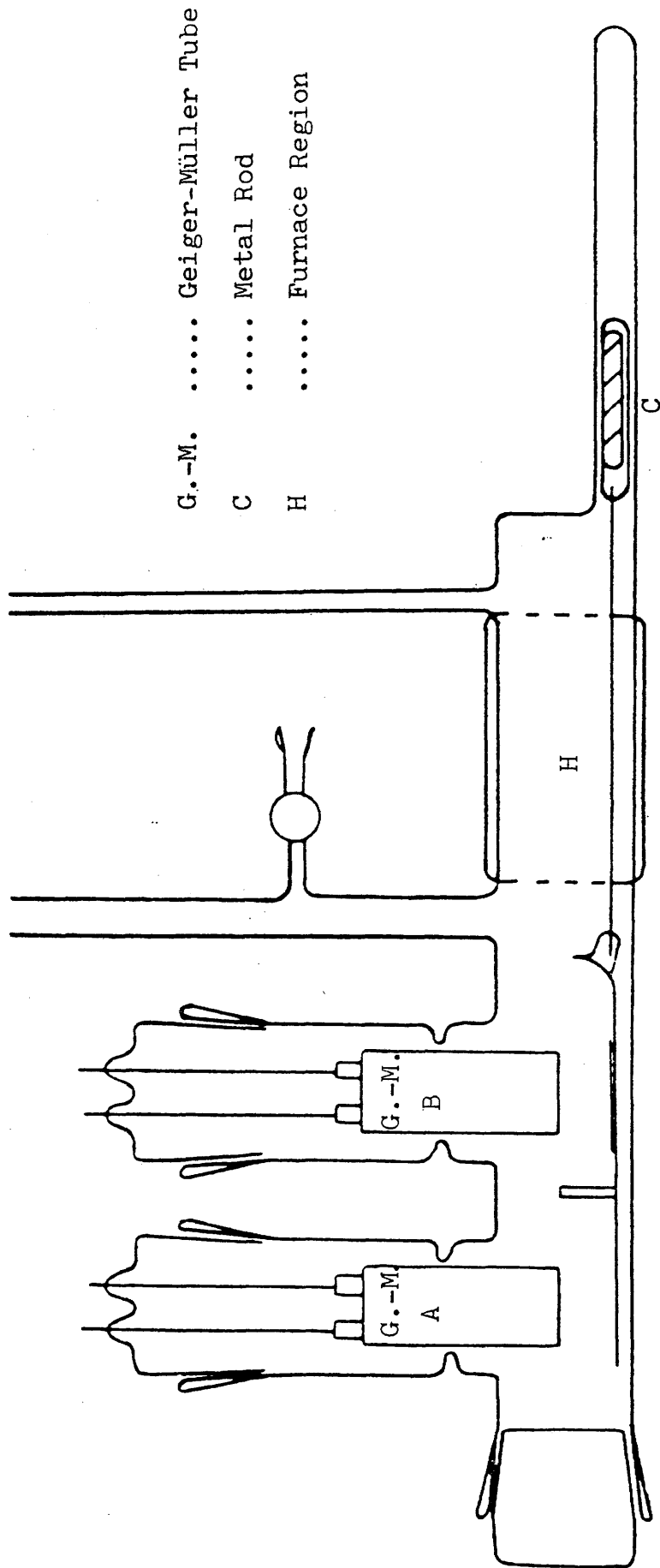


Figure 3.1 The Reaction Vessel

sealed with Araldite into B34 cones, were in turn sealed into the B34 sockets of the reaction vessel with Apiezon 'W' wax. The Geiger Müller tubes were suspended over a boat divided into two identical portions by a circular glass wall ca. 3 mm thick. The catalyst was spread thinly and uniformly on to the surface of one portion of the boat by first slurrying with a small amount of distilled water and then drying over a jet of hot air. Rotation of the boat during this drying procedure ensured a thin uniform spread. The boat could be moved into the furnace region (H), for catalyst activation, by the application of an external magnet to the glass-enclosed metal rod (C), and then withdrawn into position under the Geiger-Müller tubes for adsorption and reaction studies.

Geiger-Müller tube (A) monitored gas phase radioactivity while Geiger-Müller tube (B) monitored surface plus gas phase. Equal volumes of gas were seen by each tube and therefore surface activity could be obtained by subtraction. Since radiation could be emitted at any angle from the catalyst surface, a thick circular glass wall was incorporated to prevent the detection of surface radioactivity by Geiger-Müller tube (A). Experiments with a solid [^{14}C]polymethylmethacrylate source in position under Geiger-Müller tube (B) indicated that this was satisfactory since only background count rate was detected by Geiger-Müller (A).

The reaction vessel could be evacuated through a 4 mm tap connected directly to the main manifold. The vessel was

also coupled to a sample U-tube (volume 15 cm^3) which in turn was coupled to a combined gas chromatograph-proportional counter. The gas mixture was separated by gas chromatography and the individual components passed through the proportional counter (section 3.6) to be analysed for radioactivity.

3.2 Volumes of the Apparatus

It was necessary to determine the volumes of the various parts of the vacuum line so that accurate dilutions of radioactive gases could be carried out.

The volumes were determined by expansion of gas at known pressures from a standard volume (69.0809 cm^3). Pressures were measured by a two-limb mercury manometer, using a cathetometer to measure the heights of the mercury columns. Corrections were made to allow for the changing volume of the manometer with changing pressure.

Each volume (accurate to within $\pm 0.5 \text{ cm}^3$) was determined as an average of four separate determinations. These are shown in Table 3.1.

Table 3.1

Apparatus Volumes

	Volume (cm ³)
Secondary manifold	212
Main manifold	537
Connection between main manifold and reaction vessel	15
Connection between mixing vessel and pressure transducer	29
Mixing vessel (excluding condensing limb)	581
Condensing limb of mixing vessel	3
Storage vessel 1	1274
Storage vessel 2	1270
Storage vessel 3	1280
Storage vessel 4	1295
Storage vessel 5	252
Reaction vessel (with boat and G.-M. tubes in position)	418
Sample U-tube	15
Pressure transducer - reference side	15
Pressure transducer - measuring side	9

3.3 The Geiger-Müller System

For this work Mullard ZP1481 Geiger-Müller tubes were used. These had mica windows (thickness 3 mg cm^{-2}) and were filled with a mixture of neon, argon and halogen. The electronics consisted of an EKO Scaler Type N529B used with an EKO Probe Unit Type N558B. The discriminator bias control of the scaler was set at a value of 20, so that counts were not obtained from electronic noise produced in the counting system.

The plateau region of each G.-M. tube was determined by placing a source under the tube and measuring the count rate as a function of the applied voltage. A typical plateau is shown in figure 3.2. No counts were detected until the threshold was reached. The count rate rose rapidly until a plateau was reached where count rate increased only very slowly with voltage. At the end of the plateau the count rate began to rise rapidly again and the tube moved into a region of continuous discharge. The mid-point of the plateau region was selected as the working voltage.

After determination of the working voltages an estimate was made of the reliability of the counter performances by taking 20 separate counts of the source at the working voltage. The mean, \bar{N} , and the standard deviation, σ , were determined, where

$$\sigma = \sqrt{\frac{\sum (\bar{N} - N_i)^2}{n - 1}} .$$

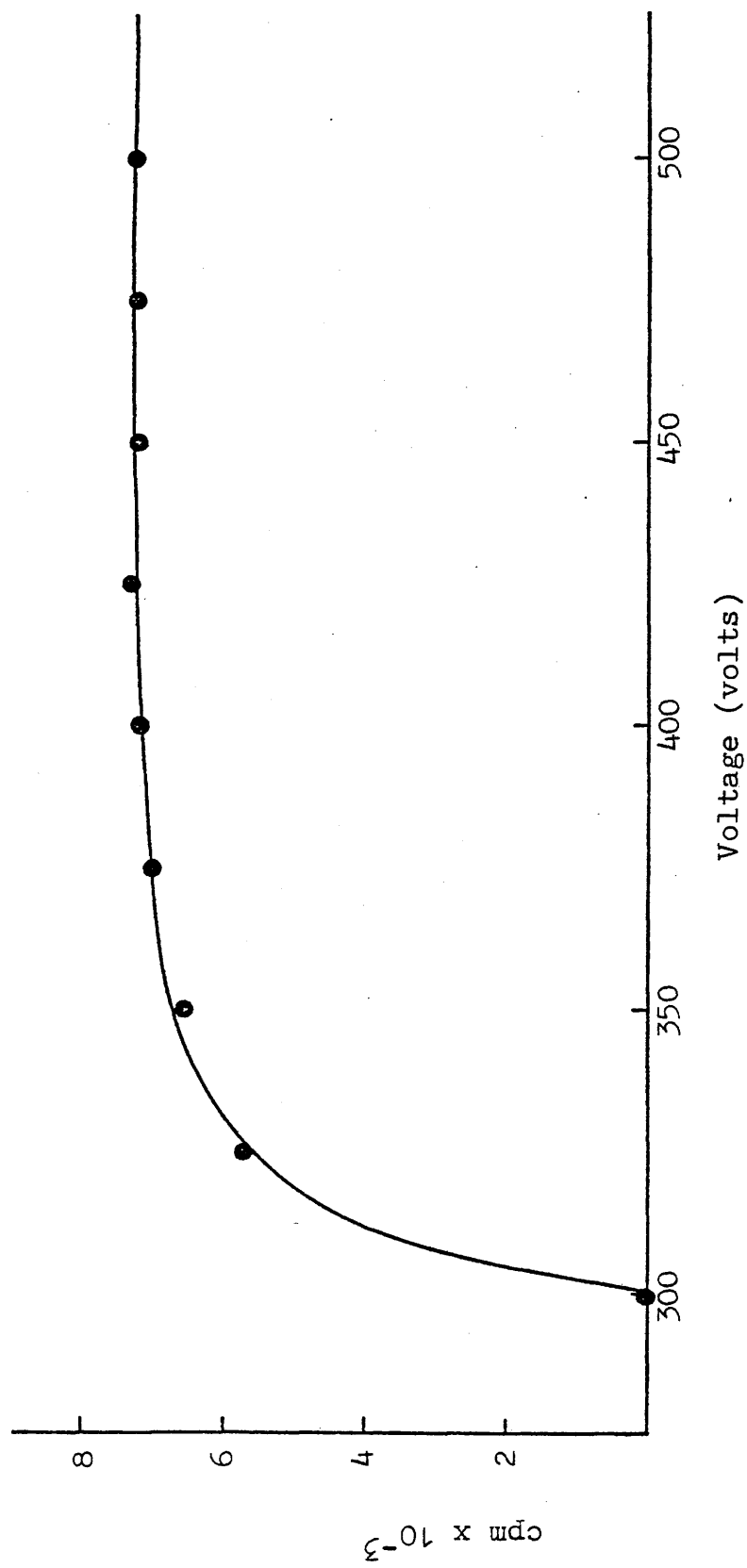


Figure 3.2 Geiger Müller Plateau

According to statistical theory, for a normal distribution of N_i values about the mean \bar{N} , 68.3% of the N_i values should fall within the range $\bar{N} \pm \sigma$; 95.1% within $\bar{N} \pm 2\sigma$ and >99% within $\bar{N} \pm 3\sigma$.

The results for this apparatus were as follows:-

	G.-M.1	G.-M.2	Theoretical
$\bar{N} \pm \sigma$	75%	70%	68.3%
$\bar{N} \pm 2\sigma$	95%	95%	95.1%
$\bar{N} \pm 3\sigma$	100%	100%	99%

Although twenty determinations of a count rate is a small sample for the application of statistical theory the results suggested that the system was reliable.

Corrections to Observed Count Rates

Three corrections were made:

- (a) dead time corrections,
- (b) background corrections,
- (c) multiplication of G.-M.(B) count rates by the intercalibration factor.

These are described separately.

Dead Time

After a particle has been detected the counter is unable to detect another for a period of a few hundred microseconds. This is known as the dead time. Since the dead time of a G.-M. tube is difficult to determine and may not be consistent it is often desirable to control it electronically. In the present work this was achieved by using a probe unit which controlled the G.-M. tube voltage so that the applied potential was diminished for a finite period after detection of a pulse. The dead times of the probe units were set at 300 μ sec, that is, at a value greater than the dead time of the tubes (specified by Mullard as less than 120 μ sec).

At high count rates a correction for dead time was made. If the dead time is T and the observed count rate is N_o , the true count rate N_T , is given by

$$N_T = \frac{N_o}{1 - N_o T} .$$

Background

Before each experiment it was necessary to determine the background count rate, i.e. the activity due to external radiation, and subtract this from all experimental count rates.

Intercalibration

The efficiencies of the two G.-M. tubes were slightly

different and thus it was necessary to obtain a relationship between counts obtained on G.-M.(A) and those obtained on G.-M.(B).

With the boat in position under the G.-M. tubes increasing pressures of radioactive gas were admitted to the reaction vessel and the count rates determined. A graph of G.-M.(A) count rate against corresponding count rate for G.-M.(B) was plotted (after correction of results for dead time losses and background) and from the gradient of this an intercalibration factor was determined (figure 3.3). All count rates measured subsequently on G.-M.(B) were then multiplied by this factor.

Absorption Effects

It was necessary to check for losses in the amount of radioactive emission reaching the counters. Two effects were considered:-

- (a) Self-absorption within the gas phase, that is losses in count rate detected from gas phase with increasing gas pressure.
- (b) Absorption of β^- radiation from the surface by the gas phase.

Effect (a) was investigated by determining the count rate as a function of gas pressure. A graph of count rate (corrected for dead time and background) versus pressure is shown in figure 3.4. It can be seen that at pressures less

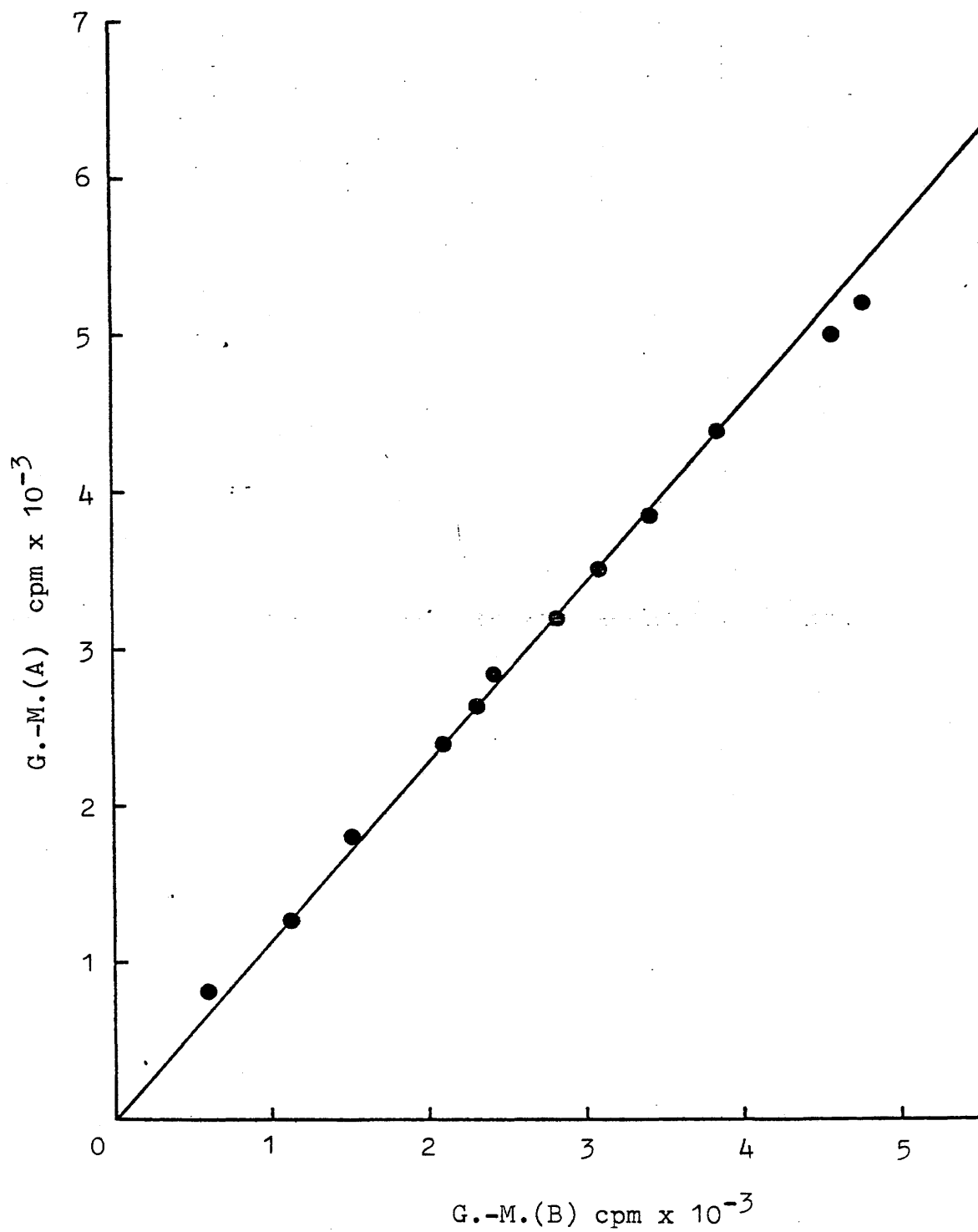


Figure 3.3 Intercalibration Plot for G.-M. Tubes

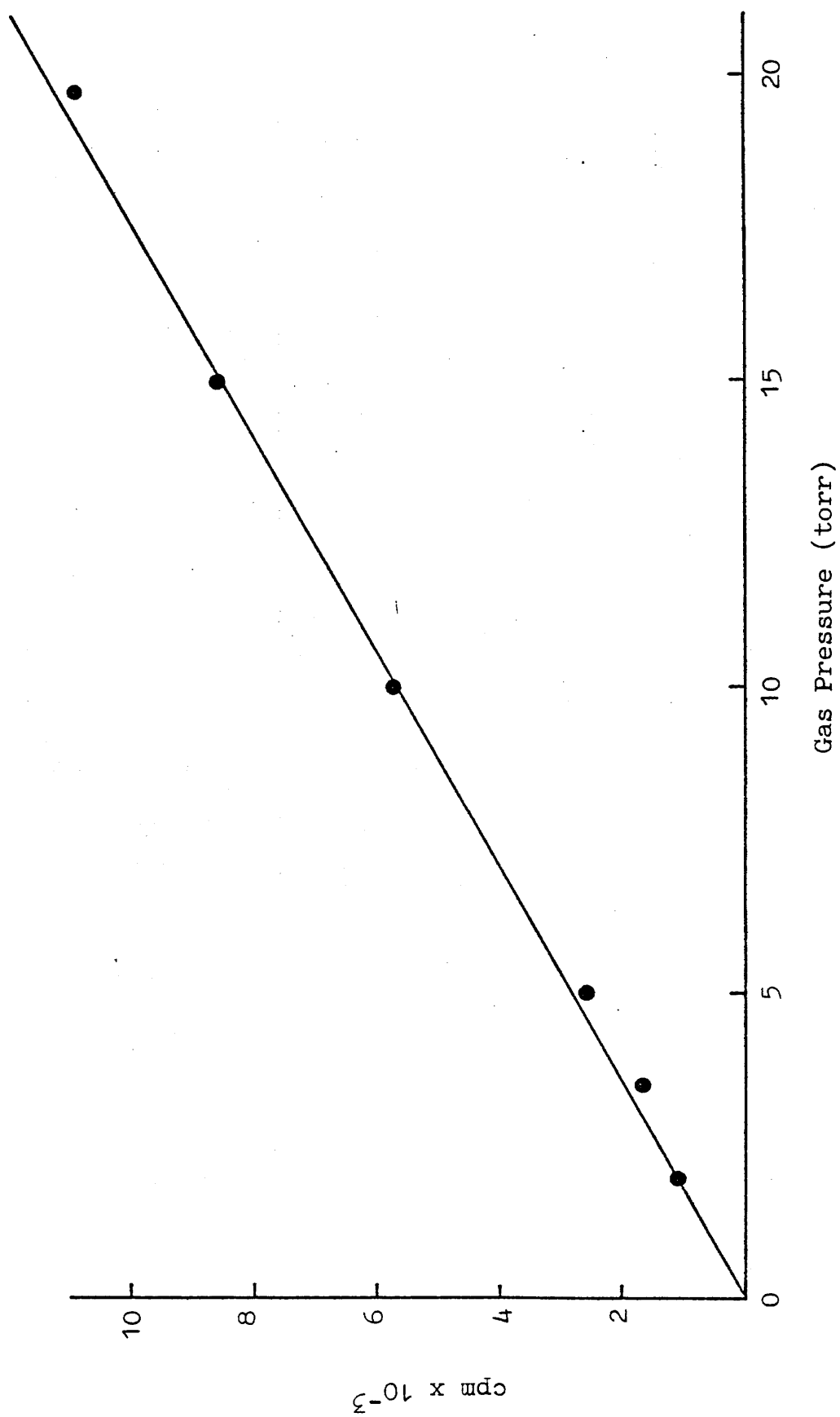


Figure 3.4 Count Rate as a Function of Gas Pressure

than 15 torr the effect was negligible.

Effect (b) was investigated by placing a [^{14}C]poly-methylmethacrylate source under G.-M.(B), evacuating the reaction vessel and then adding increasing pressures of air. A graph of count rate of source versus air pressure is shown in figure 3.5. It can be seen that at pressures less than 50 torr this effect was almost negligible.

3.4 The Pressure Transducer

A differential pressure transducer, supplied by Ackers Electronics Ltd. (type 810), was used to monitor pressure within the reaction vessel (figure 3.6). The range of the instrument was -35 to +35 torr.

The transducer consisted of a piezo-resistive half bridge element mounted in a substantial brass housing. The silicon beam on which the resistors were mounted was deflected by movement of a pressure-sensitive membrane. The input circuitry of the measuring electronics and the transducer formed a Wheatstone bridge circuit. The bridge output was a voltage proportional to the applied pressure differential.

The electronic circuit (figure 3.7) consisted of a differential cross-coupled voltage-follower pair feeding a differential amplifier. The voltage-follower pair gave a high common-mode rejection and a high input resistance, thus minimising errors in subsequent amplification. The differential amplifier converted the differential input signal to a single ended output suitable for use with a

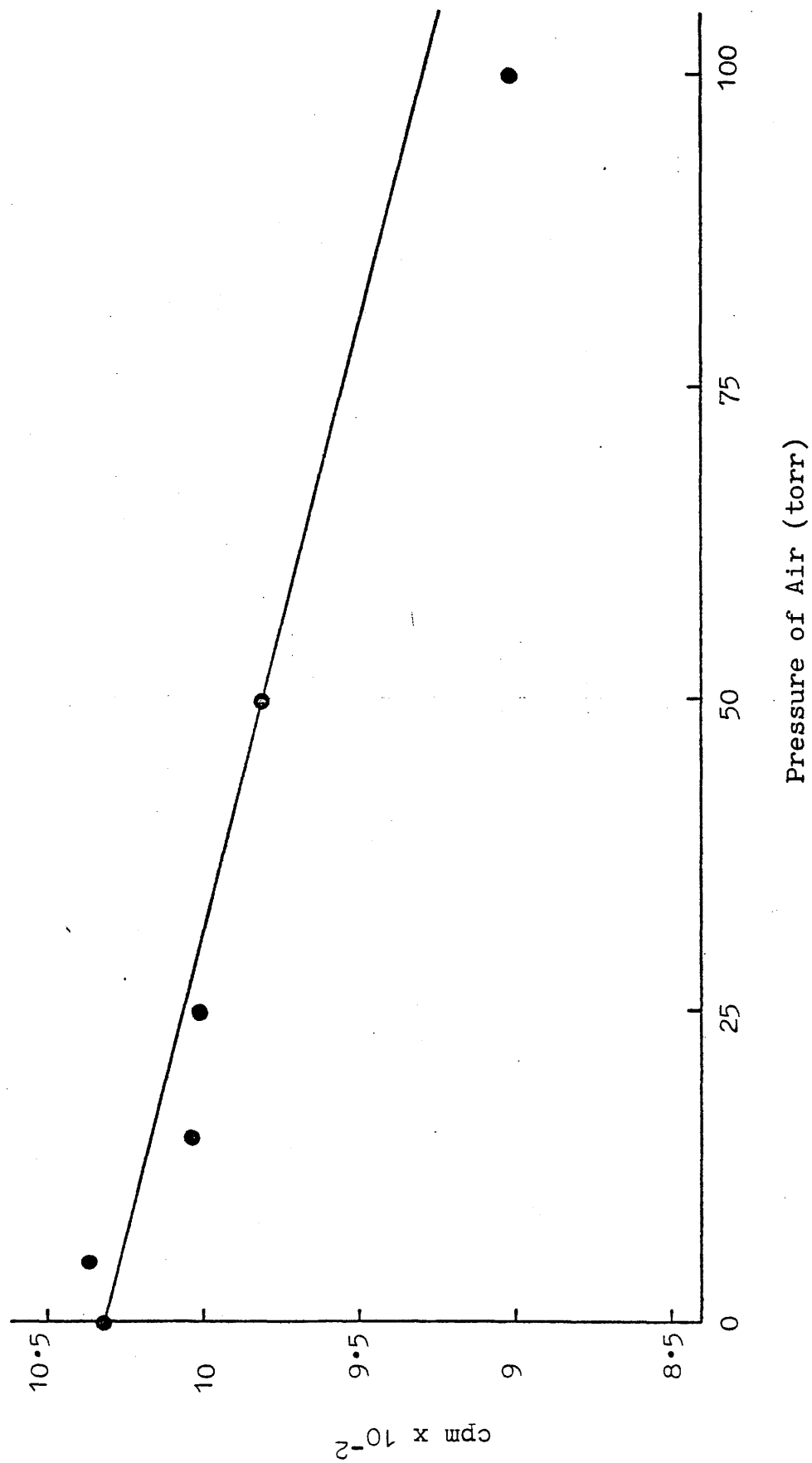


Figure 3.5 Count Rate from [¹⁴C]Polymethylmethacrylate Source versus Air Pressure

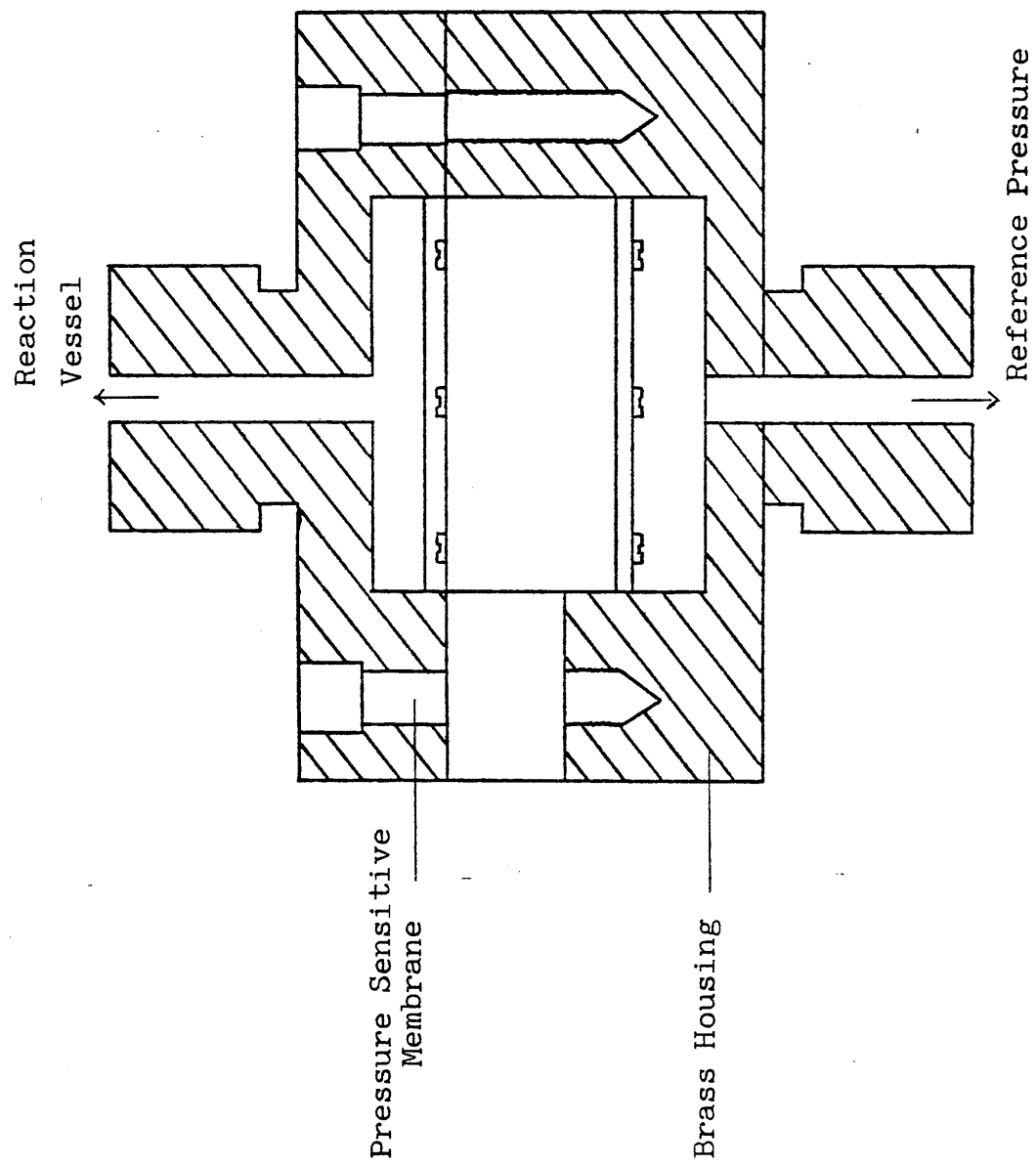


Figure 3.6 The Pressure Transducer

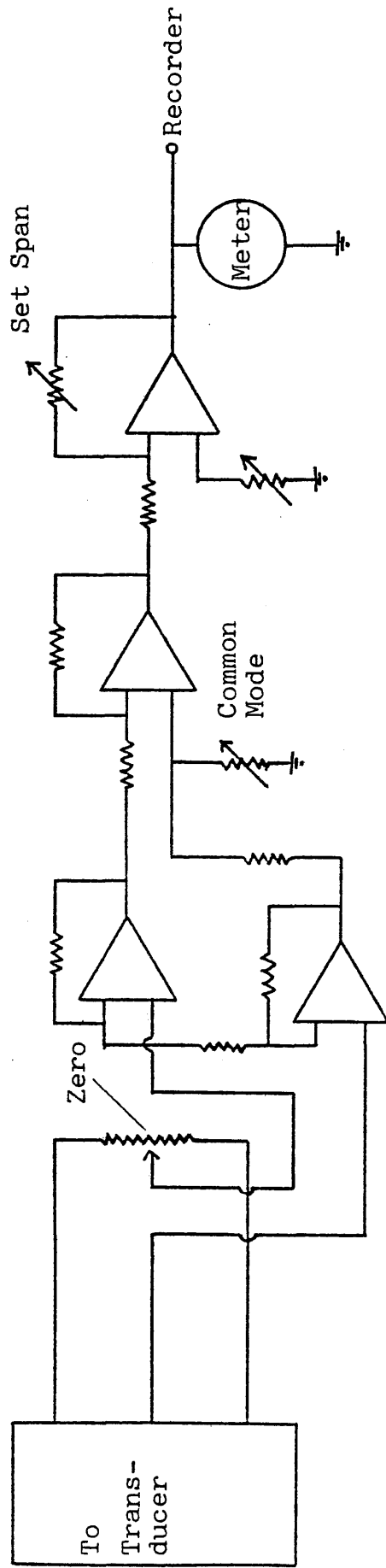


Figure 3.7 Pressure Transducer Electronics

moving coil meter and a chart recorder.

Balance and calibrating controls were provided. Adjustment of the calibrating control allowed the amount of deflection on the meter, for a given pressure, to be altered. The transducer was calibrated against the mercury manometer, using a cathetometer to measure the heights of the mercury columns. The calibrating control was adjusted until two units on the meter corresponded to a pressure difference of 1 torr. Thereafter the calibrating control was never altered. The balance control was used to set the output at zero for a given reference pressure. The response of the transducer was found to be linear within the pressure range used.

The transducer output was fed into a Servoscribe chart recorder. This allowed the direct monitoring of pressure change with time during the hydrogenation reactions.

3.5 The Gas Chromatography System

The reaction vessel was connected to a sample U-tube (volume 15 cm^3) into which samples of products could be extracted for analysis in the gas chromatograph-proportional counter. Samples were thus separated in the gas chromatograph and the amount of radioactivity in each individual product determined with the proportional counter.

Separation of mixtures was attained using a 1 metre column packed with 44-60 mesh activated silica gel. The column was operated at 80°C with helium as carrier gas (flow rate $60 \text{ cm}^3 \text{ min}^{-1}$).

The detector was a Gow-Mac thermal conductivity cell Model 10-285 operated at a filament current of 200 mA. The output from the detector was fed into a Servoscribe potentiometric chart recorder. A typical trace is shown in figure 3.8.

The conditions described above gave good separation of the hydrocarbons. The retention times (measured from the air peak) are given in table 3.2. However since the chromatographic detector depended on thermal conductivity, the quantitative analysis of hydrogen was impossible when helium was used as carrier gas.

Peak areas were measured using a fixed arm planimeter. Calibration was accomplished by introducing accurately known pressures of each gas into the chromatograph and calculating response factors (S_A) where

$$S_A = \frac{\text{Peak area}}{\text{Pressure of gas.}}$$

Using the individual response factors the partial pressures of each component in the product mixture could be calculated and hence the percentage composition of each product mixture could be determined. Since the sensitivity of the detector varied slightly from day to day a calibration was carried out each day.

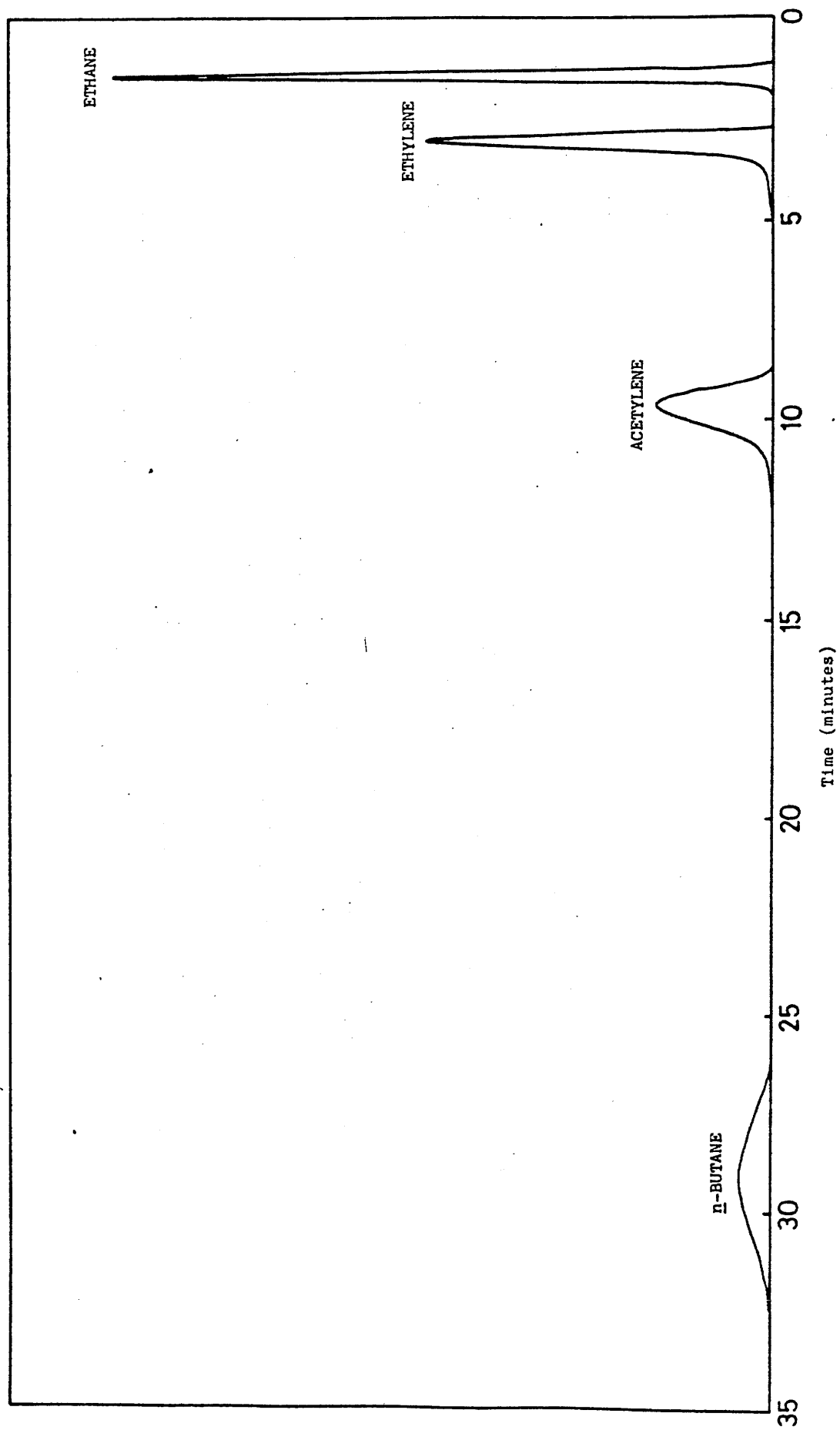


Figure 3.8 Gas Chromatography Trace

Table 3.2

Retention Times

	Retention time (minutes)
Ethane	1.5
Ethylene	3.1
Acetylene	9.8
<u>n</u> -Butane	29.3

3.6 The Proportional Counter

A gas-flow proportional counter was coupled to the gas chromatograph to determine the amount of radioactivity in each product (figure 3.9). The counter, (of similar design to that used by Schmidt-Bleek and Rowland(69)), was constructed of brass and Teflon with a stainless steel anode (figure 3.10). This had several advantages over the widely used glass counters with silver cathodes, namely that it was inert to possible components in the flow stream. It was very robust and because of the thickness of the brass cylinder (1 cm) the background was low even without further shielding. By simply unscrewing the counter it could be taken apart and cleaned. The volume of the counter was 36 cm^3 .

The counting mixture was a blend of helium and methane. The plateau length and slope, determined using an external caesium-137 source, was very much dependent on the ratio of helium to methane. A helium flow rate of $60 \text{ cm}^3 \text{ min}^{-1}$ had to be maintained for efficient chromatographic separation, so mixture proportions were altered by varying the methane flow rate. On elution from the column the helium plus sample was mixed with the required amount of methane (controlled by a fine metering valve on the methane supply line) before entering the proportional counter.

The electronics consisted of an ESI Nuclear Ratemeter type 5350 used with an ESI Nuclear Pre-amplifier unit type 425. The ratemeter settings which gave optimum working conditions were found to be:-

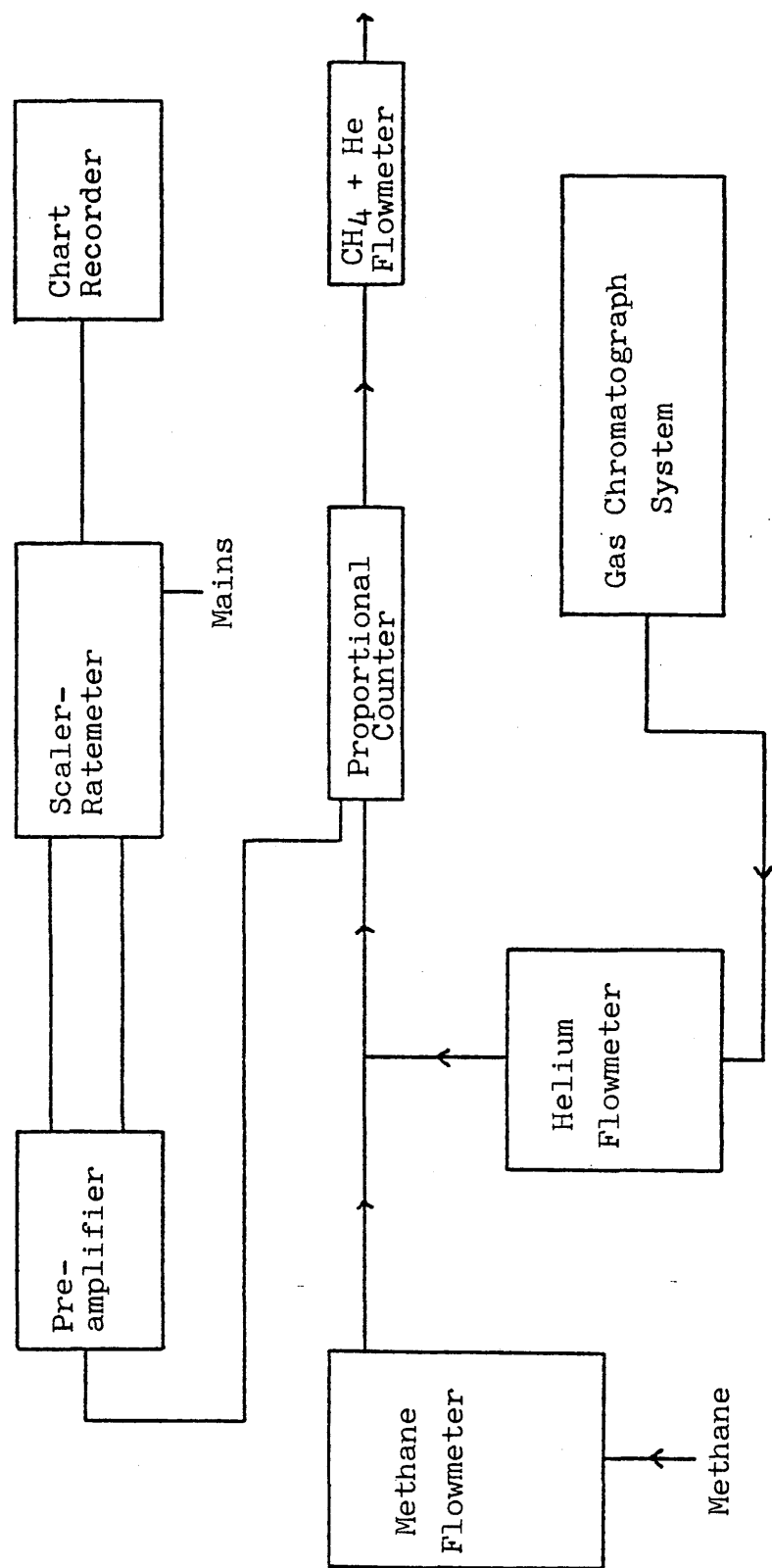


Figure 3.9 Block Schematic Diagram of Gas Chromatography - Proportional Counter System

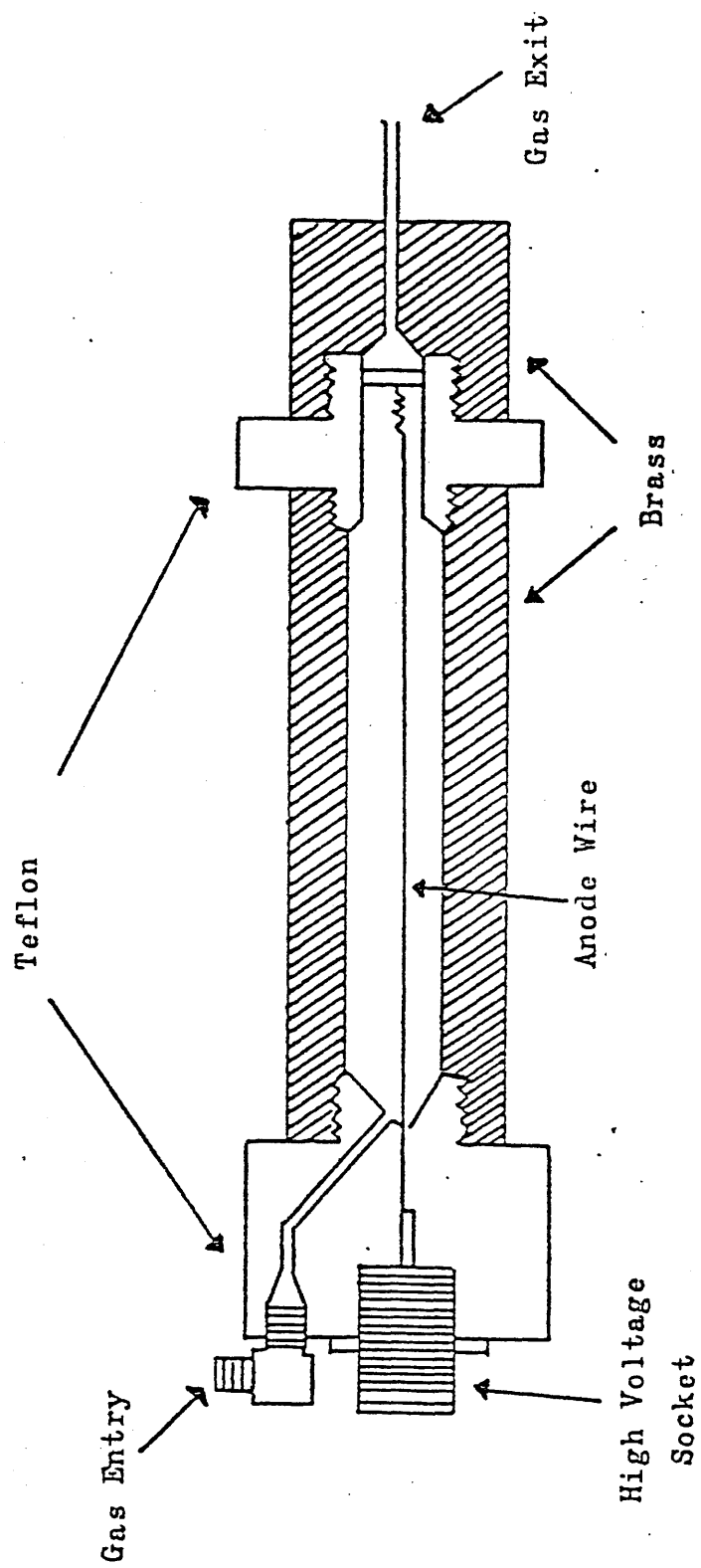


Figure 3.10 The Proportional Counter

Function	A - ∞
A	150
Gain	4
TC	0.3 sec
EHT	2.02 kV

It was found that the best plateau was obtained when the helium to methane ratio was 11:1 (figure 3.11). This had a length of approximately 100 volts and a slope of ca. 5%. The working voltage was selected as 2.02 kV. This value was slightly lower than the mid-point of the plateau and was chosen because proportional counter plateaus are known to shift to lower voltages with counter use.

As with the Geiger-Müller system, an estimate of the reliability of the counter was made by taking twenty determinations of the count rate with a caesium-137 external source placed under the counter.

The following results were obtained:-

	P.C.	Theoretical
$\bar{N} \pm \sigma$	80%	68.3%
$\bar{N} \pm 2\sigma$	95%	95.1%
$\bar{N} \pm 3\sigma$	95%	>99%

Again, allowing for the small sample of count rates taken, the results indicate reliable behaviour.

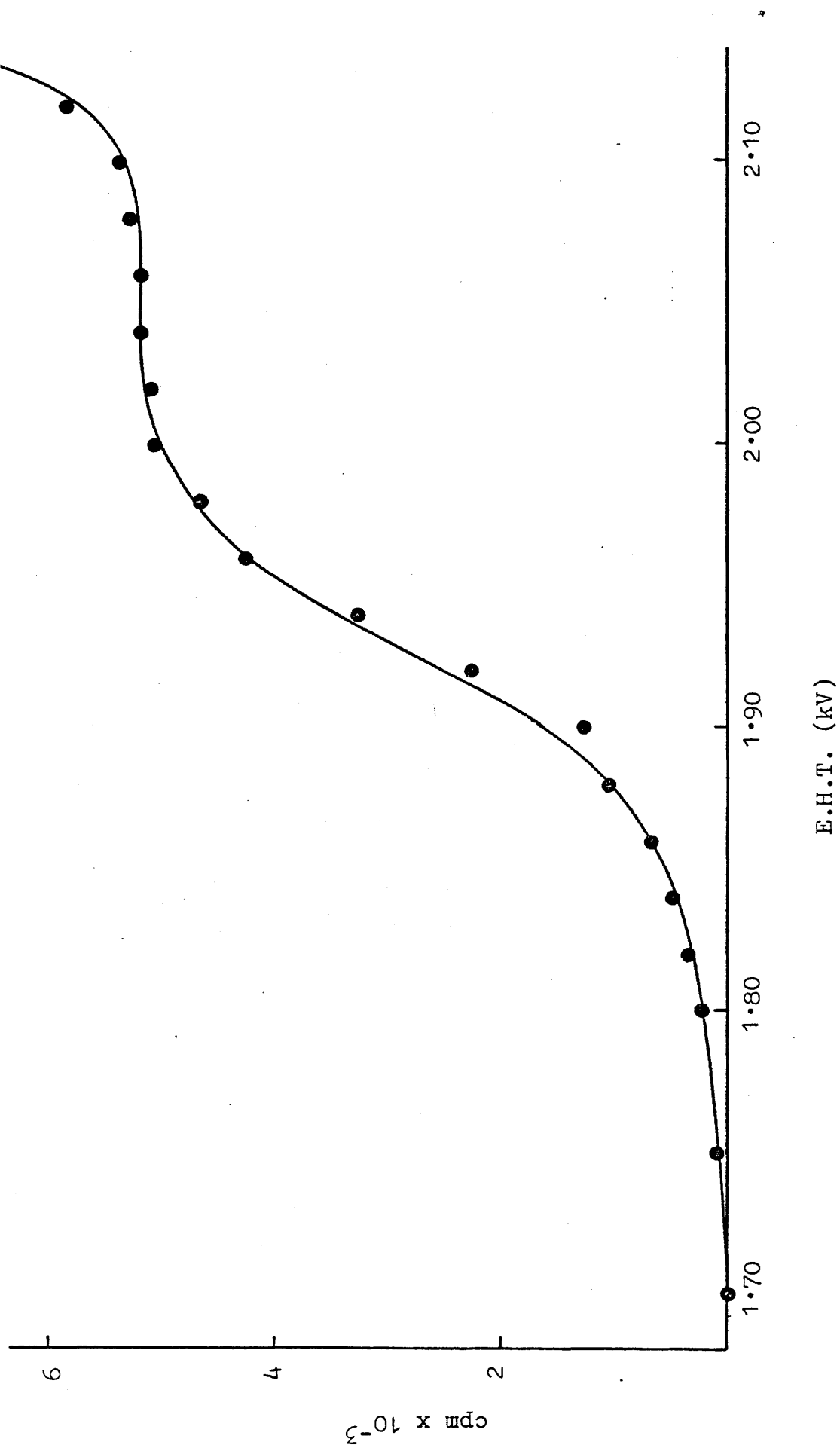


Figure 3.11 Proportional Counter Plateau

The 100 mV output of the ratemeter was fed into a Servoscribe chart recorder. This gave a visual display of the passage of radioactive gases through the counter. A two channel chart recorder was used, one channel of which was connected to the gas chromatography detector (see section 3.5) and the other channel to the proportional counter. In practice the peaks from the proportional counter were used to determine when to start and stop counting with the scaling circuit.

Before any experiments were carried out it was necessary to obtain calibrations between radioactive gas pressures and measured counts. This was done by passing various pressures of each gas through the gas chromatography-proportional counter system and determining the number of counts under each peak. It was found that a straight-line relationship existed provided the gas pressure was not in excess of 15 torr.

It was also necessary to investigate whether the passage of a large peak of eluted material through the counter would have any effect on the count rate. With an external caesium-137 source in position under the counter a series of count rates were taken. Then a series of pulses of inactive ethane, ethylene or acetylene, at different pressures, were passed through the counter. No quenching of the count rate was observed for partial pressures of added gas as large as 20 torr.

3.7 Catalyst

The catalyst used in this work was a sample of Euro-nickel-1 containing 25.4% (w/w) nickel on silica. It was prepared at Nijmegen University, The Netherlands, by the following method.

50 litres of demineralised water, 3 Kg $\text{Ni}(\text{NO}_3)_2$ and 1.4 Kg silica (Degussa Aerosil 200) were heated to 90°C. Then a warm solution containing 1.8 Kg urea was added. The slurry was well mixed and maintained at 90°C for 20 hours. The urea decomposed slowly to carbon dioxide and ammonia, the pH rose and nickel hydroxide precipitated homogeneously on to the silica. The slurry was filtered hot (to wash out ammonium nitrate), then the precipitate was slurried in hot water and filtered again. This process was repeated once more. The final precipitate was slurried again and spray-dried.

The catalyst was stored as the supported salt until required. It was activated before experiments by reduction in the reaction vessel in a flow of hydrogen (ca. $25 \text{ cm}^3 \text{ min}^{-1}$) at 500°C for 18 hours, followed by evacuation at 450°C for 6 hours and finally being cooled in vacuo to ambient temperature.

3.8 Materials

Acetylene (Air Products Ltd.) contained both acetone and air. Air was removed by cooling the mixture in a liquid nitrogen trap and then pumping. Acetone was removed by a series of bulb to bulb distillations using a liquid nitrogen trap (-196°C) and a methylene chloride/solid carbon dioxide trap (-78°C). The purified acetylene contained no impurities detectable by gas chromatography.

Hydrogen (B.O.C. Ltd. Commercial grade), for hydrogenation reactions, was purified by diffusion through a heated palladium-silver thimble. For reduction of catalysts, cylinder hydrogen was used without further purification.

Methane (Air Products Ltd. C.P. grade) was used for the operation of the proportional counter. From the manufacturer's specification this was $>99\%$ pure.

Helium (B.O.C. Ltd. Grade A) was used without further purification.

Ethane and ethylene (Air Products Ltd. C.P. grade) contained no impurities detectable by gas chromatography and were merely degassed before use.

Carbon monoxide (Air Products Ltd. C.P. grade) was used without further purification. It was specified by the manufacturers as being 99.5% pure.

$[^{14}\text{C}]$ Labelled hydrocarbons (Radiochemical Centre, Amersham) were diluted to the required specific activity with the purified inactive hydrocarbon before use.

3.9 Preparation of [^{14}C]Carbon Monoxide

[^{14}C]Carbon monoxide was prepared by reduction of [^{14}C]carbon dioxide (Radiochemical Centre, Amersham) with metallic zinc (70).

The apparatus consisted of a Pyrex loop with a cold finger and a B14 socket for attachment of the [^{14}C]CO₂ ampoule (figure 3.12). A portion of the loop had a furnace around it.

Zinc pellets, approximately 5mm in diameter, were made from a moistened mixture containing 95% by weight zinc dust (Analar) and 5% Aerosil silica (Degussa Ltd.). The silica was used to give greater porosity and to prevent clogging. The pellets were dried in an air oven at 120°C for 24 hours. They were then placed inside the furnace region of the converter and degassed at 320°C by pumping continuously for 24 hours.

[^{14}C]Carbon dioxide was converted to [^{14}C]carbon monoxide by circulation around the converter at 400°C for 48 hours. After conversion a liquid nitrogen trap was placed around the cold finger to trap out any unconverted [^{14}C]carbon dioxide and the [^{14}C]carbon monoxide was then allowed to expand into a storage vessel.

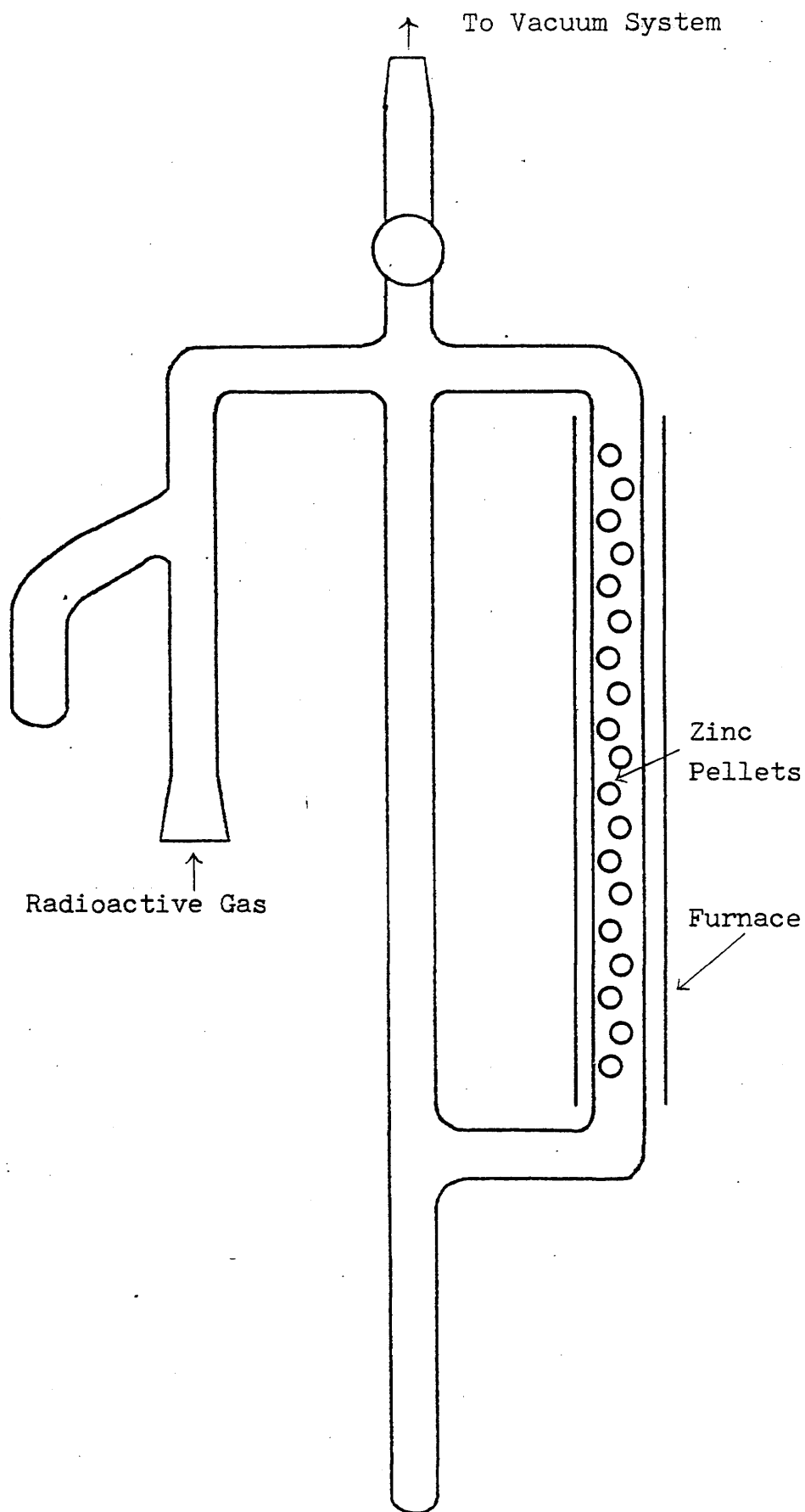


Figure 3.12 Reaction Vessel for Reduction of
[^{14}C]Carbon Dioxide

3.10 Experimental Procedure

Adsorption Isotherms

Adsorption isotherms were built up by introducing small batches of radioactive gas to the reaction vessel. After each introduction five minutes were allowed for equilibration before counting with the intercalibrated Geiger-Müller tubes. One of the tubes counted gas phase plus surface while the other counted gas phase only. Hence surface count rate could be obtained by subtraction. The process was repeated until sufficient data had been accumulated to plot the adsorption isotherm.

Hydrogenation Reactions

Hydrogenation mixtures were prepared by admitting the required pressure of hydrocarbon to the mixing vessel, condensing the hydrocarbon into the cold finger, then admitting the required pressure of hydrogen. The cold trap was then removed and the mixture allowed to warm to ambient temperature. For acetylene hydrogenation the normal mixture was 3:1 (v/v) hydrogen:acetylene.

Hydrogenations were carried out by admitting the required pressure (normally 50 torr) of mixture to the reaction vessel and monitoring the subsequent pressure fall with the pressure transducer. Samples could be removed

from the reaction vessel and injected into the combined gas chromatography-proportional counter at any stage of the reaction. The identity of the products was obtained from the gas chromatograph while the amount of radioactivity in each product was determined using the proportional counter.

CHAPTER 4

4. RESULTS

4.1 Catalyst Deactivation by C_2H_2/H_2 Mixtures

4.1.1 Pressure Fall-Time Curves

A mixture of 12.5 torr acetylene and 37.5 torr hydrogen was introduced to the reaction vessel containing 0.082g freshly reduced catalyst at room temperature. The progress of the hydrogenation reaction was followed by monitoring the fall in total pressure. Figure 4.1 shows some typical pressure fall-time curves from which it can be seen that the reaction takes place in two distinct stages, the onset of the second stage being accompanied by a sharp increase in rate.

The acceleration point, denoted as $-\Delta P_a$, was obtained by extrapolating the first and second stages of the reaction and finding the point of intersection. The acceleration occurred at a pressure fall of 17 ± 1 torr.

Analysis of the products by gas chromatography showed that in the initial stage both ethane and ethylene were produced. After the acceleration point the major process occurring was the further hydrogenation of ethylene to ethane, although very late in the reaction some butane was also observed.

A series of hydrogenations, using mixtures of 12.5 torr acetylene and 37.5 torr hydrogen, were carried out consecutively on the same catalyst sample. Between each reaction the reaction vessel was evacuated for 15 minutes to remove all the products of the previous hydrogenation. As can be seen from figure 4.1, the reaction rate progressively

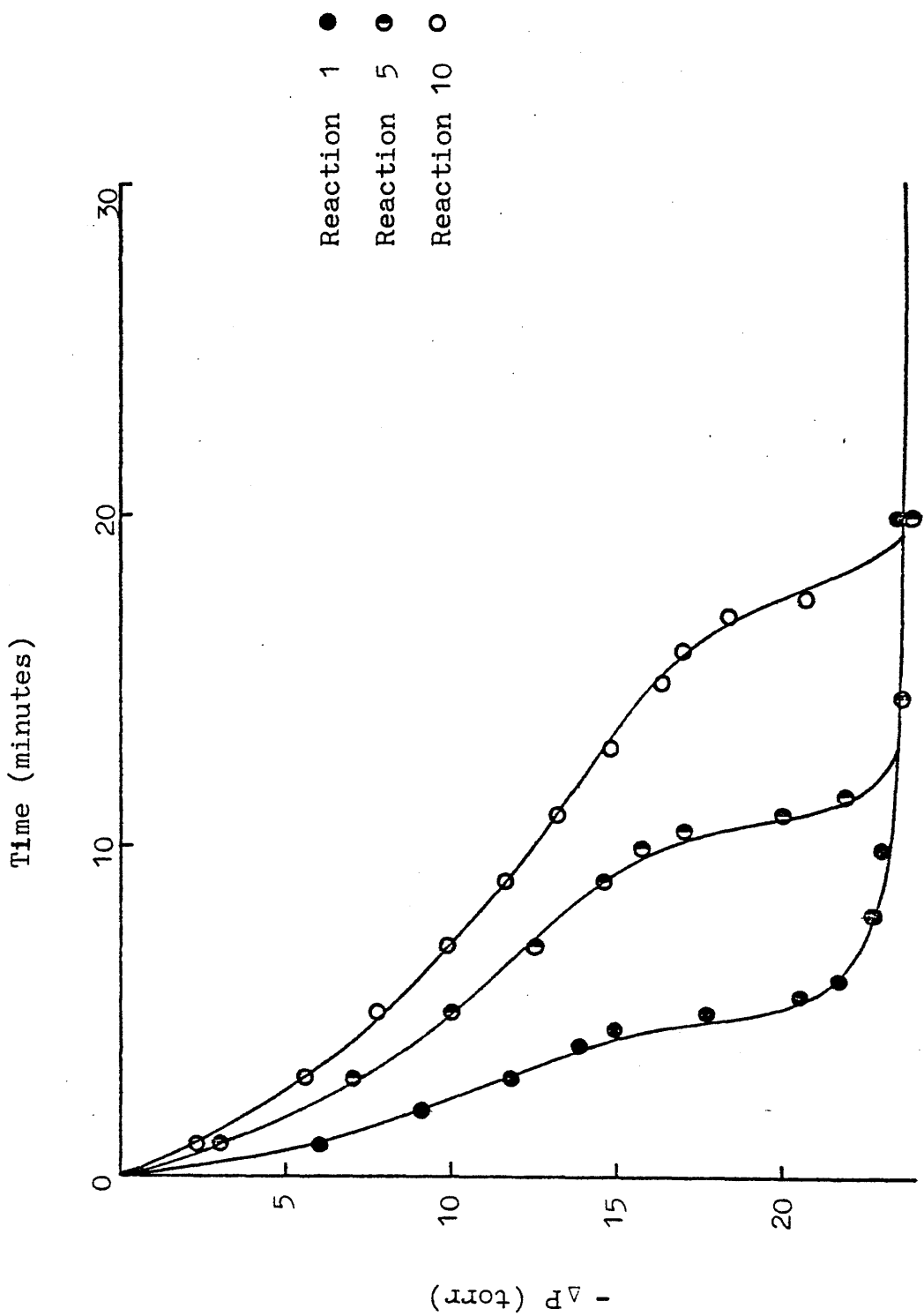


Figure 4.1 Pressure Fall-Time Curves

decreased from reaction to reaction, both stages of the reaction being decelerated.

The first stage of the reaction was found to be first order in total pressure. Plots of $\ln (P_0 + \Delta P)$ against time (figure 4.2) were found to be straight lines, the gradients of which yielded values of the first order rate constant (k). Figure 4.3 shows the variation of the first order rate constant ($k \text{ min}^{-1}$) with reaction number for hydrogenations on a 0.082g sample of Ni/SiO₂. From this it can be seen that initially the rate of reaction was high but this progressively decreased until, after approximately 15 reactions, a constant 'steady state' activity was achieved. The reaction rate did not tend to zero. Variations in the value of the rate constant at the steady state were probably due to small fluctuations in room temperature, which was $18.5 \pm 2^\circ\text{C}$.

4.1.2 Deactivation

Catalyst deactivation could only be accomplished using acetylene/hydrogen mixtures. When 12.5 torr acetylene alone was admitted to the catalyst no deactivation was observed. After a period of 48 hours in contact with the catalyst, analysis showed that a very small amount of the acetylene (<0.5 torr) had been self-hydrogenated to ethane. No ethylene was observed.

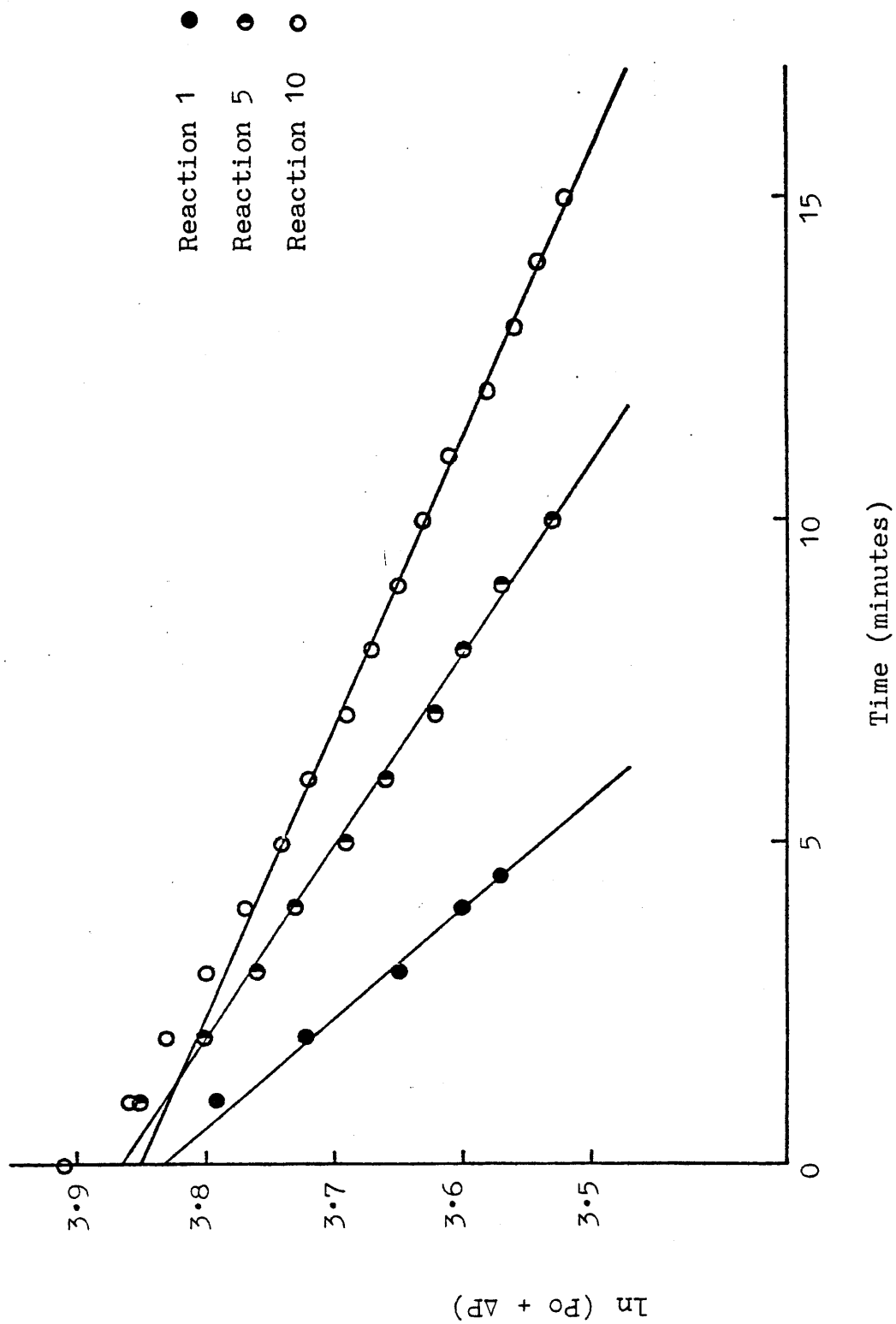


Figure 4.2 First Order Plots

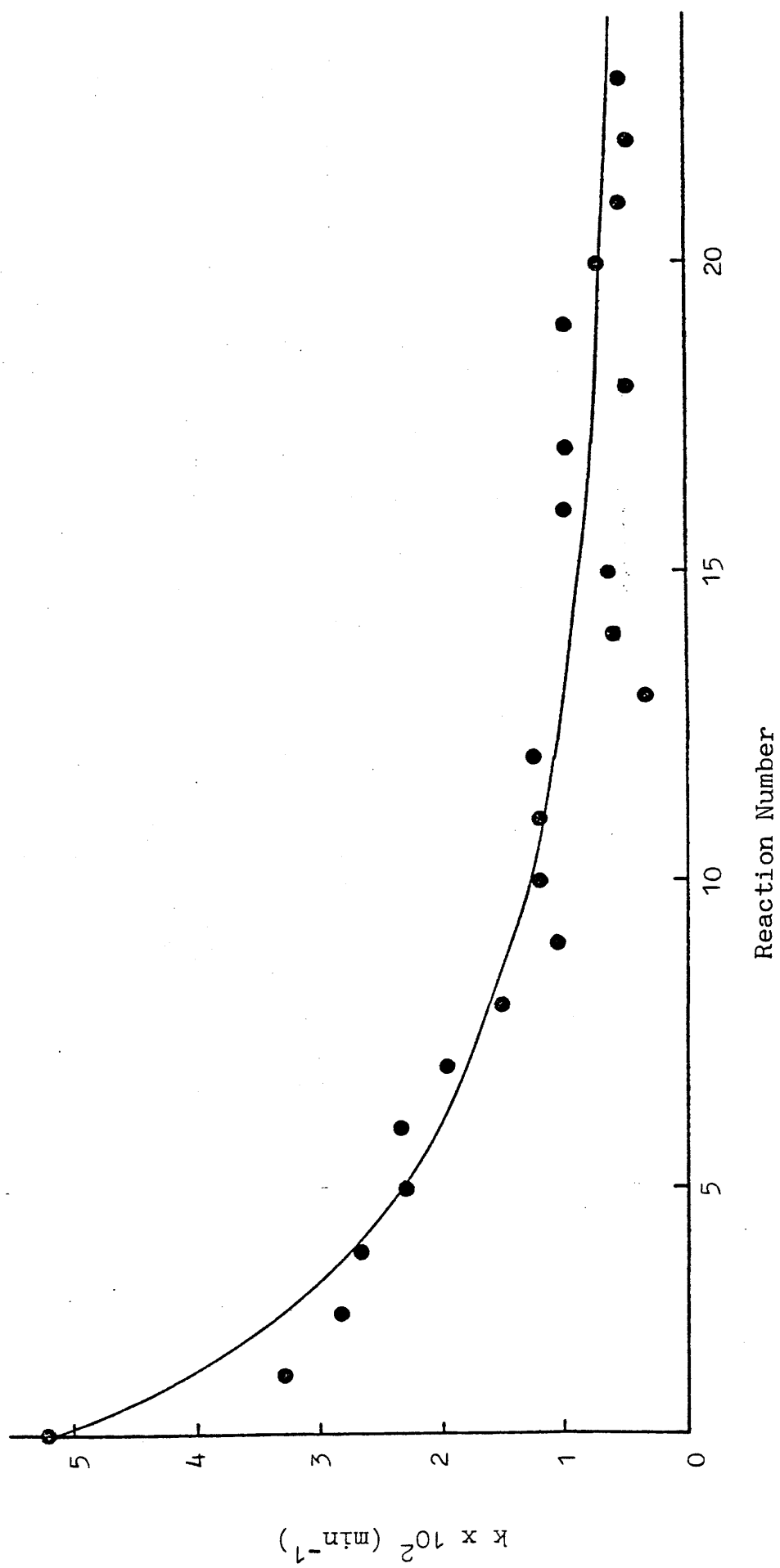


Figure 4.3 Variation of the First Order Rate Constant with Reaction Number

4.1.3 Regeneration

For a catalyst in the steady state, it was found that the initial activity could only be restored by reduction in a flow of hydrogen (flow rate $30 \text{ cm}^3 \text{ min}^{-1}$) at 500°C for 4 hours, followed by evacuation at 450°C for 2 hours and cooling under vacuum for a further 2 hours. During regeneration, methane and ethane were produced, methane being by far the major product. However, because these were continuously produced in a hydrogen flow, quantitative analysis of the amounts of each hydrocarbon was difficult.

4.1.4 Effect of Catalyst Deactivation on Selectivity

For the purposes of this thesis selectivity, S , for ethylene formation is defined as

$$S = \frac{P_{\text{C}_2\text{H}_4}}{P_{\text{C}_2\text{H}_4} + P_{\text{C}_2\text{H}_6}}$$

where $P_{\text{C}_2\text{H}_4}$ and $P_{\text{C}_2\text{H}_6}$ represent the partial pressures of ethylene and ethane respectively.

The percentage conversion has been calculated from the product distribution. It can be considered as a measure of moles of hydrogen consumed per mole of hydrocarbon present in the reaction mixture and thus, since the formation of a mole of ethane requires two moles of hydrogen and the formation of a mole of ethylene requires one mole of hydrogen, it can be calculated as:

$$\% \text{ conversion} = (2 \times \text{ethane yield}) + (1 \times \text{ethylene yield}).$$

When butane was observed as a reaction product, the term (3 x butane yield) was added to the above formula.

For a series of consecutive hydrogenation reactions, such as that described in section 4.1.1, samples were extracted at approximately 65% conversion and analysed in the gas chromatograph. In this way it was possible to investigate the effect of catalyst deactivation on selectivity for ethylene formation. As can be seen from table 4.1, deactivation had a negligible effect on selectivity.

Table 4.1 Effect of Catalyst Deactivation on Selectivity

Reaction Number	% Conversion	Selectivity
2	68.41	0.774
3	66.99	0.771
13	67.91	0.788
15	64.66	0.760
18	65.31	0.759
20	65.62	0.751
21	66.31	0.770

4.2 $[^{14}\text{C}]$ Acetylene Adsorption

4.2.1 $[^{14}\text{C}]$ Acetylene Adsorption on Freshly Reduced Ni/SiO₂

The adsorption of $[^{14}\text{C}]$ acetylene, on 0.049g freshly reduced catalyst, was followed using the direct monitoring technique described earlier (section 3.1). The specific activity of $[^{14}\text{C}]$ acetylene was 1.18×10^{-2} mCi/mM. Small aliquots of the labelled adsorbate were admitted to the reaction vessel and the surface and gas phase count rates determined after each addition.

Figure 4.4 shows an adsorption isotherm for $[^{14}\text{C}]$ acetylene adsorbed on a freshly reduced catalyst. It can be seen that adsorption occurs in two distinct stages, a steep 'primary' region followed by a linear 'secondary' region. The secondary region of adsorption continued to increase linearly with increasing gas pressure. No plateau region was observed although gas pressures in excess of 6 torr were used.

Analysis of the gas phase during the build-up of the primary region indicated that $[^{14}\text{C}]$ ethane was present. No ethylene was ever observed as a product from $[^{14}\text{C}]$ acetylene adsorption isotherm experiments. From the yields of ethane it was possible to estimate the average composition of the adsorbed acetylenic species on the primary region. Assuming, as observed previously (71) that the amount of catalyst hydrogen (retained from the reduction procedure) available for hydrogenation was negligible, the average composition

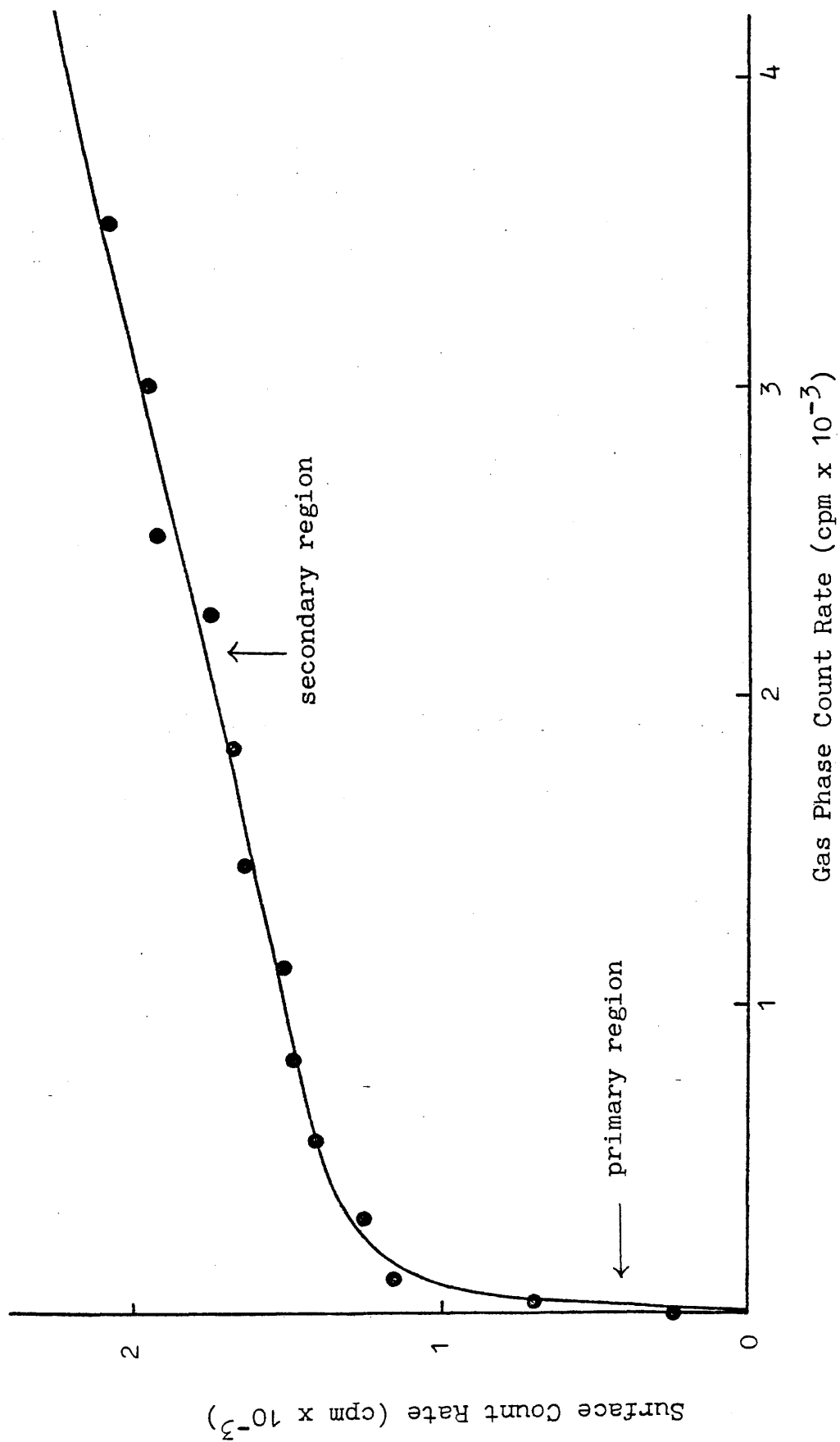


Figure 4.4 Adsorption Isotherm for $[^{14}\text{C}]$ Acetylene on Freshly Reduced Ni/SiO_2

of the adsorbed species on the primary region was found to be $C_2H_{1.9}$.

After determination of the isotherm the reaction vessel was evacuated for 15 minutes. Subsequently, the surface count rate was still much greater than background indicating that strongly bound hydrocarbon species remained on the surface. These species did not undergo exchange with non-radioactive acetylene and could not be removed by treatment with hydrogen at room temperature.

It was found that regenerating the catalyst in a stream of hydrogen at $500^\circ C$ for 16 hours removed nearly all of the surface radioactivity. Thus, it was possible to determine the reproducibility of the $[^{14}C]$ acetylene isotherm. Three isotherms, performed on the same catalyst sample with regeneration between each isotherm, are shown in figure 4.5. This indicates the reproducibility of the adsorption process.

4.2.2 Reactivity of Species Adsorbed on Primary Region

The reactivity of the acetylenic species adsorbed on the primary region of a freshly reduced catalyst was examined by covering the surface with $[^{14}C]$ acetylene to a point corresponding to the completion of the primary region. The reaction vessel was evacuated for 15 minutes. A premixed sample of 12.5 torr non-radioactive C_2H_2 and 37.5 torr H_2 was admitted to the catalyst and the change in total pressure monitored. During the hydrogenation the surface and gas phase count rates were monitored. No significant change in

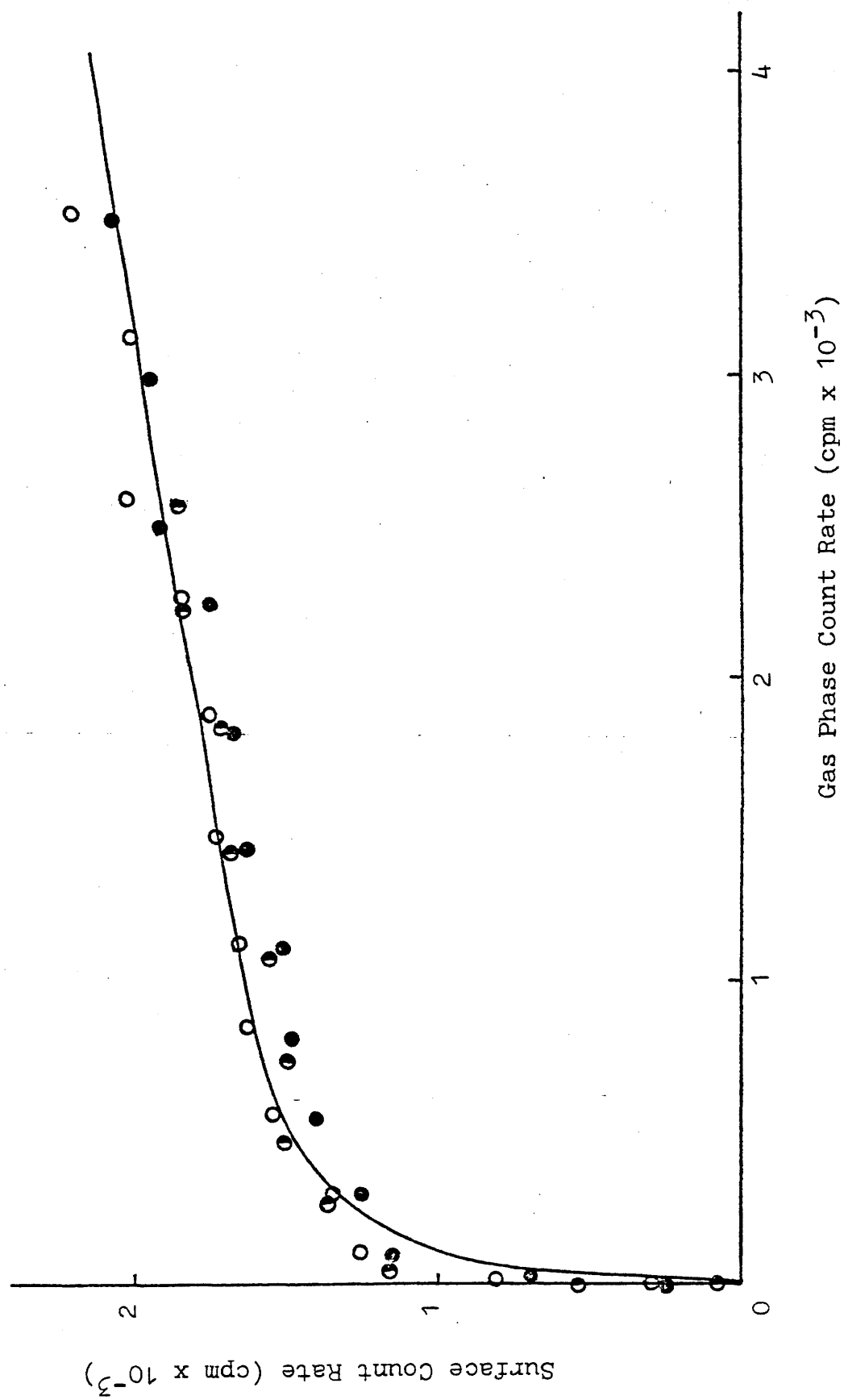


Figure 4.5 Adsorption Isotherms for [¹⁴C]Acetylene after Catalyst Regeneration

surface count rate was observed. Also, no radioactivity was detected in any of the products when these were analysed in the gas chromatography-proportional counter system. Evacuation for 15 minutes did not result in the removal of any radioactive species.

4.2.3 Removal of Adsorbed Species by C_2H_2/H_2 Mixtures

It has already been established (section 4.2.1) that strongly retained surface species cannot be removed by evacuation for 15 minutes, by treatment with hydrogen at room temperature, or by treatment with acetylene alone. The effect of C_2H_2/H_2 mixtures was investigated.

A hydrogenation reaction using a premixed sample of 12.5 torr [^{14}C]acetylene and 37.5 torr hydrogen was carried out using 0.153g of freshly reduced catalyst. The reaction vessel was evacuated for 25 minutes. A second hydrogenation was performed under similar experimental conditions. The reaction vessel was evacuated for 15 minutes, left under vacuum for 35 minutes and evacuated for a further 70 minutes, to ensure complete removal of the gas phase. The surface count rate was 9341 cpm. A number of hydrogenations were then carried out using mixtures of 12.5 torr non-radioactive acetylene and 37.5 torr hydrogen. The surface count rate was determined after each reaction. The results are shown in table 4.2. It can be seen that some surface [^{14}C]species were removed during each of the first nine reactions. After this the surface count rate remained almost constant. However,

even after treatment with twelve hydrogenation mixtures,
78.84% of the initial radioactivity was still present.

Table 4.2 Removal of Adsorbed Species by C₂H₂/H₂ Mixtures

Number of Reactions Performed	Surface Count Rate (cpm)
0	9341
1	8851
2	8699
3	8597
4	8393
5	8257
6	8010
7	7745
8	7471
9	7480
10	7433
11	7358
12	7364

4.2.4 $[^{14}\text{C}]$ Acetylene Adsorption on 'Deactivated' Ni/SiO₂

0.049g catalyst was reduced at 500°C for 14 hours, evacuated at 450°C for 1 hour and allowed to cool under vacuum for 3½ hours. A $[^{14}\text{C}]\text{C}_2\text{H}_2$ isotherm was built up on the catalyst. The reaction vessel was evacuated for 15 minutes to remove gas phase $[^{14}\text{C}]\text{C}_2\text{H}_2$ and loosely bound surface species. A pre-mixed sample of 12.5 torr acetylene and 37.5 torr hydrogen was introduced to the reaction vessel. The reaction was followed in the usual way by monitoring the change in total pressure. The catalyst activity (first order rate constant, $k \text{ min}^{-1}$) was determined. Samples were analysed during the course of the reaction. Gas chromatographic analysis revealed that the product distribution was as expected, ethane and ethylene being produced up to the acceleration point, and subsequently ethylene being hydrogenated to ethane. From proportional counter analysis it was found that no radioactivity had been incorporated into any of the products.

Surface count rates were monitored during this reaction. As can be seen from table 4.3 there was a very small decrease during the course of the reaction. The amount of radioactivity removed from the surface was so small that, in any one sample removed for analysis, it was below the level of detection in the proportional counter.

The above results suggested that $[^{14}\text{C}]$ hydrocarbon material, retained from the adsorption experiment, was present in two forms, type I species which were strongly

Table 4.3 Effect of a C₂H₂/H₂ Mixture on
[¹⁴C]Acetylene Residues

Initial surface count rate = 2770 cpm

Time (min)	-ΔP (torr)	Surface Count Rate (cpm)
0	0	2877
3	1.96	2724
6	3.92	2751
9	4.90	2787
12	5.88	2747
15	6.86	2650
18	7.84	2764
21	9.31	2702
24	10.29	2651
27	11.27	2692
30	13.24	2672
33	13.73	2691
36	15.69	2710
42	24.51	2603

bound to the catalyst surface and could only be removed by C_2H_2/H_2 mixtures, and type II which were so strongly bound that they did not undergo exchange or reaction. It was possible, however, that type II species were becoming increasingly dehydrogenated during the course of the reaction. The amount of type II species on the surface far exceeded the amount of type I.

After the hydrogenation reaction a second adsorption isotherm was built up. This procedure was repeated several times during the process of deactivation. Before each isotherm was determined the catalyst was allowed to stand for 1 - 16 hours under the hydrogen-rich reaction products. This period was long enough for the complete removal of all the 'removable' preadsorbed [^{14}C]acetylene (see section 4.2.3). The reaction vessel was then evacuated. This procedure allowed catalyst activity to be compared with adsorption characteristics. Figure 4.6 shows the adsorption isotherms during deactivation. In each case the surface count rates have been corrected for the background activity arising from permanently retained acetylenic residues. It can be seen that during deactivation the primary region progressively decreased, suggesting that, as the catalyst activity decreased, the extent of permanent retention of species on the primary region increased. Deactivation had no effect on the secondary region.

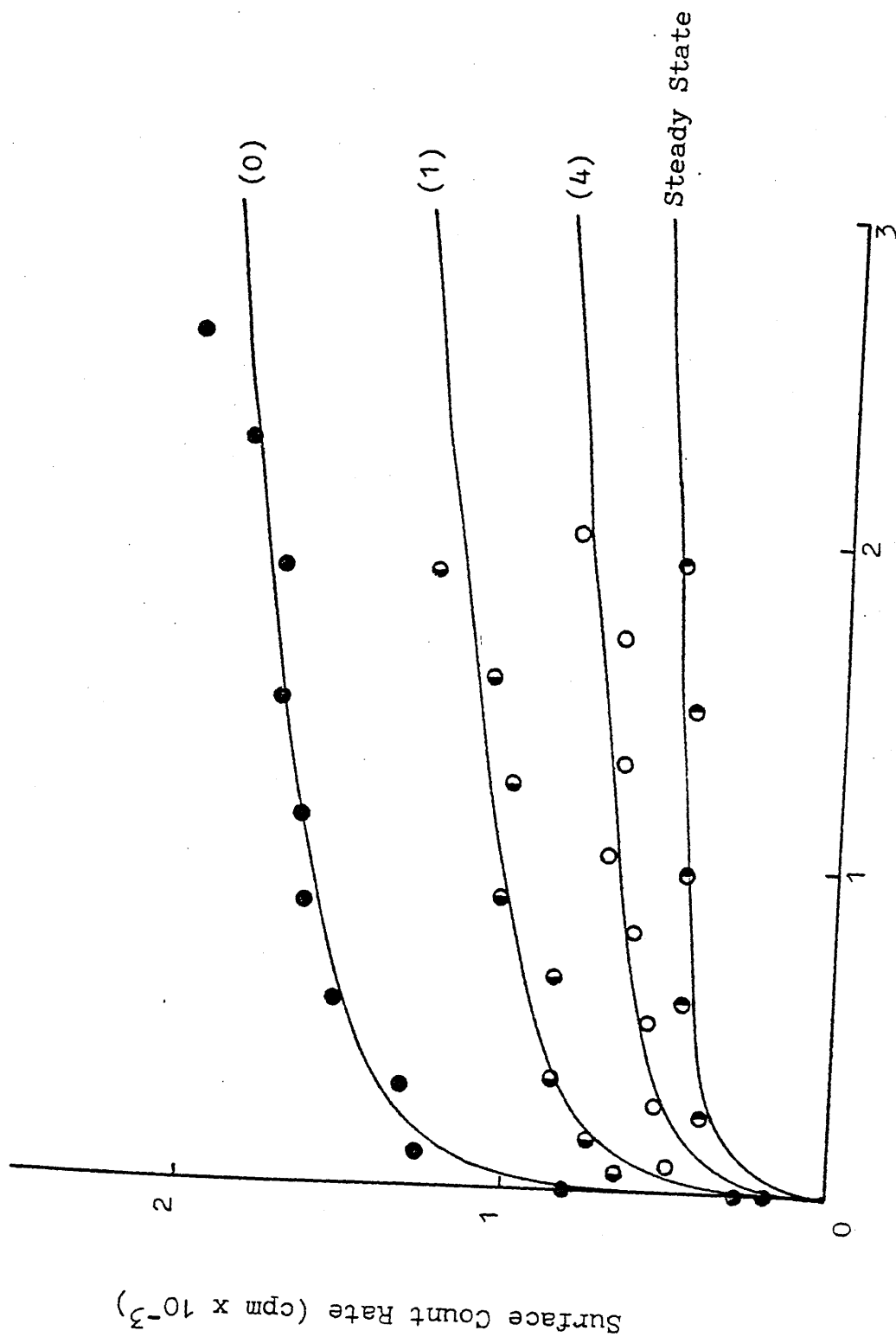


Figure 4.6 Adsorption Isotherms for $[^{14}\text{C}]$ Acetylene after varying numbers of reactions have been carried out.

4.2.5 Permanent Retention During Adsorption Isotherm

Experiments

Before each new isotherm (section 4.2.4) the surface count rate was determined. As has already been described, surface count rates in subsequent isotherms were corrected for this background activity arising from permanently retained acetylenic species. It is of interest to plot residual background against isotherm number (figure 4.7) to obtain information about the amount of retention which takes place with each experiment. The graph shows that from the fourth isotherm the amount of radioactivity retained on the surface increased linearly with isotherm number. This suggests that a similar proportion of [^{14}C]acetylene was being retained each time.

4.2.6 [^{14}C]Acetylene Adsorption on Steady State Ni/SiO₂

For catalysts which had been 'run-in' to their steady state by performing approximately 15 reactions, the adsorption isotherms for [^{14}C]acetylene showed almost no primary region. The secondary region was unaffected, and, within the limits of experimental error, had the same gradient as that obtained with a freshly reduced catalyst (figure 4.6).

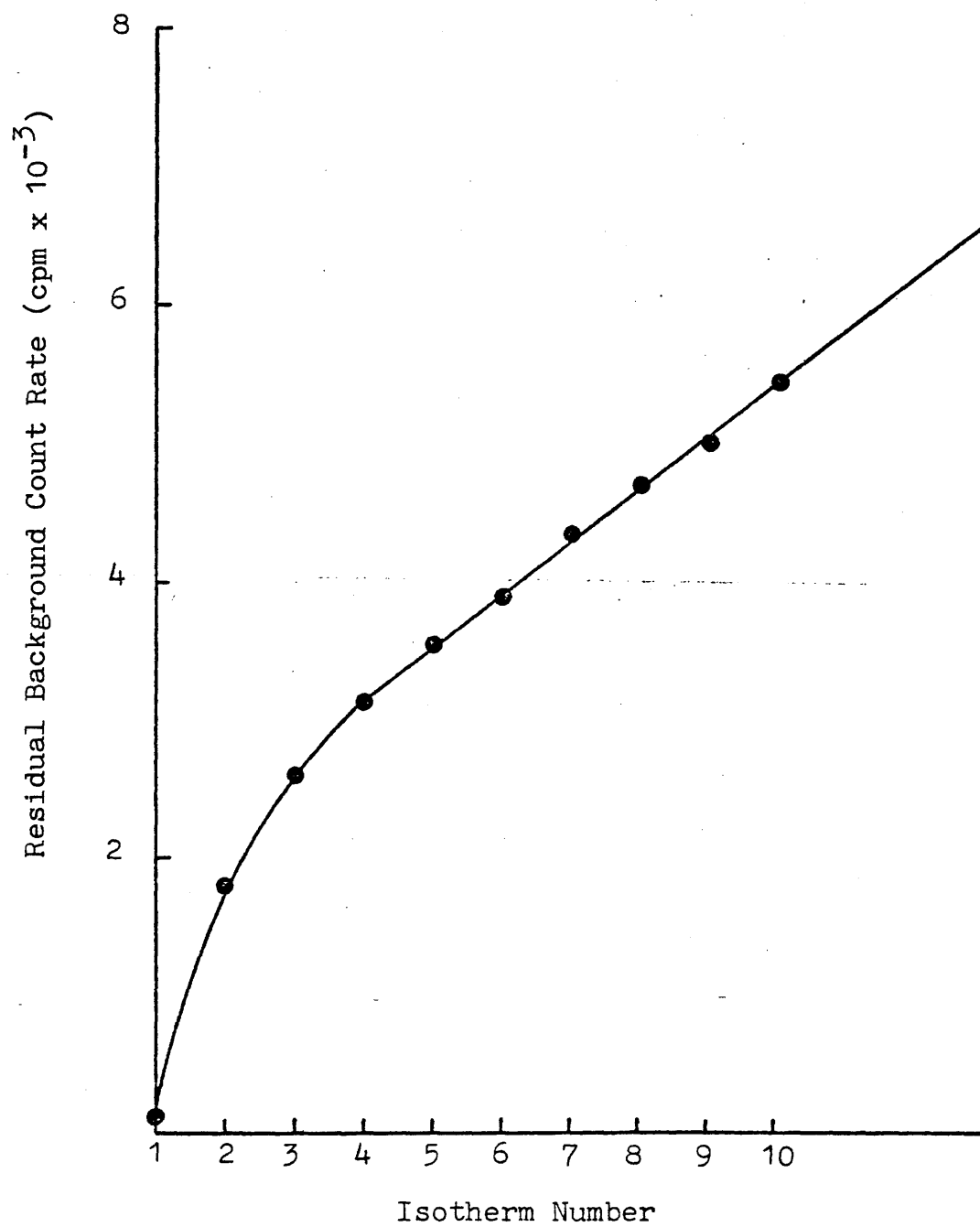


Figure 4.7 Residual Background Count Rate versus Isotherm Number

4.3 $[^{14}\text{C}]$ Carbon Monoxide Adsorption

4.3.1 $[^{14}\text{C}]$ Carbon Monoxide Adsorption on Freshly Reduced Ni/SiO₂

The adsorption of $[^{14}\text{C}]$ carbon monoxide (specific activity 2.70×10^{-2} mCi/mM) was examined on 0.049g freshly reduced Ni/SiO₂ using a similar technique to that used for the adsorption of $[^{14}\text{C}]$ acetylene. The adsorption isotherm is shown in figure 4.8. The surface count rate increased sharply with increasing pressure, until a constant value was attained at a surface count rate of 2060 cpm. The pressure range studied in the experiment was 0 - 6 torr. The plateau region was observed up to the 6 torr limit and there was no evidence to suggest that it did not continue indefinitely. The shape of the isotherm suggests that carbon monoxide adsorption reaches a saturation level, this corresponding to the completion of a monolayer of adsorbed species.

The catalyst was evacuated for 35 minutes to determine the amount of $[^{14}\text{C}]$ carbon monoxide which could be removed by evacuation. Before evacuation the saturation surface count rate was 2060 cpm. After evacuation the surface count rate was found to be 1515 cpm, corresponding to a removal of 26.5% of the adsorbed carbon monoxide. Subsequent treatment with acetylene/hydrogen mixtures did not cause any further displacement.

After the above treatment, it was found that a second $[^{14}\text{C}]$ carbon monoxide isotherm could be built up. This is

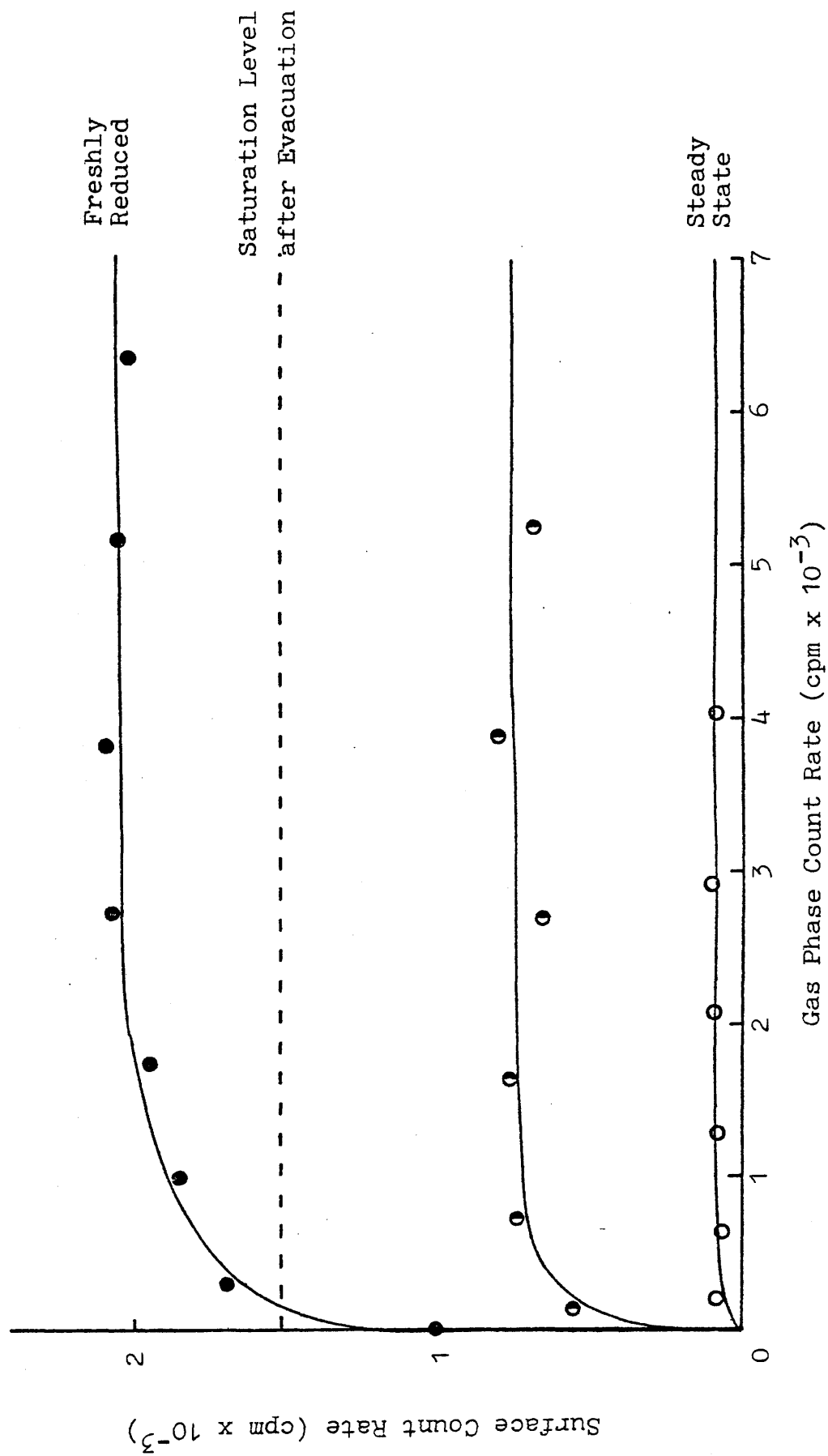


Figure 4.8 Adsorption Isotherms for $[^{14}\text{C}]$ Carbon Monoxide on Ni/SiO_2

also shown in figure 4.8. As can be seen, the saturation count rate of this isotherm was 740 cpm. However, since surface count rates have been corrected for the background activity, arising from permanently retained [^{14}C]carbon monoxide molecules from the previous isotherm, the total surface count rate was actually 2255 cpm. The saturation surface count rate after the first isotherm was 2060 cpm and therefore, it would appear that there had been an overall increase of approximately 10% in the number of molecules of carbon monoxide which the surface was capable of adsorbing.

4.3.2 [^{14}C]Carbon Monoxide Adsorption on Steady State Ni/SiO₂

The catalyst which was used in section 4.3.1 was regenerated in a flow of hydrogen ($25\text{ cm}^3\text{ min}^{-1}$) at 500°C for 14 hours, evacuated at 450°C for 1 hour, and finally cooled to room temperature. Sufficient acetylene hydrogenation reactions were carried out to reach a steady state constant activity. A [^{14}C]carbon monoxide isotherm was built up. As can be seen from comparison with adsorption on a freshly reduced catalyst (figure 4.8), the amount of adsorption on a steady state catalyst is substantially less, the saturation surface count rate being 80 cpm.

4.3.3 Poisoning of Acetylene Hydrogenation by Carbon Monoxide

The catalyst used in section 4.3.2 was regenerated in a flow of hydrogen ($30 \text{ cm}^3 \text{ min}^{-1}$) at 500°C for 1 hour, evacuated at 450°C for 1 hour and finally allowed to cool to room temperature. A [^{14}C]carbon monoxide isotherm was built up until the pressure in the gas phase was 6 torr. The reaction vessel was evacuated for 35 minutes to remove all gas phase carbon monoxide. From the surface count rate it was known that a substantial amount of carbon monoxide was still adsorbed on the surface (surface coverage approximately 75%). To this catalyst was added a premixed sample containing 12.5 torr acetylene and 37.5 torr hydrogen. The progress of the hydrogenation reaction was followed by monitoring change in total pressure. It was found that hydrogenation was still possible despite the high surface coverage of carbon monoxide, but that reaction proceeded at a much diminished rate. The first order rate constant was found to be $2.8 \times 10^{-3} \text{ min}^{-1}$ compared with a value of $9.0 \times 10^{-3} \text{ min}^{-1}$ on a similar weight of regenerated catalyst without carbon monoxide pretreatment.

The catalyst was regenerated in a flow of hydrogen ($25 \text{ cm}^3 \text{ min}^{-1}$) at 500°C for 14 hours, evacuated at 450°C for 1 hour and finally cooled to room temperature. A sufficient number of hydrogenation reactions were carried out to bring the catalyst to the steady state. A [^{14}C]carbon monoxide

isotherm was built up until the pressure in the gas phase was 6 torr. The amount of [^{14}C]carbon monoxide which became adsorbed on the surface was very low. After evacuating the reaction vessel for 30 minutes to remove gas phase [^{14}C]carbon monoxide, a 1:3 acetylene/hydrogen mixture was added.

Although the amount of carbon monoxide adsorbed on the surface was very small, it was still sufficient to cause a reduction in the rate of the subsequent hydrogenation reaction. The first order rate constant decreased from a steady state value of $6.5 \times 10^{-3} \text{ min}^{-1}$ to $2.9 \times 10^{-3} \text{ min}^{-1}$.

It was found that pretreatment of the 'steady state' catalyst with [^{14}C]carbon monoxide, as described above, caused a change in the selectivity of the catalyst for ethylene production. There was an increase from a value of 0.760 on a normal steady state catalyst to 0.822 on a [^{14}C]carbon monoxide pretreated catalyst.

4.4 [^{14}C]Ethylene Adsorption

4.4.1 [^{14}C]Ethylene Adsorption on Freshly Reduced Ni/SiO₂

The adsorption of [^{14}C]ethylene (specific activity $1.31 \times 10^{-2} \text{ mCi/mM}$) on 0.082g freshly reduced catalyst was followed by the direct monitoring technique. Small aliquots of the labelled adsorbate were admitted to the reaction vessel and the surface and gas phase count rates determined after each addition.

Figure 4.9 shows a typical adsorption isotherm for

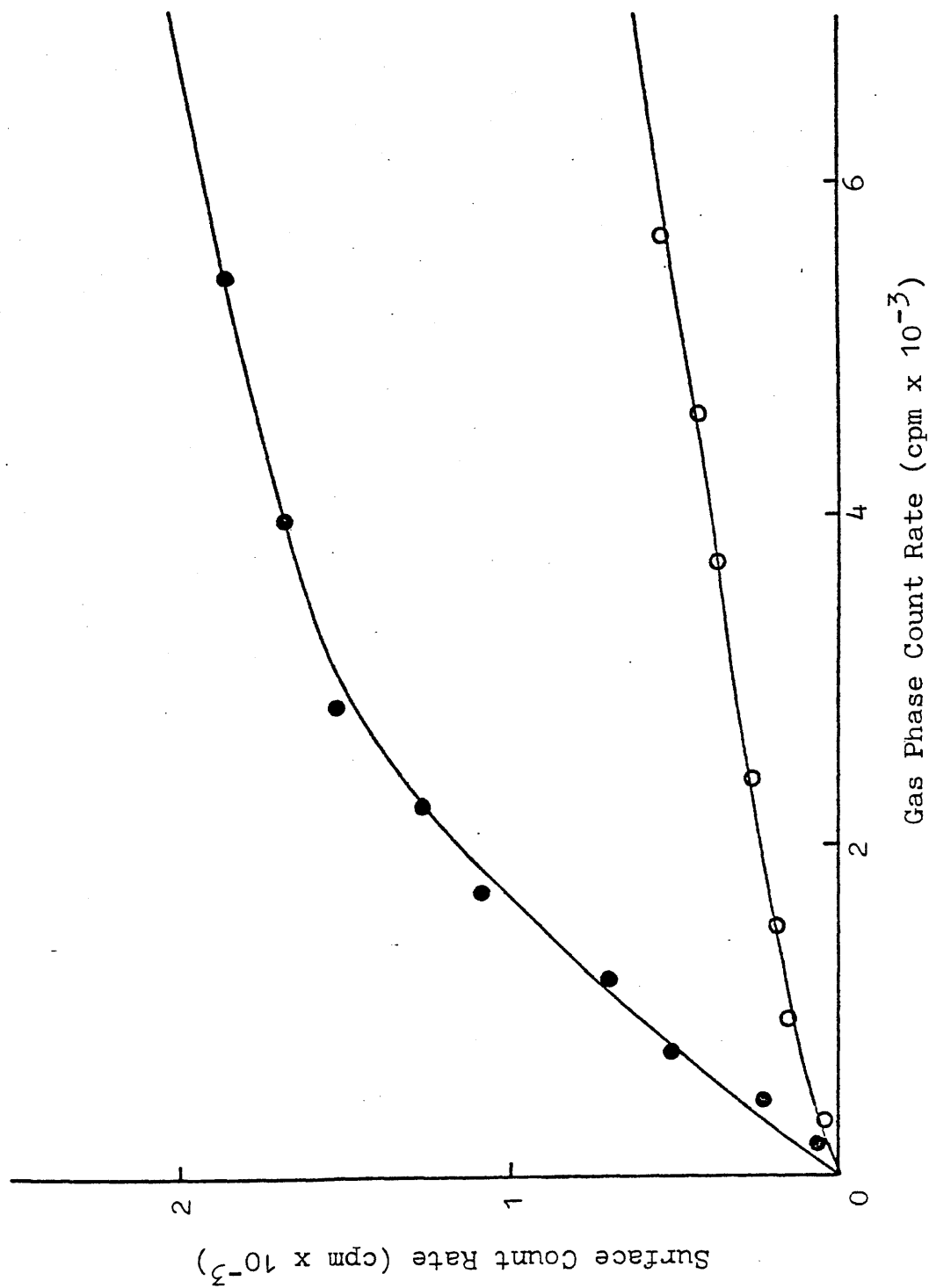


Figure 4.9 Adsorption of $[^{14}\text{C}]$ Ethylene on Freshly Reduced (●) and Steady State (○) Ni/SiO_2

[^{14}C]ethylene on a freshly reduced catalyst. Again the isotherm has primary and secondary regions, but the primary region is less steep than was found with [^{14}C]acetylene. The secondary region continued to increase linearly with increasing gas pressure although pressures in excess of 6 torr were used.

After evacuation for 15 minutes the surface count rate had decreased markedly but was still above background, indicating some degree of permanent retention. It was found that regenerating the catalyst in a stream of hydrogen at 500°C removed almost all of the surface radioactivity. Hence it was possible to test the reproducibility of the results.

4.4.2 [^{14}C]Ethylene Adsorption on Steady State Ni/SiO₂

The 0.082g sample of catalyst used in section 4.4.1 was regenerated in a stream of hydrogen at 500°C for 4 hours. A sufficient number of acetylene hydrogenation reactions were carried out to bring the catalyst to the steady state. A [^{14}C]ethylene isotherm was built up (figure 4.9). It was found that the amount of adsorption was substantially less than that observed on a freshly reduced catalyst.

4.5 The Acetylene Hydrogenation Reaction

4.5.1 Product Distribution on Steady State Catalysts

For 0.082g of catalyst, which had been 'run-in' to the steady state, samples were extracted and analysed several times during the reactions in order to follow the changes in product distribution throughout the reaction. A typical product distribution curve for a steady state catalyst is shown in figure 4.10. The results have been corrected for the small losses of material due to withdrawing samples for analysis. From figure 4.10 it can be seen that at approximately 125% conversion all of the acetylene had reacted. This point corresponded almost exactly with the acceleration point on the pressure fall against time curve (see, for example, figure 4.1). At conversions less than 125% the yields of ethane and ethylene increased almost linearly with % conversion. When all the acetylene had been consumed the ethylene yield decreased rapidly and simultaneously the ethane yield increased rapidly. In this second stage the ethane and ethylene yields did not change linearly with % conversion.

Comparison of analyses for a set of reactions at the steady state showed that the product distributions were similar for each reaction. Figure 4.10 corresponds to reaction 17 and figure 4.11 to reaction 40 on the same catalyst sample. Some butane was always observed in the late stages of reaction. At completion the butane yield constituted approximately 15% of the total product.

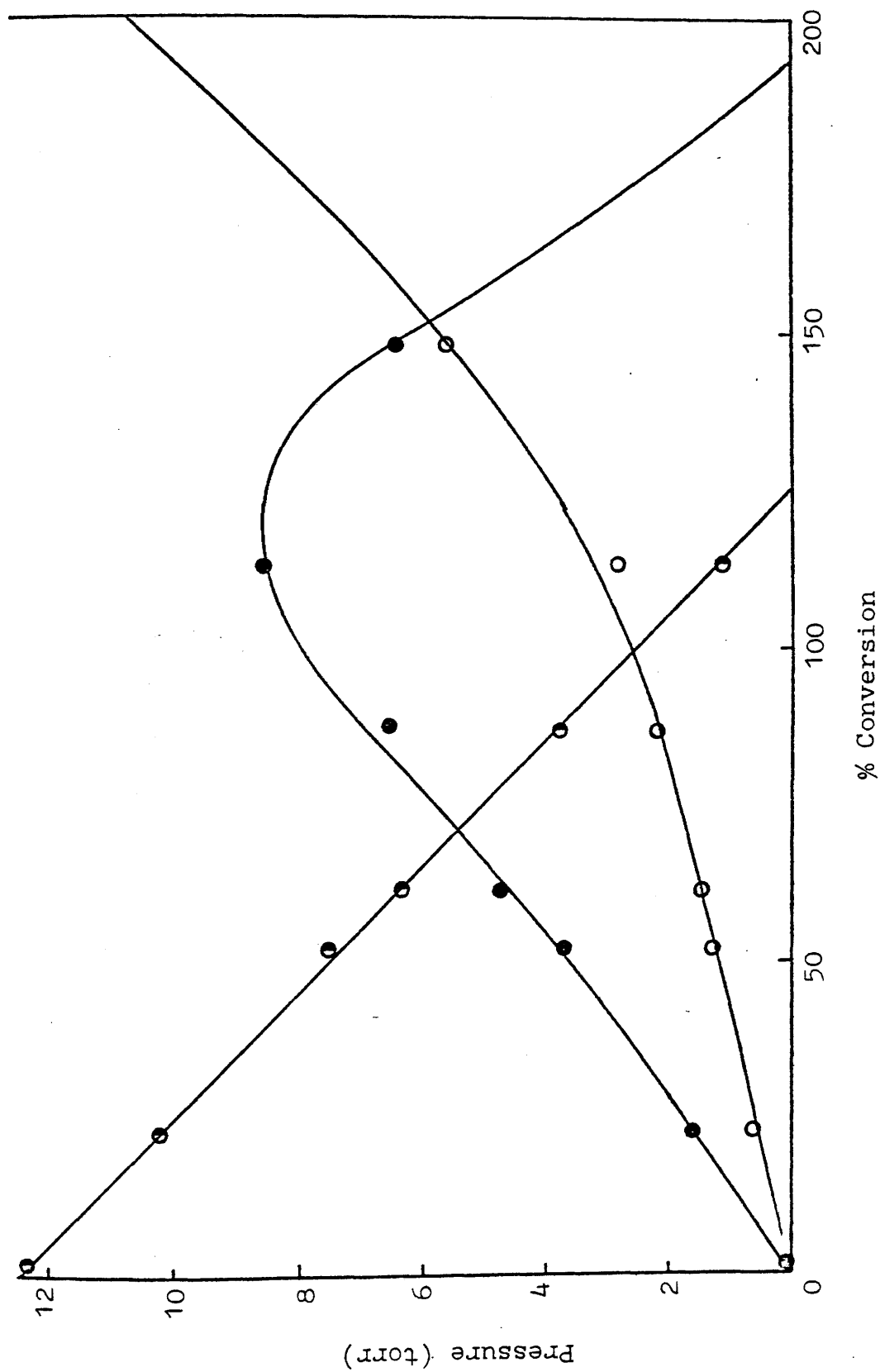


Figure 4.10 Product Distribution Curves for a Steady State Catalyst (Reaction 17).
(○ = Ethylene, ● = Acetylene, ○ = Acetylene)

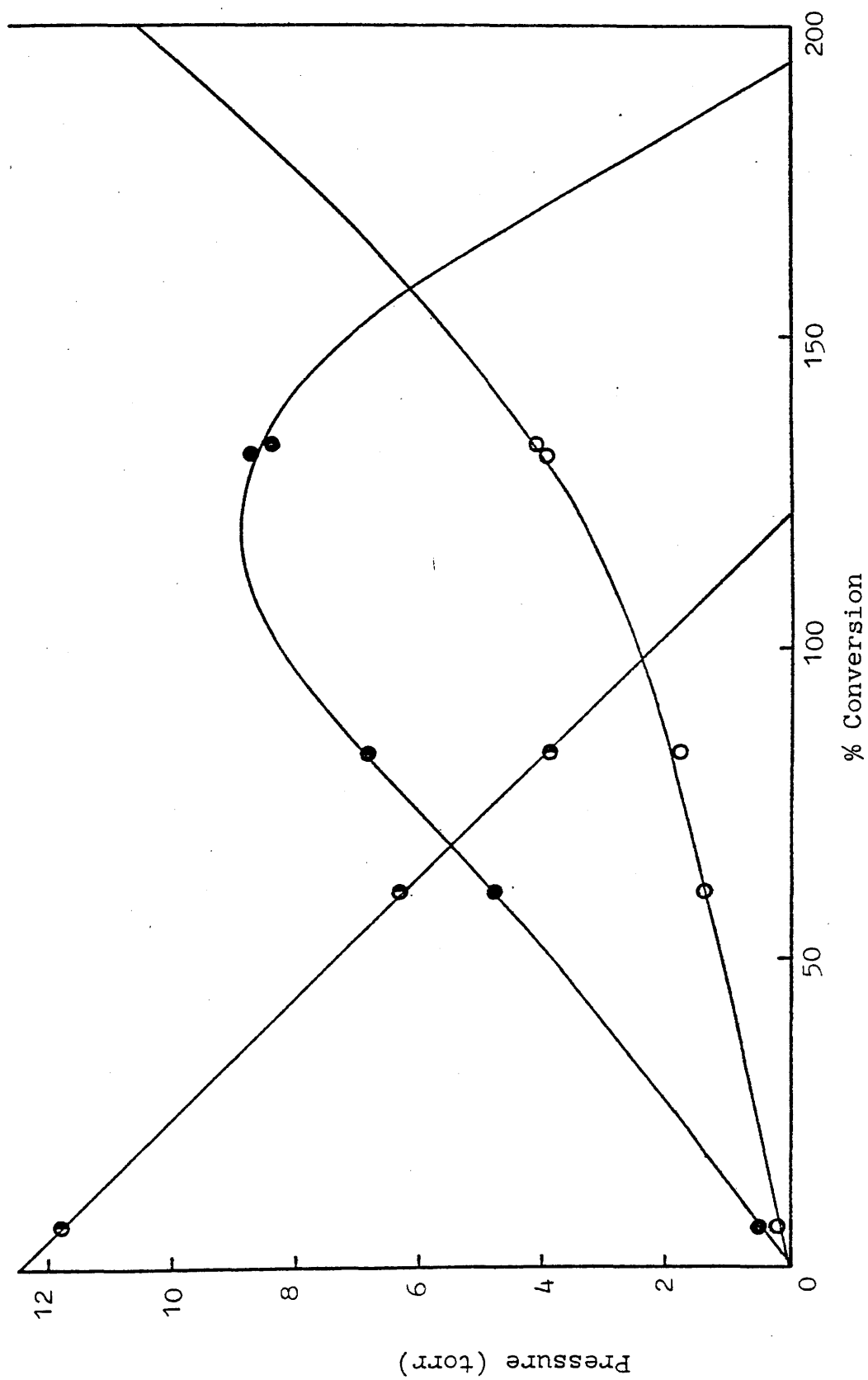


Figure 4.11 Product Distribution Curves for a Steady State Catalyst (Reaction 40)
 (○ = Ethane, ● = Ethylene, ○ = Acetylene)

4.5.2 Variation of Selectivity during a Steady State Reaction

The variation of selectivity with respect to conversion is shown in figures 4.12 and 4.13. The selectivity for ethylene was initially zero but increased rapidly to a value of 0.750 ± 0.02 at approximately 15% conversion. This value was maintained until all the acetylene had reacted. Comparison of figures 4.12 and 4.13 suggests that this behaviour was repeated throughout the steady state.

4.5.3 [^{14}C]Ethylene Tracer Studies of Acetylene Hydrogenation

The addition of small amounts of [^{14}C]ethylene to acetylene/hydrogen reaction mixtures provided a method whereby information could be obtained about possible reaction pathways. Thus it was possible to assess the amount of ethane formed directly from acetylene and the amount formed via a gas phase ethylene intermediate (section 1.3).

0.082g Ni/SiO₂ was reduced then brought to the steady state by performing 23 hydrogenation reactions at ambient temperature. A pre-mixed sample, containing 1 torr [^{14}C]ethylene (specific activity 1.31×10^{-2} mCi/mM), 12.5 torr acetylene and 37.5 torr hydrogen, was introduced to the reaction vessel. Samples were extracted at different stages of the reaction and analysed in the gas chromatography-proportional counter system. The total ethane, ethylene and acetylene yields and the [^{14}C]ethane and [^{14}C]ethylene yields were determined and, from these, the [^{12}C]hydrocarbon yields. The results, corrected for small losses of material due to

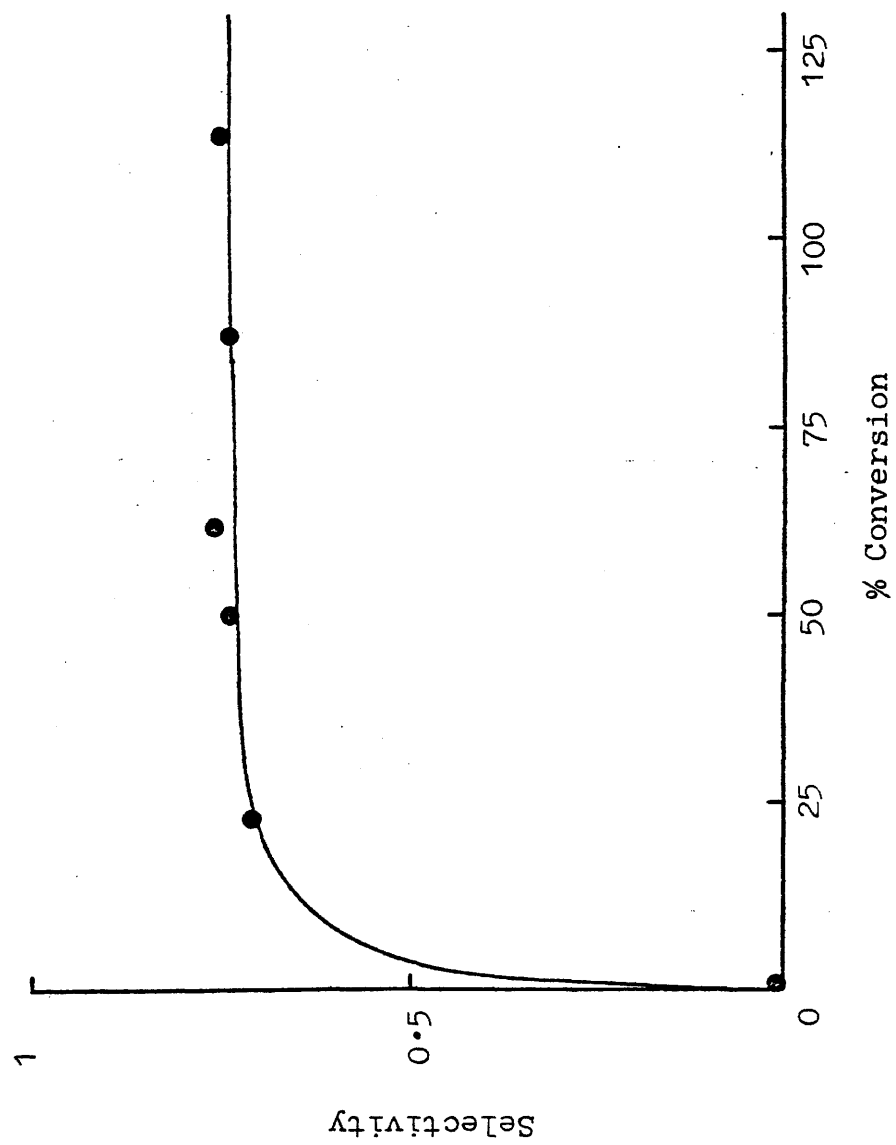


Figure 4.12 Selectivity versus % Conversion for a Steady State Catalyst (Reaction 17)

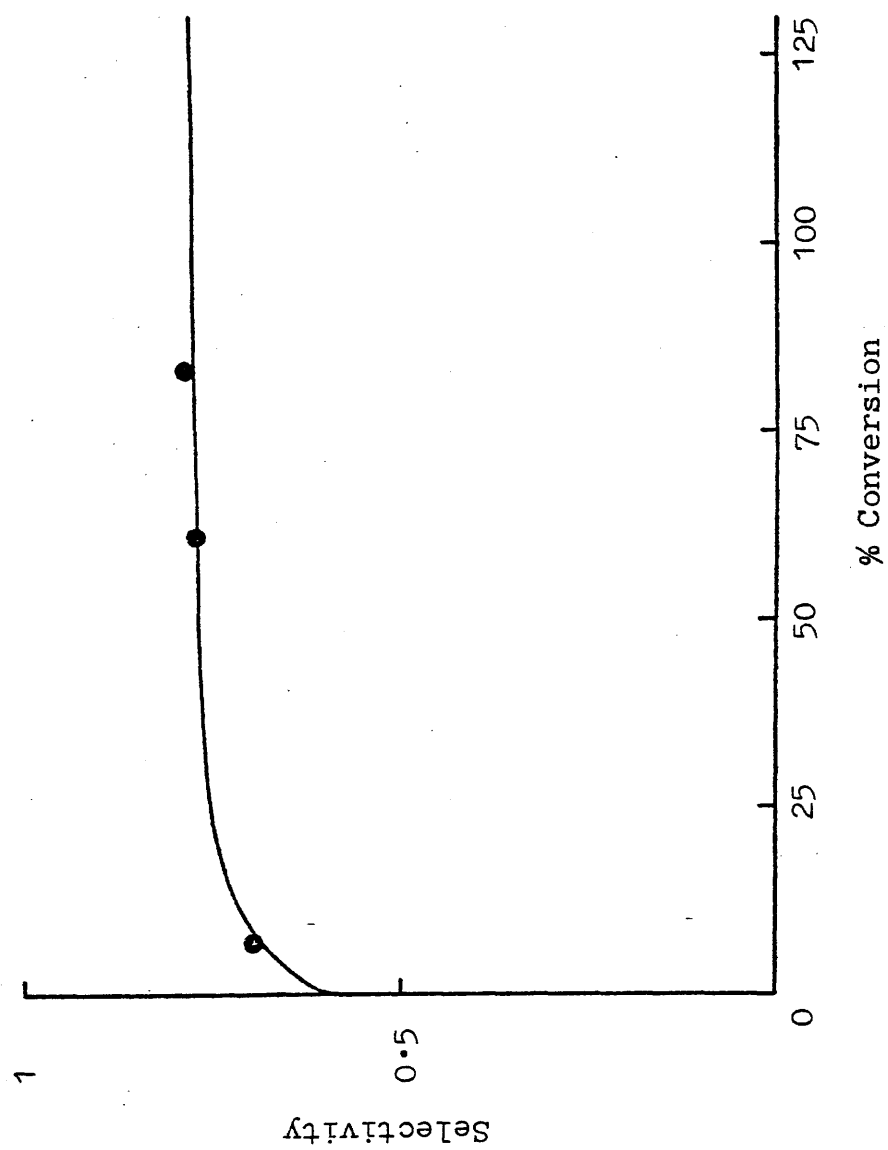


Figure 4.13 Selectivity versus % Conversion for a Steady State Catalyst (Reaction 40)

the withdrawal of samples for analysis, are shown in tables 4.4 and 4.5.

To the same steady state catalyst sample a pre-mixed sample, containing 2 torr [^{14}C]ethylene, 12.5 torr acetylene and 37.5 torr hydrogen, was introduced. Again, samples were analysed at various conversions. The results, corrected for small losses of material due to the withdrawal of samples for analysis, are shown in tables 4.6 and 4.7.

The procedure was repeated using a mixture containing 3 torr [^{14}C]ethylene, 12.5 torr acetylene and 37.5 torr hydrogen and the same catalyst sample. The results from this reaction are shown in tables 4.8 and 4.9.

Graphs of [^{12}C]hydrocarbon yields against conversion were drawn (figures 4.14 - 4.16). The general characteristics of these are similar to the results of hydrogenation experiments on steady state catalysts in the absence of [^{14}C]ethylene. A direct comparison can be made with figures 4.10 and 4.11, which are the product distribution curves for the same catalyst sample, before it was used for the added [^{14}C]ethylene experiments.

The results in tables 4.4 - 4.9 indicate that it is possible to hydrogenate [^{14}C]ethylene in the presence of acetylene. However, the reaction proceeds very slowly until all the acetylene has been consumed. At conversions less than approximately 125% the yield of [^{14}C]ethane increased almost linearly with hydrogen uptake (figures 4.17 - 4.19) indicating that the hydrogenation of [^{14}C]ethylene

Table 4.4

1 torr added [^{14}C]ethylene (0.0816g Ni/SiO₂)

% conversion	total C ₂ H ₆ (torr)	total C ₂ H ₄ (torr)	total C ₂ H ₂ (torr)	[^{14}C]C ₂ H ₆ (counts)	[^{14}C]C ₂ H ₄ (counts)
2.92	0.141	1.083	12.276	0	4580
11.14	0.345	1.711	11.444	41	4539
35.72	0.854	3.762	8.884	23	4557
42.39	0.998	4.309	8.193	27	4553
48.62	1.155	4.781	7.564	60	4520
70.05	1.653	6.480	5.367	137	4443
76.64	1.893	6.808	4.799	64	4516
110.03	2.710	9.363	1.427	133	4447
129.62	3.797	9.703	0	431	4149

Table 4.5

1 torr added [^{14}C]ethylene (0.0816g Ni/SiO₂)

% conversion	[^{14}C]C ₂ H ₆ (torr)	[^{14}C]C ₂ H ₄ (torr)	[^{12}C]C ₂ H ₆ (torr)	[^{12}C]C ₂ H ₄ (torr)	S	S'
2.92	0	1	0.141	0.083	0.371	0.371
11.14	0.009	0.991	0.336	0.720	0.682	0.686
35.72	0.005	0.995	0.849	2.767	0.765	0.768
42.39	0.006	0.994	0.992	3.315	0.770	0.773
48.62	0.013	0.987	1.142	3.794	0.769	0.777
70.05	0.030	0.970	1.623	5.510	0.772	0.791
76.64	0.014	0.986	1.879	5.822	0.756	0.764
110.03	0.029	0.971	2.681	8.392	0.758	0.775
129.62	0.094	0.906	3.703	8.797	0.704	0.759

Table 4.6

2 torr added [^{14}C]ethylene (0.0816g Ni/SiO₂)

% conversion	total C ₂ H ₆ (torr)	total C ₂ H ₄ (torr)	total C ₂ H ₂ (torr)	[^{14}C]C ₂ H ₆ (counts)	[^{14}C]C ₂ H ₄ (counts)
19.10	0.472	3.462	10.566	81	8919
27.03	0.616	4.178	9.706	126	8874
33.21	0.805	4.576	9.119	158	8843
59.91	1.316	6.914	6.270	257	8744
112.77	2.719	10.746	1.035	396	8604
117.56	2.955	10.904	0.641	536	8465
125.85	3.517	10.980	0.003	707	8294

Table 4.7

2 torr added [^{14}C]ethylene (0.0816g Ni/SiO₂)

% conversion	[^{14}C]C ₂ H ₆ (torr)	[^{14}C]C ₂ H ₄ (torr)	[^{12}C]C ₂ H ₆ (torr)	[^{12}C]C ₂ H ₄ (torr)	S	S'
19.10	0.018	1.982	0.454	1.480	0.765	0.770
27.03	0.028	1.972	0.588	2.206	0.790	0.798
33.21	0.035	1.965	0.770	2.611	0.772	0.783
59.91	0.057	1.943	1.259	4.971	0.798	0.817
112.77	0.088	1.912	2.631	8.834	0.771	0.799
117.56	0.119	1.881	2.836	9.023	0.761	0.799
125.85	0.157	1.843	3.360	9.137	0.731	0.780

Table 4.8

3 torr added [^{14}C]ethylene (0.0816g Ni/SiO₂)

% conversion	total C ₂ H ₆ (torr)	total C ₂ H ₄ (torr)	total C ₂ H ₂ (torr)	[^{14}C]C ₂ H ₆ (counts)	[^{14}C]C ₂ H ₄ (counts)
35.02	0.612	6.190	8.698	149	12268
42.72	0.848	6.692	7.960	199	12218
54.43	1.079	7.706	6.715	248	12167
67.22	1.352	8.761	5.387	261	12156
97.01	2.017	11.192	2.291	414	12003
103.17	2.055	11.913	1.532	526	11891
118.54	2.839	12.340	0.321	832	11585
138.00	5.426	10.074	0	2793	9619

Table 4.9

3 torr added $[^{14}\text{C}]$ ethylene (0.0816g Ni/SiO₂)

% conversion	$[^{14}\text{C}]\text{C}_2\text{H}_6$ (torr)	$[^{14}\text{C}]\text{C}_2\text{H}_4$ (torr)	$[^{12}\text{C}]\text{C}_2\text{H}_6$ (torr)	$[^{12}\text{C}]\text{C}_2\text{H}_4$ (torr)	S	S'
35.02	0.036	2.964	0.576	3.226	0.849	0.833
42.72	0.048	2.952	0.800	3.740	0.824	0.835
54.43	0.060	2.940	1.019	4.766	0.824	0.838
67.22	0.063	2.937	1.289	5.824	0.819	0.833
97.01	0.100	2.900	1.917	8.292	0.812	0.836
103.17	0.127	2.873	1.928	9.040	0.824	0.855
118.54	0.201	2.799	2.638	9.541	0.783	0.830
138.00	0.676	2.324	4.750	7.750	0.620	0.756

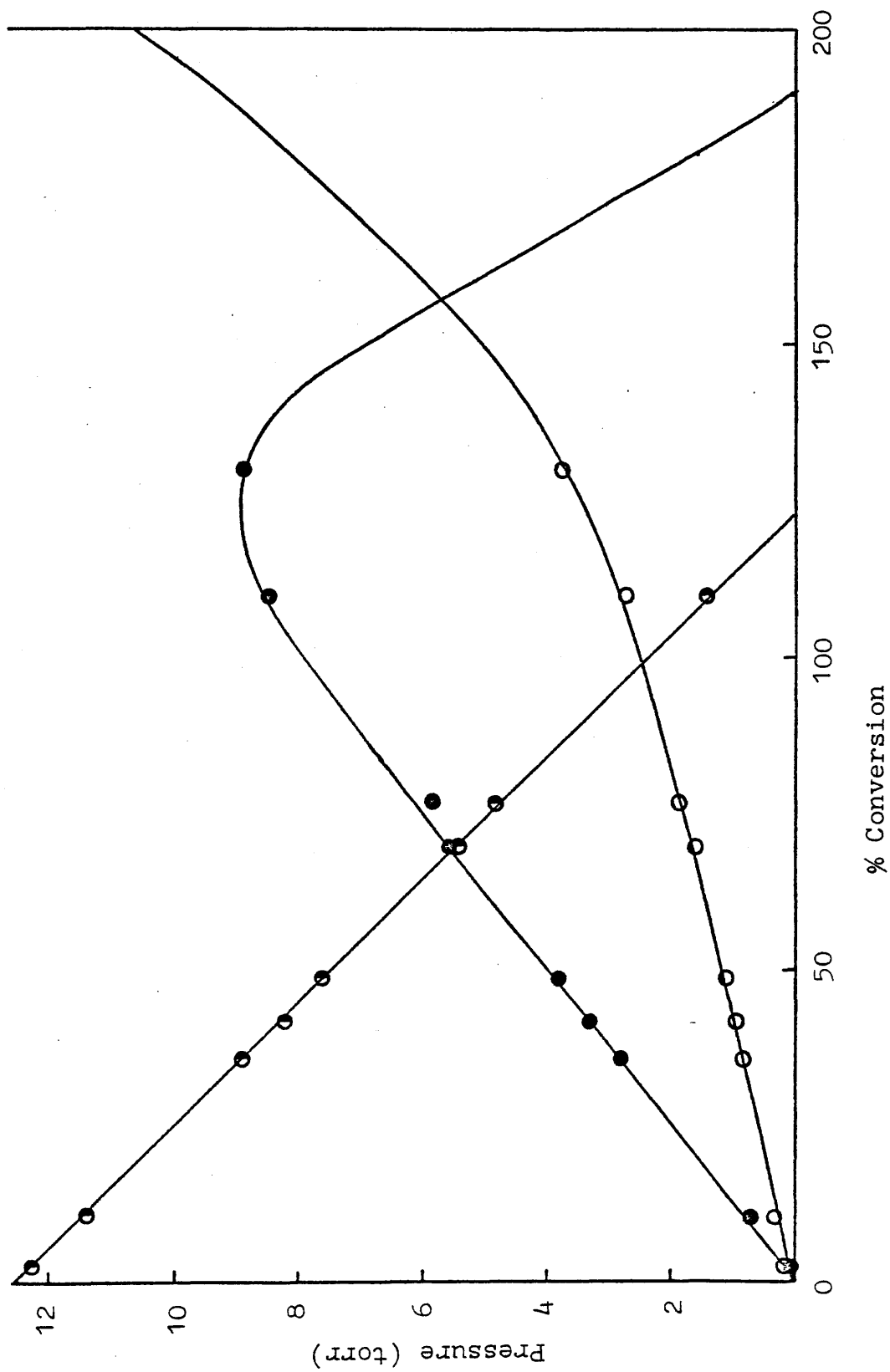


Figure 4.14 $[^{12}\text{C}]$ Product Distribution Curves - 1 torr added $[^{14}\text{C}]$ Ethylene Experiment
 (O = Ethane, ● = Ethylene, O = Acetylene)

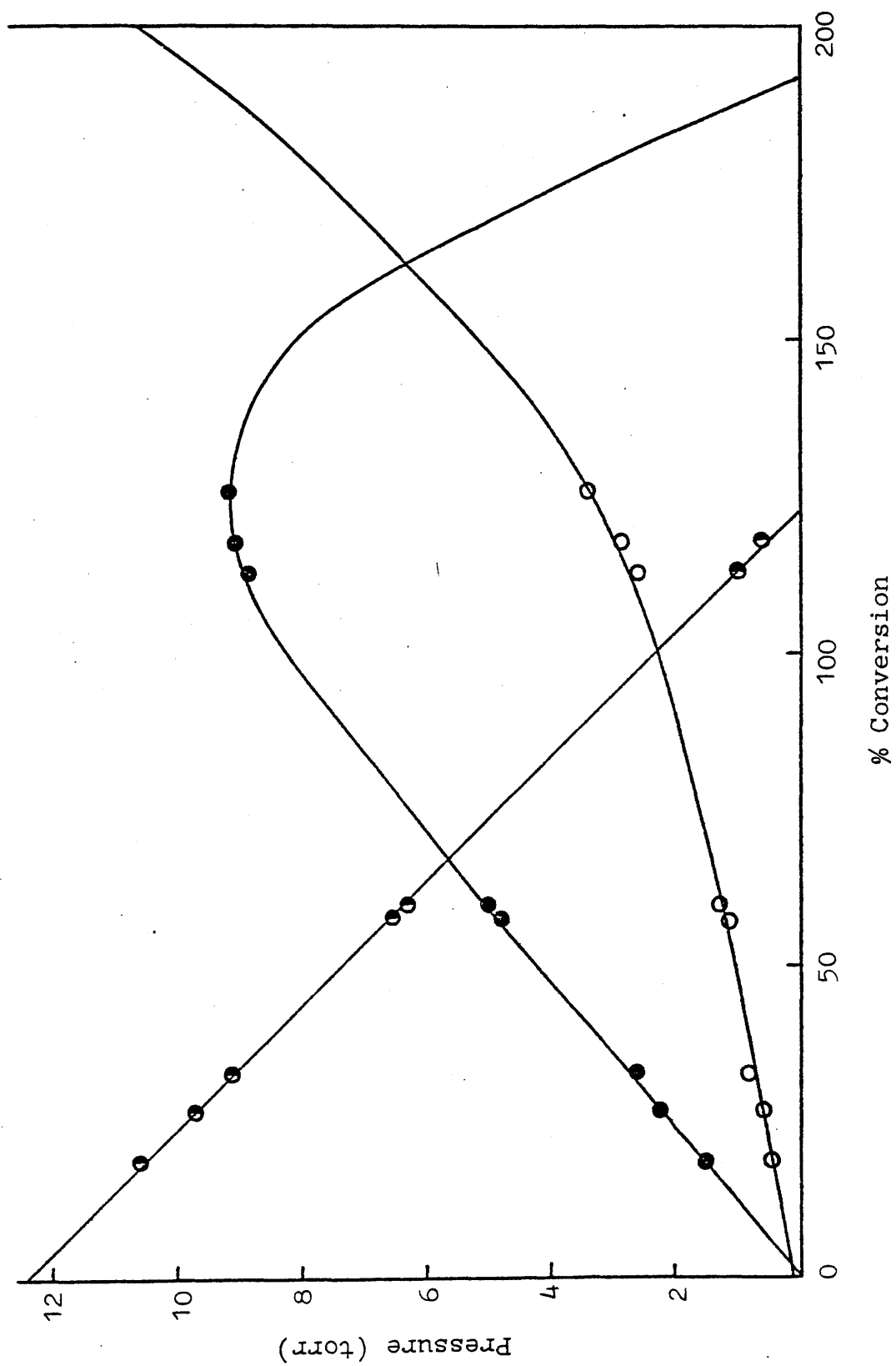


Figure 4.15 $[^{12}\text{C}]$ Product Distribution Curves - 2 torr added $[^{14}\text{C}]$ Ethylene Experiment
 (O = Ethane, ● = Ethylene, ○ = Acetylene)

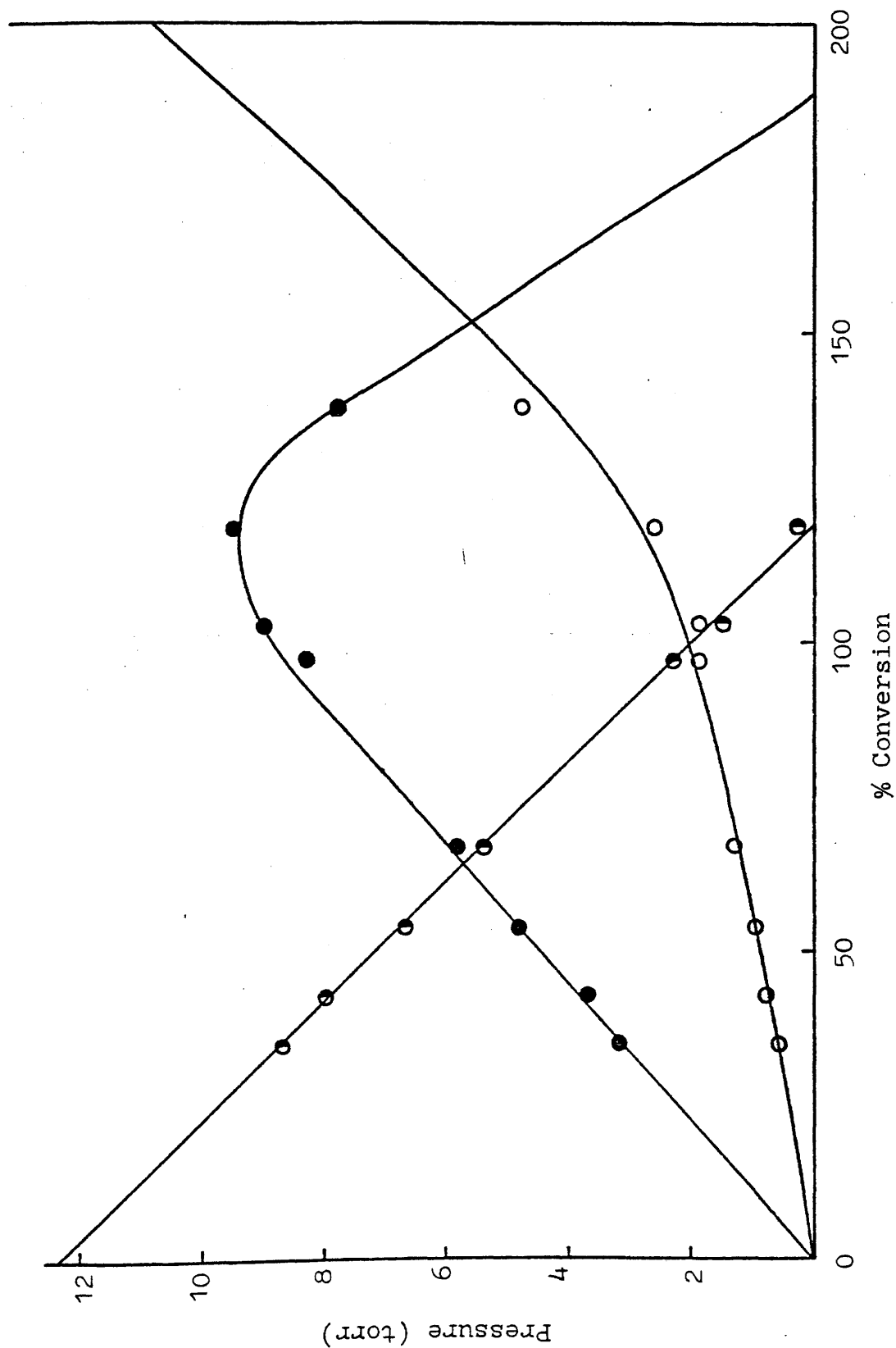


Figure 4.16 $[^{12}\text{C}]$ Product Distribution Curves - 3 torr added $[^{14}\text{C}]$ Ethylene Experiment
 (\circ = Ethane, \bullet = Ethylene, \circ = Acetylene)

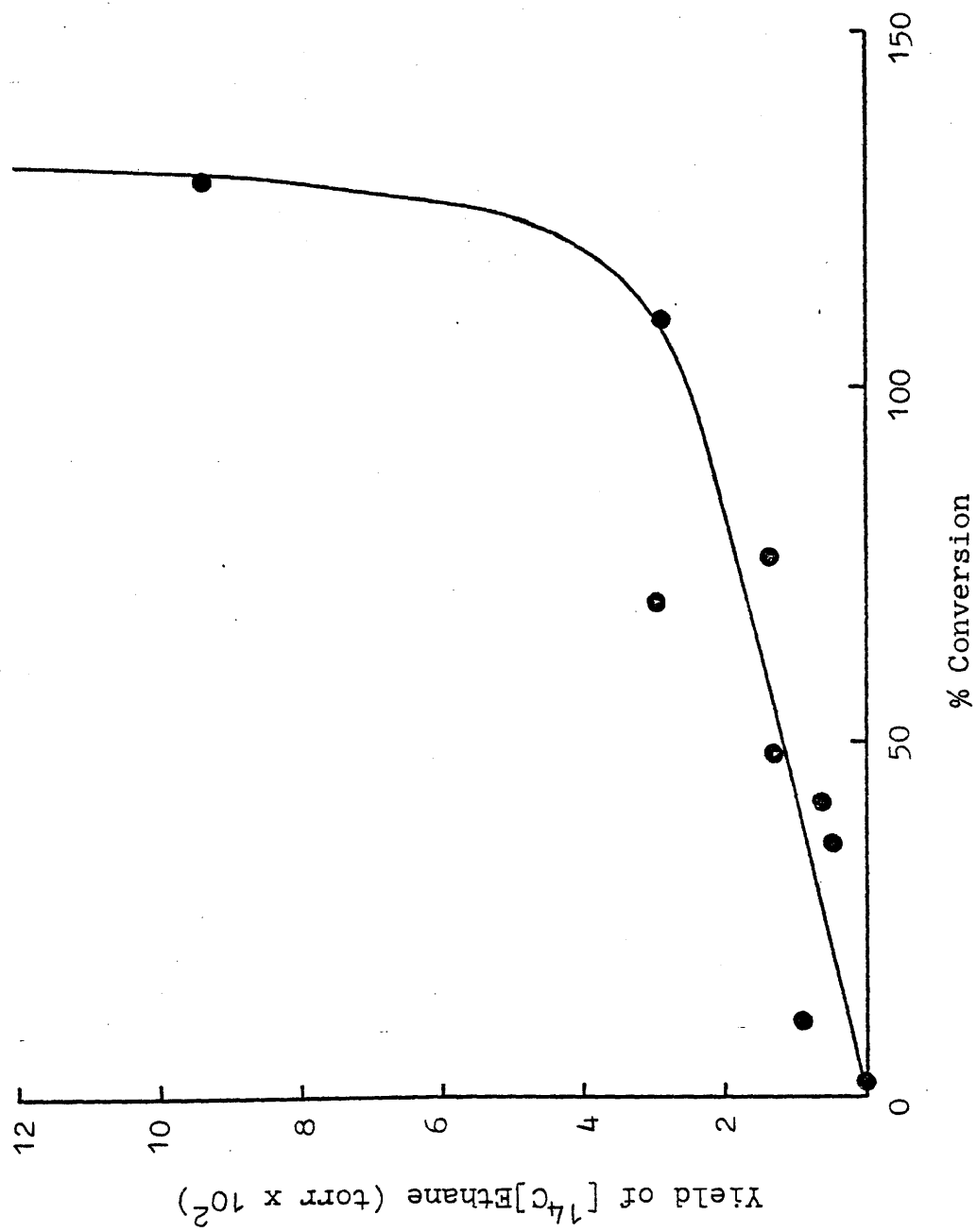


Figure 4.17 $[^{14}\text{C}]$ Ethane Yield versus % Conversion - 1 torr added $[^{14}\text{C}]$ Ethylene Experiment

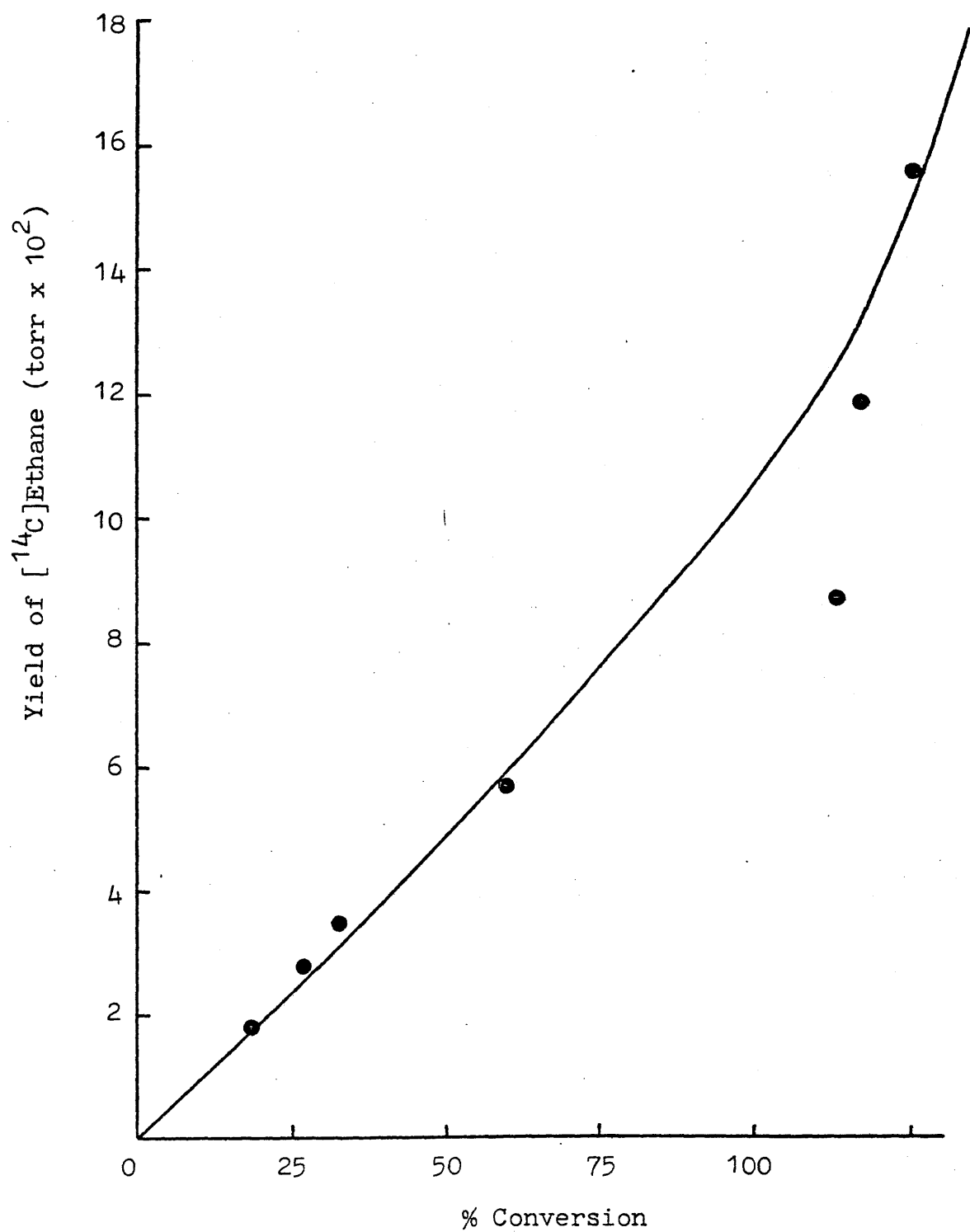


Figure 4.18 $[^{14}\text{C}]$ Ethane Yield versus % Conversion
- 2 torr added $[^{14}\text{C}]$ Ethylene Experiment

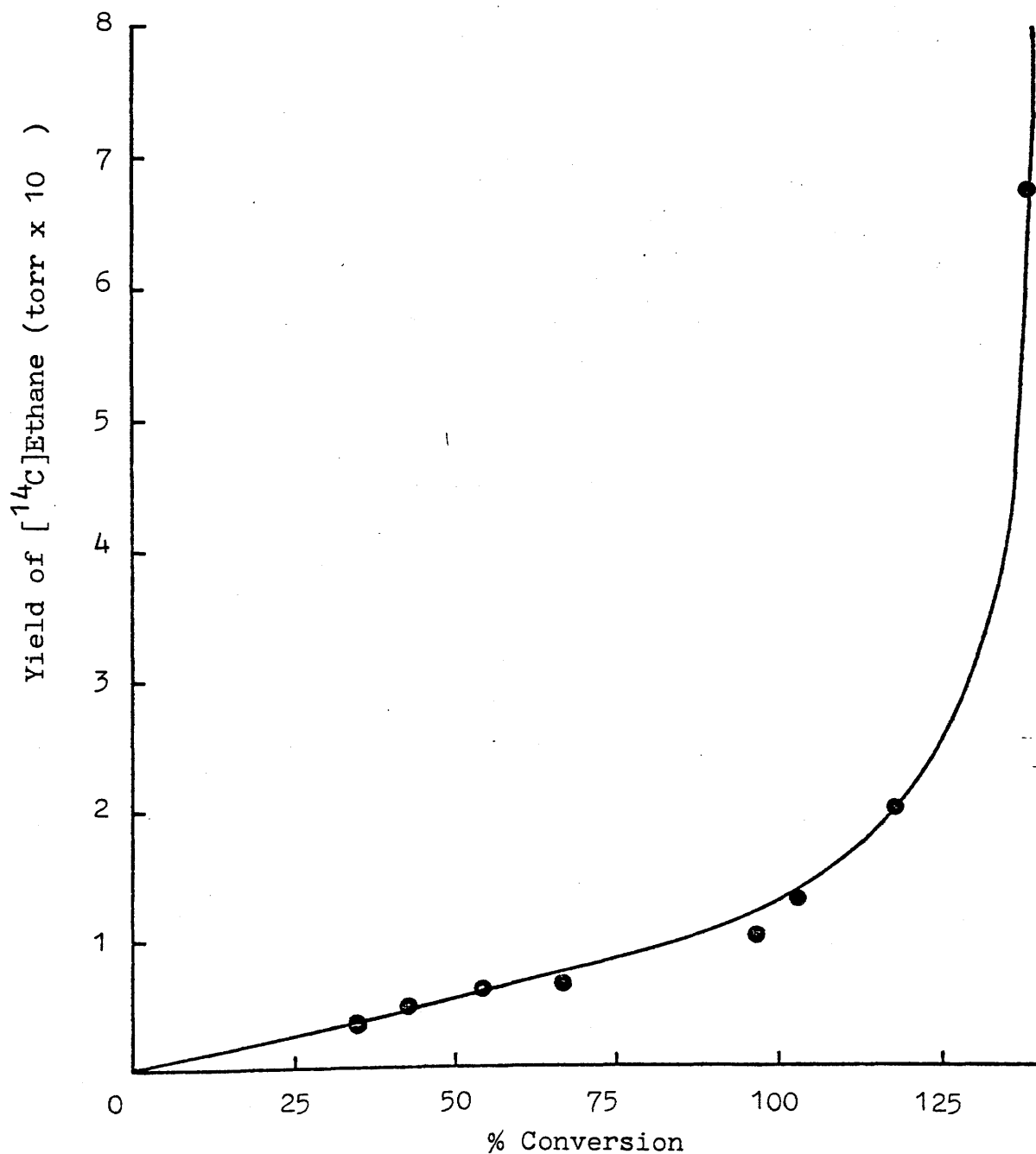


Figure 4.19 $[^{14}\text{C}]$ Ethane Yield versus % Conversion
- 3 torr added $[^{14}\text{C}]$ Ethylene Experiment

proceeded independently of the amount of acetylene in the reaction vessel. At the acceleration point, when all the acetylene had reacted, the $[^{14}\text{C}]$ ethane yield increased rapidly.

The yield of $[^{14}\text{C}]$ ethane only constituted a small, but constant, proportion of the total ethane yield at conversions less than those corresponding to the acceleration point (table 4.10). Extracting data for the $[^{14}\text{C}]$ ethane yields at 25%, 50% and 75% conversion from figures 4.17 - 4.19, it was possible to plot graphs of $[^{14}\text{C}]$ ethane yield against initial $[^{14}\text{C}]$ ethylene pressure (figure 4.20). The results indicate that the amount of $[^{14}\text{C}]$ ethane produced, at any particular conversion up to the acceleration point, was directly proportional to the initial pressure of $[^{14}\text{C}]$ ethylene.

Using the $[^{12}\text{C}]$ hydrocarbon data, the selectivity for ethylene was calculated and this is shown in tables 4.5, 4.7, and 4.9. In figures 4.21 - 4.23 selectivity is plotted against conversion. The selectivity was initially zero but increased rapidly to a constant value which was maintained up to approximately 125% conversion. This behaviour is similar to that observed in section 4.5.2 for hydrogenation reactions in the absence of $[^{14}\text{C}]$ ethylene.

It has been established above that the variation of $[^{14}\text{C}]$ ethane yield with conversion is approximately linear and that the amount of $[^{14}\text{C}]$ ethane produced at any particular conversion is directly proportional to the initial pressure of $[^{14}\text{C}]$ ethylene. Thus, since the gas phase $[^{12}\text{C}]$ ethylene,

Table 4.10

[¹⁴C]Ethane Yields

Initial [¹⁴ C]C ₂ H ₄ pressure (torr)	% conversion	$\frac{[^{14}\text{C}]\text{C}_2\text{H}_6}{(\text{C}_2\text{H}_6)_{\text{total}}}$
1	2.92	0
	11.14	0.026
	35.72	0.006
	42.39	0.006
	48.62	0.013
	70.05	0.018
	76.64	0.007
	110.03	0.011
2	19.10	0.038
	27.03	0.046
	33.21	0.044
	59.91	0.043
	112.77	0.032
	117.56	0.040
3	35.02	0.059
	42.72	0.057
	54.43	0.056
	67.22	0.047
	97.01	0.050
	103.17	0.062
	118.54	0.071

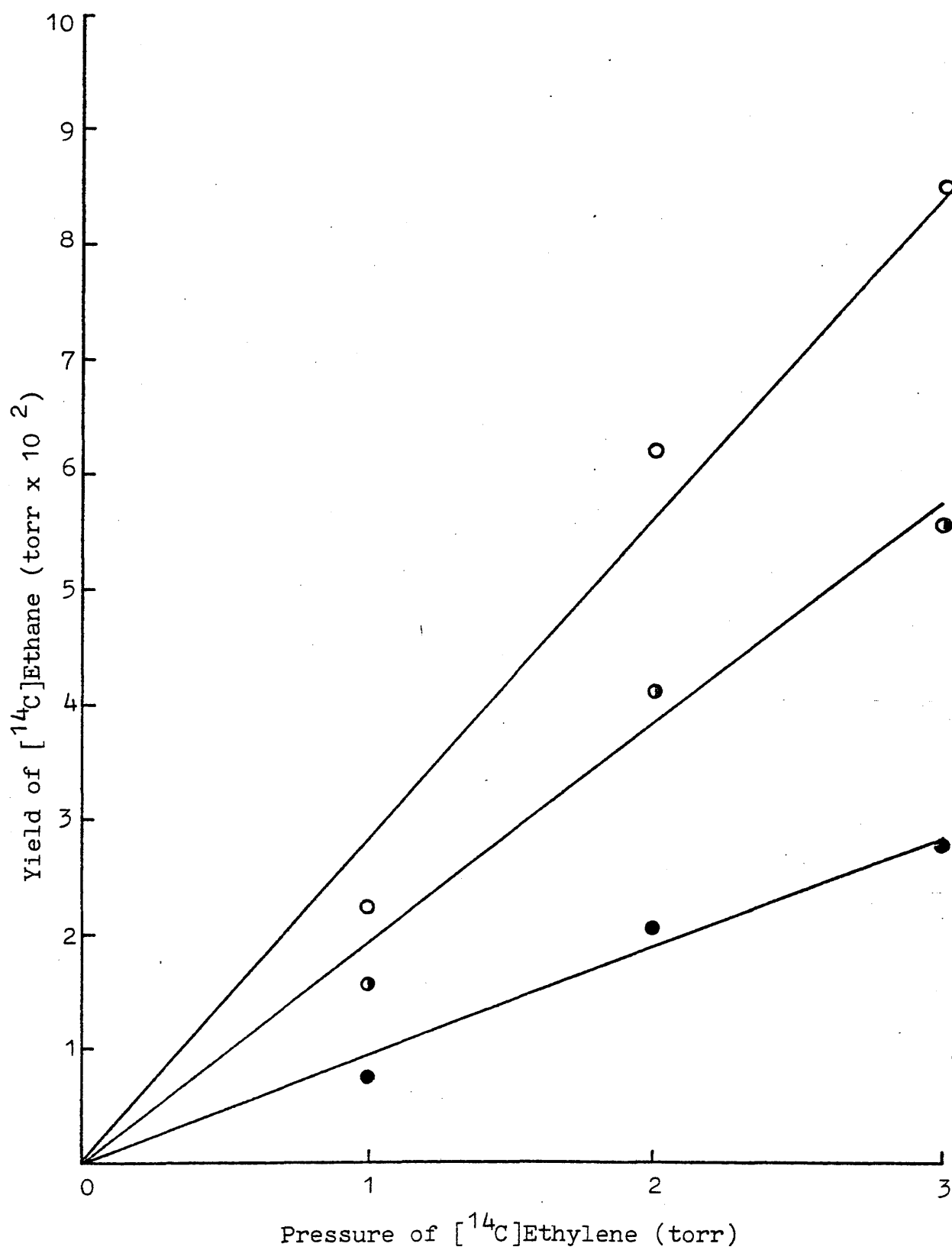


Figure 4.20 Variation of the Yield of $[^{14}\text{C}]$ Ethane with Pressure of added $[^{14}\text{C}]$ Ethylene at 25% (●), 50% (◐) and 75% Conversion (○).

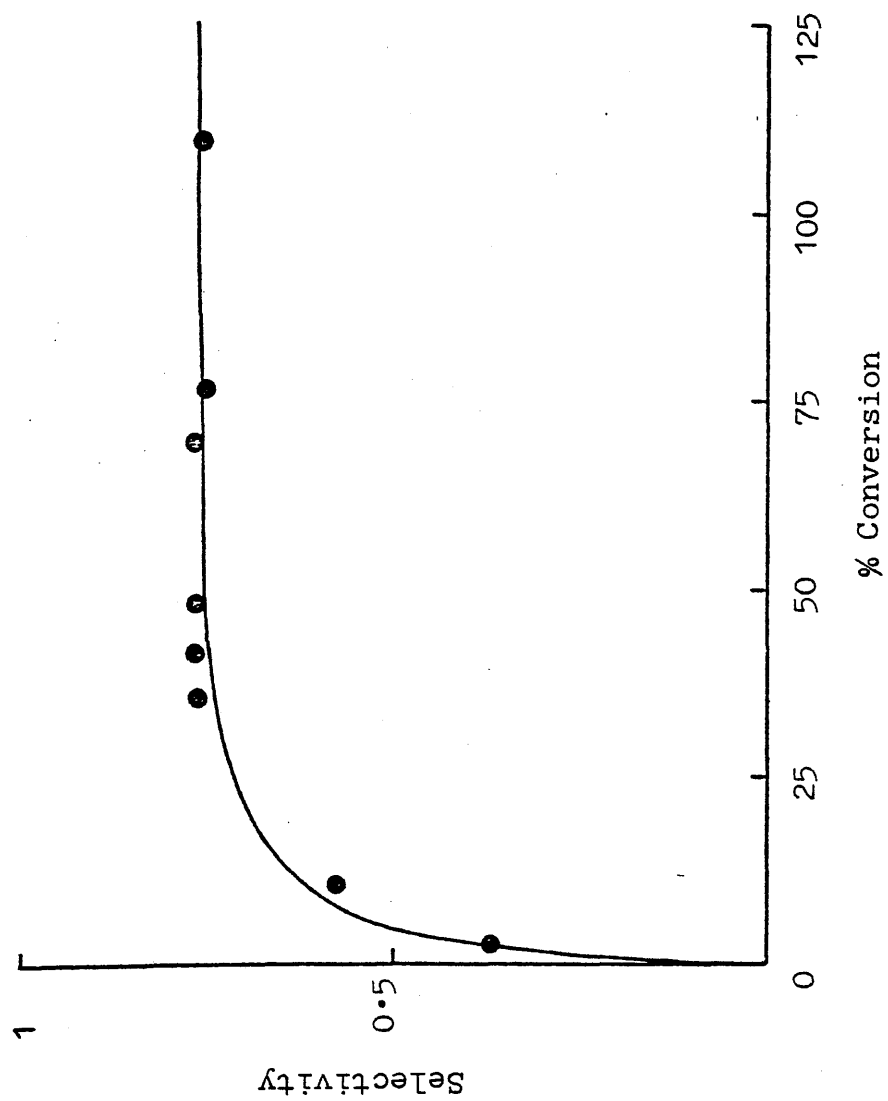


Figure 4.21 Selectivity versus % Conversion - 1 torr added [^{14}C]Ethylene Experiment

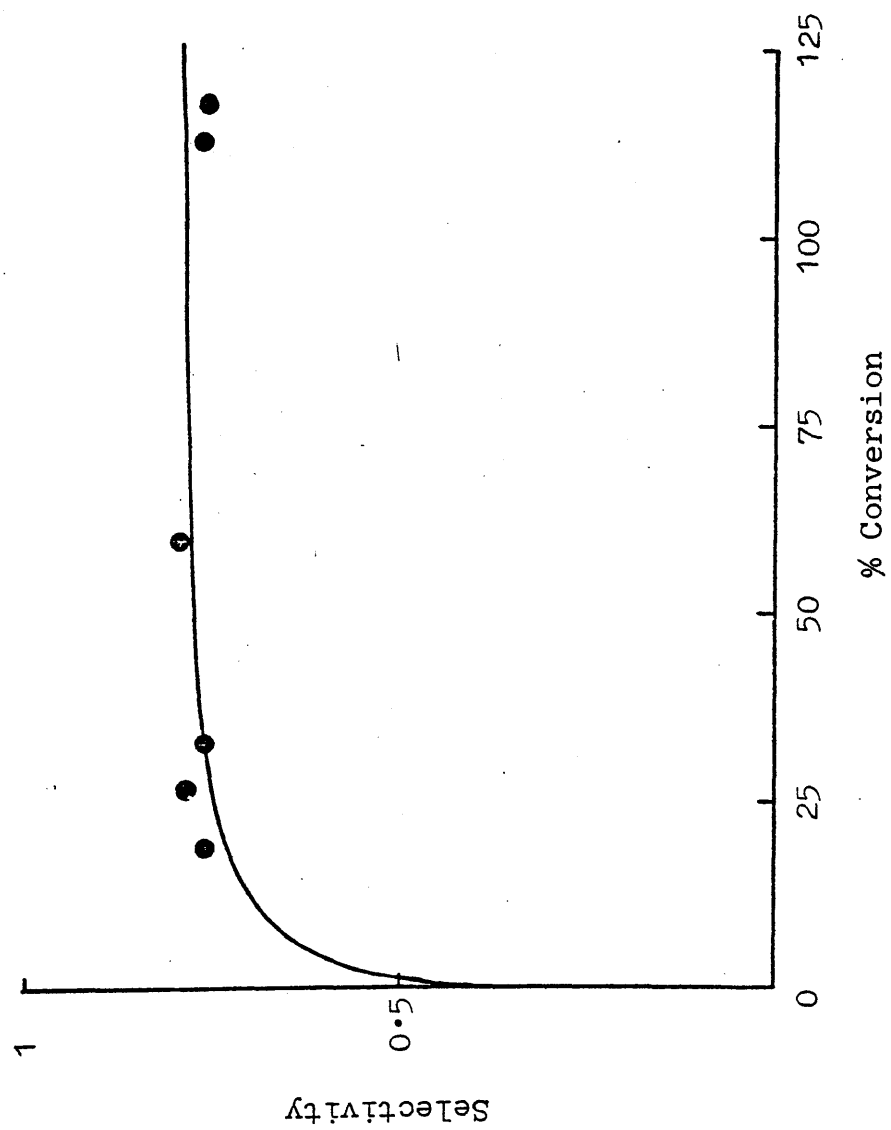


Figure 4.22 Selectivity versus % Conversion - 2 torr added $[^{14}\text{C}]$ Ethylene Experiment

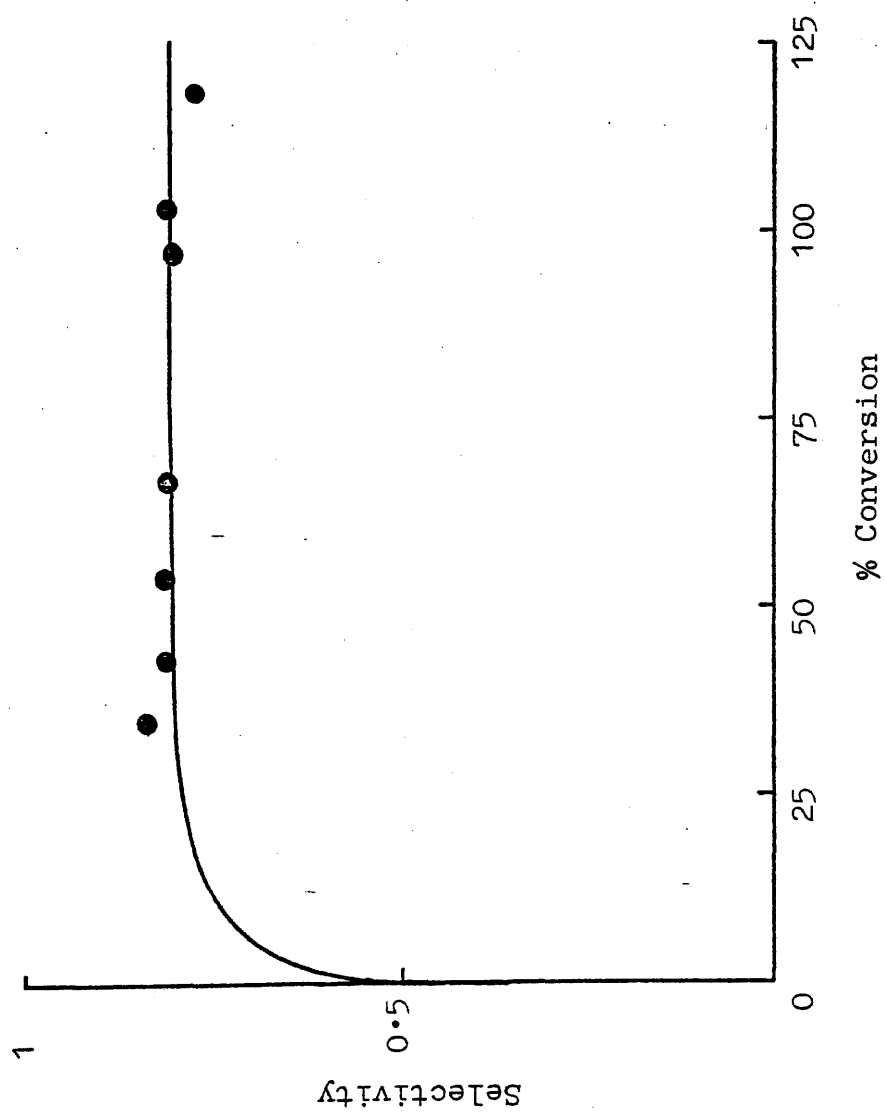


Figure 4.23 Selectivity versus % Conversion - 3 torr added $[^{14}\text{C}]$ Ethylene Experiment

produced by acetylene hydrogenation, is chemically indistinguishable from the added [^{14}C]ethylene, it is possible to calculate the yield of [^{12}C]ethane which is formed via a gas phase [^{12}C]ethylene intermediate. By subtraction, the amount of [^{12}C]ethane formed directly can be obtained. The results, shown in tables 4.11 - 4.13, indicate that the amount of ethane formed via a gas phase ethylene intermediate is small by comparison with the amount formed directly from acetylene.

From the results above it is possible to calculate the 'inherent' selectivity, S' , defined as:-

$$S' = \frac{P_{\text{C}_2\text{H}_4}}{P_{\text{C}_2\text{H}_4} + P_{\text{C}_2\text{H}_6}^*}$$

where $P_{\text{C}_2\text{H}_6}^*$ is the pressure of ethane produced directly. Values of S' are shown in tables 4.5 - 4.9. It can be seen that S' followed a similar pattern of behaviour to S , reaching a constant value at approximately 15% conversion. Also, the value of S' increased slightly as the initial pressure of added [^{14}C]ethylene was increased.

Table 4.11 1 torr added [^{14}C]ethylene

% conversion	($\text{P}_{\text{C}_2\text{H}_6}$) _{total} (torr)	($\text{P}_{\text{C}_2\text{H}_6}$) _{direct} (torr)
2.92	0.141	0.141
11.14	0.336	0.329
35.72	0.849	0.835
42.39	0.992	0.972
48.62	1.142	1.092
70.05	1.623	1.453
76.64	1.879	1.796
110.03	2.681	2.430

Table 4.12 2 torr added [^{14}C]ethylene

% conversion	($\text{P}_{\text{C}_2\text{H}_6}$) _{total} (torr)	($\text{P}_{\text{C}_2\text{H}_6}$) _{direct} (torr)
19.10	0.454	0.441
27.03	0.588	0.557
33.21	0.770	0.723
59.91	1.259	1.113
112.77	2.631	2.224
117.56	2.836	2.265

Table 4.13 3 torr added [^{14}C]ethylene

% conversion	($\text{P}_{\text{C}_2\text{H}_6}$) _{total} (torr)	($\text{P}_{\text{C}_2\text{H}_6}$) _{direct} (torr)
35.02	0.576	0.537
42.72	0.800	0.739
54.43	1.019	0.922
67.22	1.289	1.164
97.01	1.917	1.631
103.17	1.928	1.528
118.54	2.638	1.953

4.5.4 Permanent Retention of [^{14}C]Ethylene

During the experiments described in section 4.5.3 the build-up of permanently retained residues formed from [^{14}C]ethylene was monitored. The results are summarized in table 4.14.

Table 4.14 Retention of [^{14}C]Ethylene

Treatment	Surface Count Rate (cpm)
Exposure to 5 reaction mixtures each containing 1 torr [^{14}C] C_2H_4	109
Exposure to 5 reaction mixtures each containing 2 torr [^{14}C] C_2H_4	218
Exposure to 5 reaction mixtures each containing 3 torr [^{14}C] C_2H_4	321

It can be seen that the amount of permanent retention is small but that a proportion of each reaction mixture became permanently adsorbed. Similar effects were observed when [^{14}C]ethylene alone was admitted to the surface (section 4.4.1 and 4.4.2).

4.6 The Effect of Variation of Hydrogen Pressure on the Acetylene Hydrogenation Reaction

From the results in section 4.5 it can be deduced that the amount of [^{14}C]ethylene which can be hydrogenated in the presence of acetylene/hydrogen mixtures is very small. Previous studies using Rh/SiO₂, Ir/SiO₂, Pd/SiO₂ and Pd/Al₂O₃ (33, 38, 68, 72) have shown analogous behaviour both in this respect and also in the forms of adsorption isotherms on freshly reduced, deactivated and steady state catalysts. For these catalysts it was found that the amounts of [^{14}C]ethylene which can be adsorbed on the catalyst both in the presence and absence of acetylene (in the absence of hydrogen) are identical. Therefore the lack of ethylene hydrogenation, when added to acetylene/hydrogen reaction mixtures, cannot be explained in terms of adsorbed acetylene preventing the adsorption of ethylene. In an attempt to explain the observed phenomena, the other variable in the system, namely hydrogen, was considered. The initial pressure of hydrogen in the reaction mixture was varied and the effects of this on the various aspects of the reaction were examined.

4.6.1 Pressure Fall-Time Curves

A 0.082g sample of Ni/SiO₂ was reduced and brought to the steady state. Pre-mixed samples containing 1 torr [^{14}C]ethylene (specific activity 1.31×10^{-2} mCi/mM), 12.5

torr acetylene and various pressures of hydrogen were admitted to the reaction vessel. Hydrogen pressures of 20 torr, 37.5 torr, 60 torr and 100 torr were used in these experiments.

From figure 4.24 it can be seen that increasing the initial pressure of hydrogen increased the overall rate of reaction. All four reactions took place in two stages, the onset of the second stage being accompanied by an increase in rate. The pressure fall at which this acceleration took place did not appear to be related to the initial hydrogen pressure.

4.6.2 Product Distribution

For the reactions carried out in section 4.6.1, samples were analysed at various stages to obtain information about the effect of initial hydrogen pressure on product distribution. Figure 4.25 shows the yield of [^{12}C]ethane against conversion for each of the initial hydrogen pressures. As the initial pressure of hydrogen was increased the yield of ethane (at conversions up to the acceleration point) increased. A plot of [^{12}C]ethylene against conversion (figure 4.26) showed that the opposite effect was true for ethylene, that is, as the initial pressure of hydrogen was increased, the yield of ethylene decreased. The effect on acetylene removal is shown in figure 4.27. As the initial hydrogen pressure was increased the amount of acetylene consumed at any particular conversion was slightly

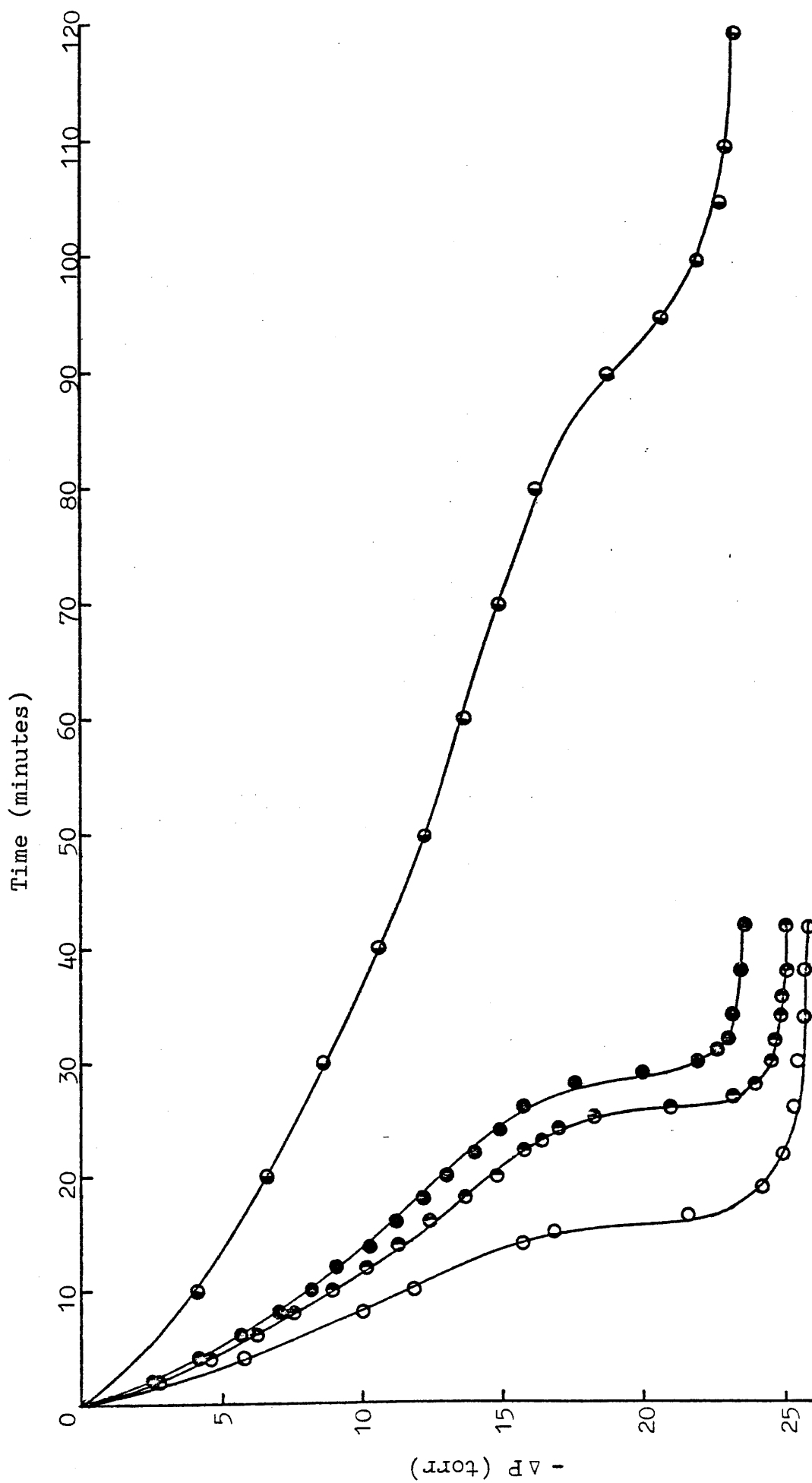


Figure 4.24 Pressure Fall - Time Curves

(Initial Pressure of Hydrogen 20 (○), 37.5 (●), 60 (●) and 100 (○) torr)

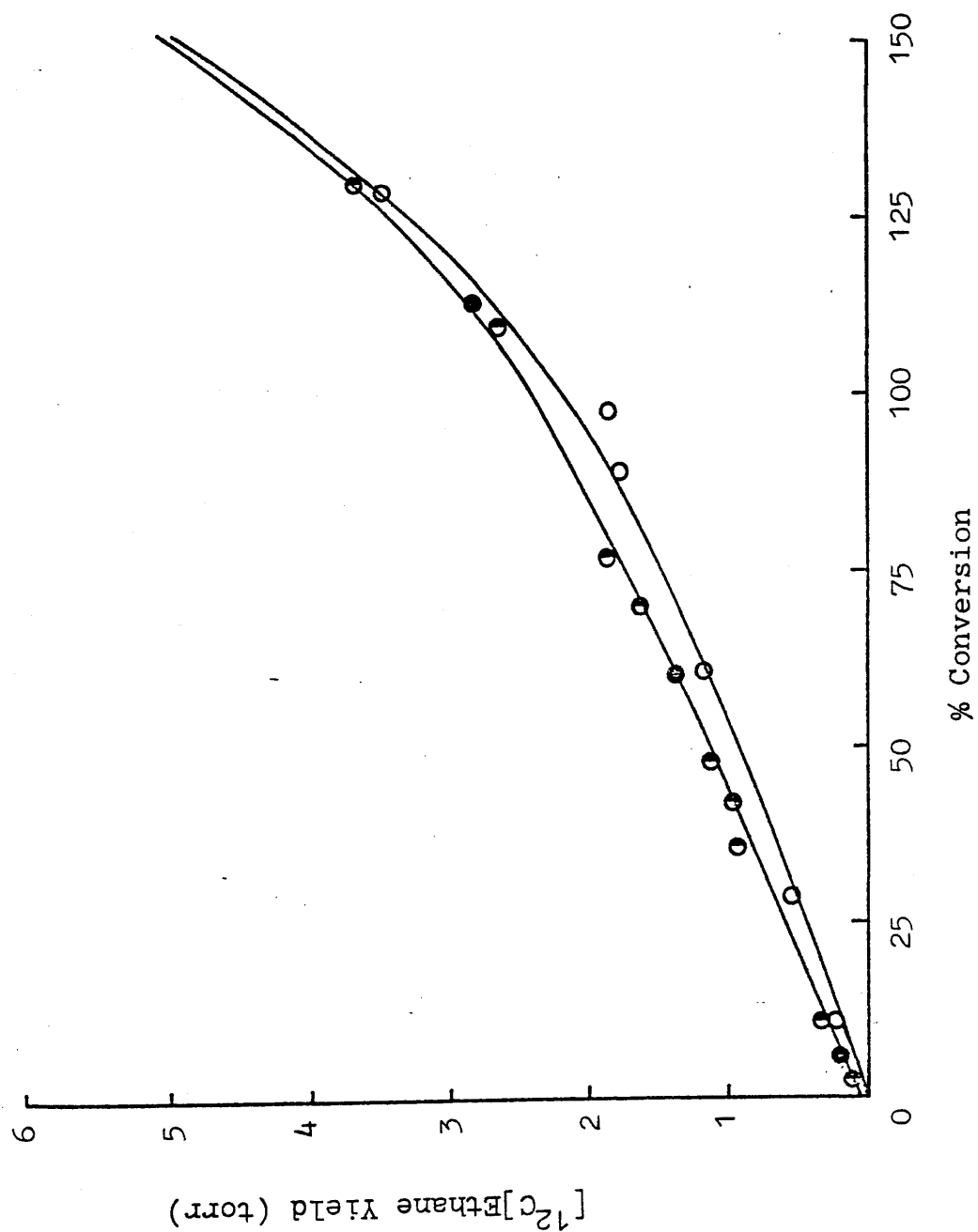


Figure 4.25 $[^{12}\text{C}]$ Ethane Yield versus % Conversion for Initial Hydrogen Pressures of 20 (○), 37.5 (◐) and 60 (●) torr.

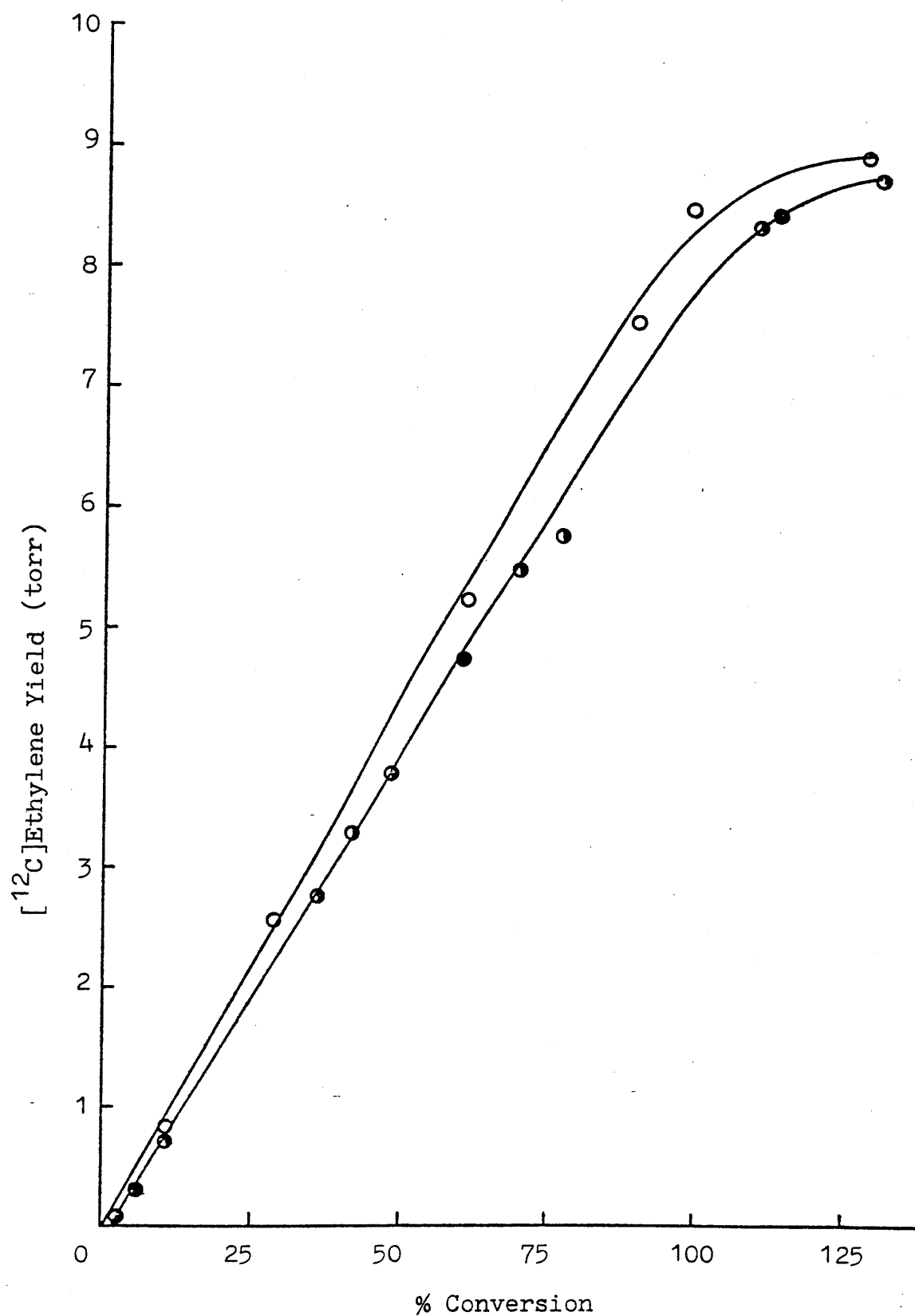


Figure 4.26 ^{12}C Ethylene Yield versus % Conversion for Initial Hydrogen Pressures of 20 (○), 37.5 (◐) and 60 (●) torr.

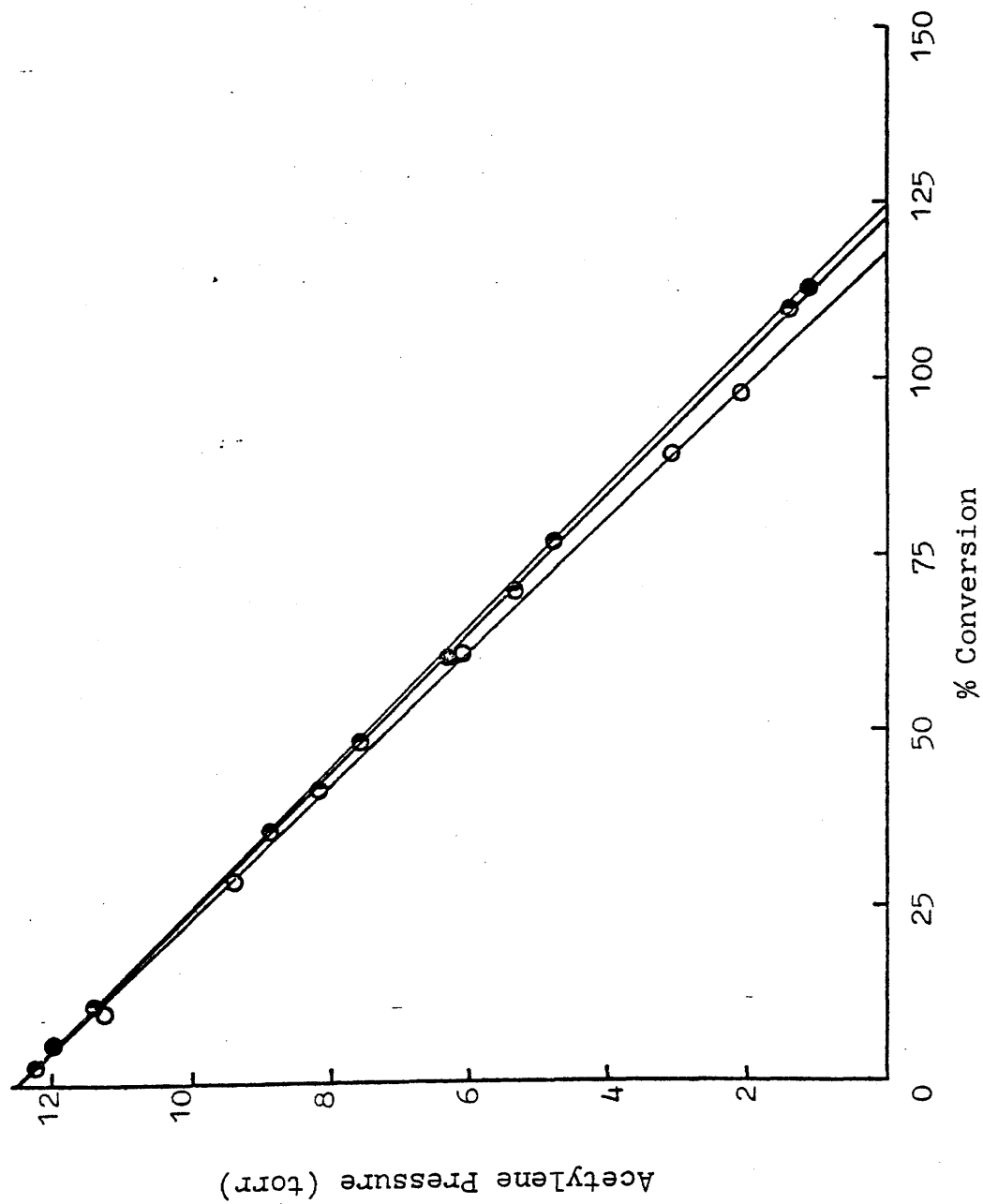


Figure 4.27 Acetylene Pressure versus % Conversion for Initial Hydrogen Pressures of 20 (○), 37.5 (●) and 60 (●) torr.

diminished. Also, as the initial hydrogen pressure was increased the value of conversion at which the acetylene concentration fell to zero was increased slightly. The effect was very small since, as has been stated above, the pressure fall at which acceleration took place was independent of initial hydrogen pressure. The variation of [^{14}C]ethane yield is shown in figure 4.28. The behaviour of [^{14}C]ethane was analogous to that of [^{12}C]ethane, that is, as the initial hydrogen pressure was increased the yield of [^{14}C]ethane increased.

4.6.3 Selectivity for Ethylene

For the product distributions given in section 4.6.2 selectivity values were calculated. These are shown in table 4.15. As in section 4.5.3, for all initial hydrogen pressures used, the selectivity was initially zero but increased rapidly to a constant value which was maintained up to approximately 125% conversion. When an initial hydrogen pressure of 20 torr was used the selectivity over the plateau region was approximately 0.83. However, when this was increased to 37.5 torr the selectivity fell to 0.78. The effect of further increasing the hydrogen pressure to 60 torr was much less apparent.

Using a similar method to that employed in section 4.5.3 it was possible to calculate the amount of [^{12}C]ethane which had been formed via a gas phase ethylene intermediate, and hence, by subtraction, the amount of [^{12}C]ethane formed

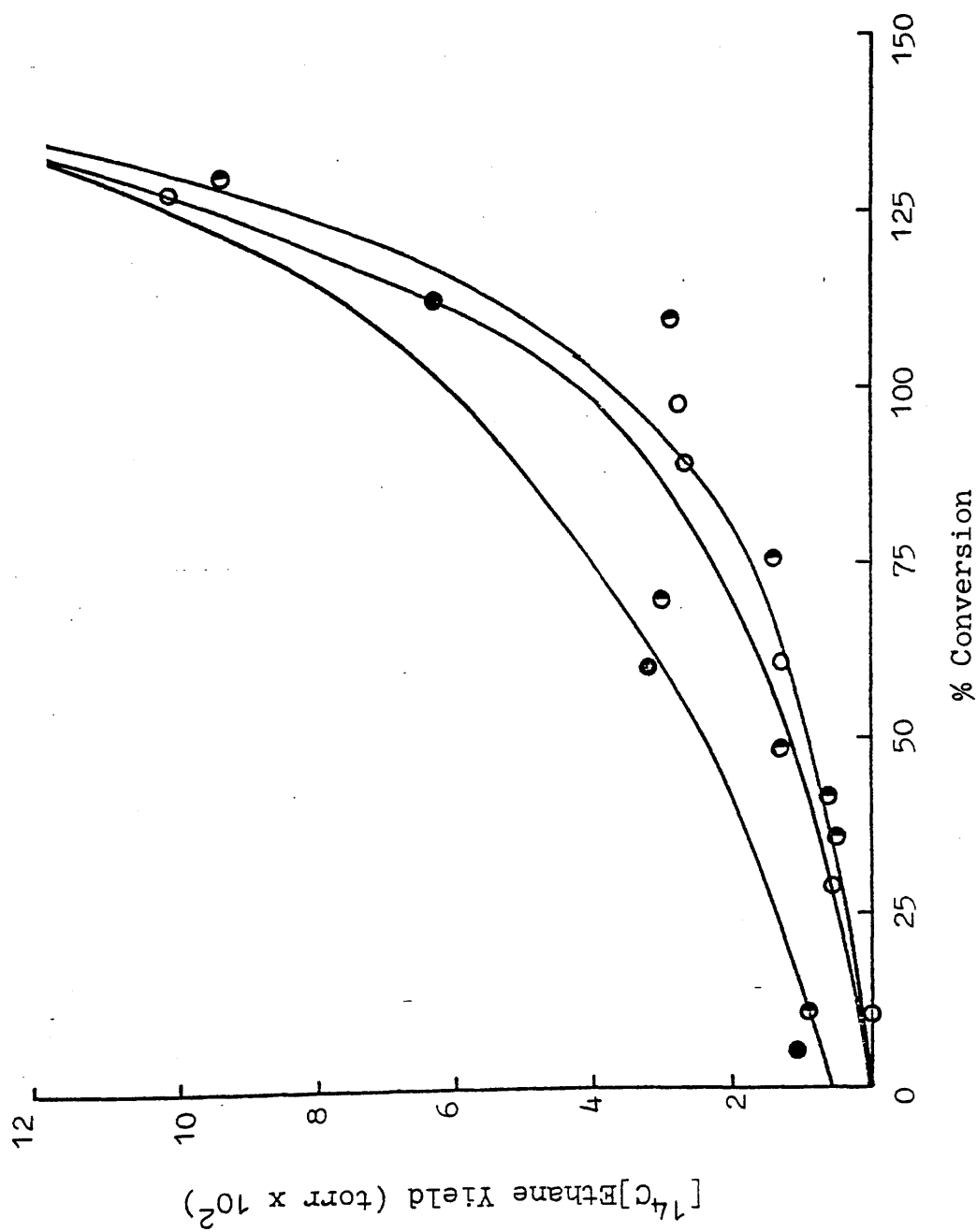


Figure 4.28 $[^{14}\text{C}]$ Ethane Yield versus % Conversion for Initial Hydrogen Pressures of 20 (○), 37.5 (◐) and 60 (●) torr.

Table 4.15 Effect of Initial Hydrogen Pressure on Selectivity

$(P_{H_2})_{\text{initial}}$ (torr)	% conversion	$(P_{[^{12}C]C_2H_6})_{\text{total}}$ (torr)	$(P_{[^{12}C]C_2H_6})_{\text{direct}}$ (torr)	S	S'
20	10.60	0.246	0.246	0.772	0.772
	28.66	0.539	0.524	0.823	0.827
	60.74	1.172	1.103	0.817	0.826
	89.49	1.786	1.575	0.810	0.829
	98.13	1.867	1.621	0.820	0.840
37.5	2.92	0.141	0.141	0.371	0.371
	11.14	0.336	0.329	0.682	0.686
	35.72	0.849	0.835	0.765	0.768
	48.62	1.142	1.092	0.769	0.777
	70.05	1.623	1.453	0.772	0.791
60	110.03	2.681	2.430	0.758	0.775
	5.71	0.199	0.195	0.614	0.618
	60.49	1.408	1.251	0.771	0.791
	113.44	2.838	2.257	0.750	0.790

directly from acetylene. The results show that, for all initial hydrogen pressures used, the amount of ethane formed via a gas phase ethylene intermediate is small by comparison with that formed directly from acetylene. From these results, values of the 'inherent' selectivity, S' , were calculated and these are also shown in table 4.15. As before (section 4.5.3) S' showed similar behaviour to S .

CHAPTER 5

5. DISCUSSION

5.1 Introduction

The research described in this thesis was undertaken to obtain information about the nature of the adsorbed species which are catalytically active in acetylene hydrogenation, the importance of permanently adsorbed hydrocarbon species, the effect of catalyst deactivation on the reaction kinetics and the relative importance of alternative reaction pathways during acetylene hydrogenation.

From the experiments described in Chapter 4 a number of interesting results have been obtained regarding the adsorption and subsequent hydrogenation of acetylene.

Under the reaction conditions used, the hydrogenation of acetylene took place in two stages, the onset of the second stage being accompanied by a sharp increase in rate. In a series of consecutive reactions the reaction rate progressively decreased from reaction to reaction until, after approximately 15 reactions, a constant 'steady state' activity was achieved. Deactivation had no effect on catalyst selectivity and could only be accomplished using acetylene/hydrogen mixtures.

The adsorption isotherms for acetylene showed two regions, a steep 'primary' region followed by a linear 'secondary' region. During catalyst deactivation the primary region progressively decreased. Deactivation had no effect on the secondary region. The adsorption isotherms for [^{14}C]ethylene

also showed primary and secondary regions but the primary region was less steep than that for acetylene. It was found that the species which are hydrogenated to give products, that is, the species involved in actual turnover during an acetylene hydrogenation reaction, are located on the secondary region.

In contrast, carbon monoxide adsorption showed typical Langmuir-type behaviour. Evacuation removed approximately 25% of the adsorbed carbon monoxide. After evacuation and treatment of the catalyst with an acetylene/hydrogen mixture it was possible not only to replace this 25%, but also to adsorb a further 10% of carbon monoxide.

The products of the acetylene hydrogenation reaction were ethane, ethylene and n-butane. At conversions less than 15% the sole product was ethane. From 15 - 125% conversion both ethane and ethylene were formed, ethylene being the major product. After the acceleration point, when all the acetylene had been consumed, the main process was the further hydrogenation of ethylene to ethane. Very late in the reaction n-butane was observed.

It was possible to hydrogenate [^{14}C]ethylene in the presence of acetylene but the reaction proceeded very slowly until all the acetylene had been consumed.

The amount of ethane formed via a gas phase ethylene intermediate was found to be small by comparison with the amount formed directly from acetylene.

Increasing the initial pressure of hydrogen in the

reaction mixture increased the overall rate of reaction. When the hydrogen pressure was increased from 20 torr to 37.5 torr a drop in selectivity for ethylene was observed. The effect on selectivity of further increasing the hydrogen pressure was much less apparent.

Pretreatment of the catalyst with carbon monoxide caused a partial reduction in the rate of hydrogenation of acetylene and caused an increase in the selectivity for ethylene.

These observations will be discussed in detail in the ensuing sections of the chapter.

5.2 Adsorption and Reactivity of Acetylene on Ni/SiO₂

It is generally considered that, before undergoing hydrogenation, acetylene is adsorbed on to the metal surface. The results of section 4.2.1 show that on a freshly reduced sample of catalyst the adsorption takes place in two distinct stages. During catalyst deactivation to a steady state activity, the primary region progressively decreases (sections 4.2.4 and 4.2.6). Similar results have been reported for [¹⁴C]acetylene adsorption on Rh/SiO₂, Ir/SiO₂, Pd/SiO₂ and Pd/Al₂O₃ catalysts (38). Since the surface count rates in each isotherm have been corrected for the background activity arising from permanently retained acetylenic residues, the observed decrease in the amount of primary adsorption is equivalent to an increase in the extent of permanent retention of species on the surface. The catalytic steady

state therefore corresponds to the attainment of a steady state concentration of strongly retained species.

Deactivation has no effect on the secondary region.

Analysis of the gas phase during the build-up of the primary region indicated that only [^{14}C]ethane was present. No ethylene or acetylene was detected. From the yields of [^{14}C]ethane it is possible to calculate the average composition of the adsorbed acetylenic species on the primary region. This is found to be $\text{C}_2\text{H}_{1.9}$, suggesting that a range of adsorbed species is present and that extensive dissociation of the C-H bonds has taken place.

In section 4.2.2 the reactivity of the acetylenic species adsorbed on the primary region of a freshly reduced catalyst was investigated. It was found that the primary adsorbed species do not desorb to give products and it would appear that the species involved in actual turnover during a hydrogenation reaction are located on the secondary region. During deactivation the extent of permanent retention on the surface increases and consequently the primary region of the [^{14}C]acetylene adsorption isotherm is observed to decrease progressively (section 4.2.4). Therefore, although the primary adsorbed species are not involved in turnover during a reaction, the rate of hydrogenation is nevertheless related to the extent of primary adsorption. The experiment described in section 4.2.2 provides no information about the fate of the hydrogen atoms of the primary adsorbed species. It is possible that these may play a part in the

hydrogenation reaction.

Comparison of the adsorption of [^{14}C]acetylene on a freshly reduced catalyst with that of [^{14}C]carbon monoxide on a similar catalyst sample has shown that the characteristics of the two isotherms are different. The adsorption of [^{14}C]carbon monoxide increases sharply with increasing pressure, and then reaches a steady value (section 4.3.1). The shape of the isotherm suggests that carbon monoxide reaches a saturation level which may be taken to correspond to the completion of a monolayer of adsorbed species. As was described in section 4.2.1, the adsorption isotherm for acetylene on a freshly reduced catalyst has a steep primary region followed by a linear secondary region. The gradient of the secondary region can be extrapolated to zero pressure. Using this value, the saturation value for the [^{14}C]carbon monoxide isotherm and the specific activities of the two gases the following relationship can be derived for the relative number of molecules of each gas:

$$[^{14}\text{C}]\text{CO} = 0.61 \times [^{14}\text{C}]\text{C}_2\text{H}_2 \dots\dots\dots (1).$$

As has been discussed in the introduction (section 1.3), carbon monoxide can adsorb as a linear, bridged or multi-centre species on nickel. Primet et al.(61) have investigated the adsorption of carbon monoxide on Ni/SiO_2 . They have obtained data to suggest that, at room temperature, the average bond number is 1.85. Assuming that at saturation every metal atom is involved in bonding, the average bond number gives the ratio of surface nickel atoms to CO

molecules. Using this information and equation (1) it can be calculated that acetylene secondary adsorption corresponds to coverage in excess of one monolayer. It is possible that secondary adsorption arises from the formation of overlayers on the primary adsorbed material (26).

After building up a [^{14}C]carbon monoxide isotherm, on a freshly reduced catalyst, evacuation of the reaction vessel for 35 minutes resulted in the removal of approximately 25% of the adsorbed species (section 4.3.1). The strengths of bonding of the carbon monoxide molecules to the nickel surface will depend on whether they are adsorbed as linear, bridged or multicentre species. Hence, some species will be more weakly bound and easily removed by, for example, evacuation.

Subsequent treatment with an acetylene/hydrogen mixture did not cause any further displacement of carbon monoxide. After this treatment it was found that a second [^{14}C]carbon monoxide isotherm could be built up. It had been expected that this would correspond to a replacement of the 25% which had been removed by evacuation. However, after such a surface had been saturated by carbon monoxide, the total surface count rate recorded indicated that it was possible to replace not only the lost 25%, but to add approximately a further 10% of carbon monoxide. Therefore there had been an overall increase of approximately 10% in the number of molecules of carbon monoxide which the surface was capable of adsorbing. Similar effects have been observed using allene/hydrogen

mixtures and a $\text{Rh}/\text{Al}_2\text{O}_3$ catalyst (73). Three possible reasons for this enhanced adsorption of carbon monoxide can be considered, (i) spillover of CO onto the support, (ii) enhanced adsorption of CO in the presence of hydrogen, or other species, and (iii) surface reconstruction on exposure to acetylene/hydrogen mixtures.

The effect of spillover of CO molecules onto the support is unlikely at room temperature. O'Neill and Yates(74) have reported that, for the Ni/SiO_2 system, the silica had little or no effect on the adsorption of carbon monoxide.

In studies of the co-adsorption of hydrogen and carbon monoxide considerable interaction of the two has been observed. A typical result of adding hydrogen to chemisorbed CO is a slight shift of the C-O stretching frequencies to longer wavelengths (43). This has been observed with rhodium and platinum (75), and with Ni/SiO_2 (76). Also, there are reports of enhanced adsorption of carbon monoxide in the presence of hydrogen. Using nickel films, Wedler et al.(77) have observed this effect to occur at 80°C but not at 0°C. Horgan and King(78) have reported enhanced adsorption at 27°C. From tritium tracer studies, using supported platinum catalysts, Altham and Webb(79) have found that the amount of hydrogen retained on the metal is small. Therefore, on this basis it is doubtful whether a hydrogen-carbon monoxide interaction could be responsible for the 10% increase in carbon monoxide adsorption observed in the present work.

An alternative explanation is that acetylene/hydrogen

mixtures, on contact with the catalyst surface, cause a perturbation of the metal atoms. It is suggested that the adsorption of acetylene results in a surface reconstruction with perhaps the migration of nickel atoms through adsorbed layers. The increase in adsorption of [^{14}C]carbon monoxide can then be explained since the surface, after treatment with acetylene/hydrogen mixtures, is a different surface from that obtained after reduction.

The amount of carbon monoxide which could be adsorbed on a catalyst in its steady state for acetylene hydrogenation was approximately 4% of the amount adsorbed at saturation on a similar weight of freshly reduced catalyst (section 4.3.2). The substantial reduction is due to the extensive coverage of a steady state catalyst by permanently retained acetylenic residues. If it is assumed that, on a freshly reduced catalyst, CO adsorbs in such a way that at saturation every surface metal atom is involved in bonding, then, using the results of sections 4.3.1 and 4.3.2 it is possible to estimate the number of bare metal atoms on a steady state catalyst. For a freshly reduced catalyst 2060cpm from [^{14}C]CO were obtained at saturation. For the same catalyst sample in the steady state the saturation level was 80cpm. Hence at the steady state approximately 4% of the total surface metal atoms are still vacant and therefore available for carbon monoxide adsorption.

Considering the surface to be an assembly of metal atoms on which 2-site random adsorption of acetylene molecules

takes place, then, for geometrical reasons, isolated metal atoms will remain vacant on the nickel surface. Statistics predict that, for a random 2-site adsorption, 7% of the metal atoms will remain vacant as single sites (80). This figure is rather higher than the 4% which was observed experimentally, suggesting that perhaps the 2-site adsorption model is not totally accurate.

The results presented in Chapter 4 and discussed above suggest that two types of adsorption take place when acetylene is admitted to a nickel surface, (a) dissociative adsorption to form $M-C_xH_y$ species of average composition $C_2H_{1.9}$ and (b) associative adsorption either by a carbon-carbon interaction with the dissociative species, or by a weak bonding with metal atoms in interstitial positions in the dissociatively adsorbed layer. Also the results of section 4.2.2 have shown that the species adsorbed on the secondary region are the ones involved in actual turnover during a hydrogenation reaction. It is suggested that hydrogenation takes place by hydrogen transfer between a dissociatively adsorbed hydrocarbon species and associatively adsorbed acetylene. Such a mechanism is consistent with that proposed by Thomson and Webb for the hydrogenation of unsaturated hydrocarbons (26).

The results of section 4.1.2 indicate that deactivation can only be achieved by treating the catalyst with acetylene/hydrogen mixtures. When acetylene alone was admitted to the catalyst no deactivation was observed. This suggests that

hydrogen is in some way responsible for the effect. Infrared studies of acetylene adsorption in the presence of hydrogen show that, with various supported metals, surface polymeric species are formed (37), although these species are absent when no hydrogen is present on the catalyst surface. This is further evidence to support the idea that the primary adsorption region consists of a range of polymeric species of which some may undergo further dissociation, some may be involved in surface polymerisation reactions and others may be active as hydrogen transfer species. The deactivation process observed in a series of consecutive reactions is a result of the progressive build-up of inactive surface polymers, thereby causing a loss of catalyst activity for acetylene hydrogenation. The steady state may be envisaged to correspond to the attainment of a steady concentration of active hydrogen transfer species.

Regeneration of the catalyst (as described in section 4.1.3) produced methane and ethane, methane being by far the major product. However, the observation of these products does not assist in the identification of surface species since, at temperatures greater than 250°C, nickel is a good catalyst for hydrocarbon cracking reactions (81). Hence surface polymers may well exist on the catalyst surface but, under regeneration conditions, these would undergo catalytic cracking and hydrogenation to form ethane and methane.

5.3 Reaction Pathways and Selectivity in the Acetylene Hydrogenation Reaction

The hydrogenation of 1:3 acetylene/hydrogen mixtures over Ni/SiO_2 always showed a sudden acceleration in the rate of reaction (sections 4.1.1 and 4.1.2). Catalyst deactivation appeared to have no effect on the pressure fall at which this acceleration took place. The first stage (up to the acceleration point) was found to be first order in total pressure with the exception of the first several minutes, where a deviation from first order behaviour was observed. Analysis of reaction products showed that during this short period ethane was the sole product. The reaction can therefore be considered to occur in three stages (i) the production of ethane from acetylene, (ii) the production of ethane and ethylene from acetylene, and the production of ethane from ethylene and (iii) the further hydrogenation of ethylene to ethane and the appearance of butane.

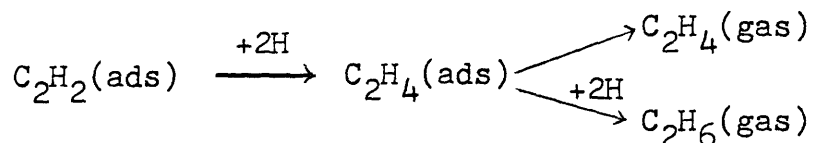
The selectivity for ethylene production was initially zero but increased rapidly to a steady value of 0.75 ± 0.02 at approximately 15% conversion. It would appear that the production of ethane and ethylene occur almost independently during the first order region of the reaction as suggested by the steady value for the selectivity and the almost linear increase of both the ethane and ethylene yield with increasing conversion. The initial production of ethane as sole product suggests that it is possible to form ethane without passing through a gas phase ethylene intermediate.

Bond et al. (17,18) have proposed that the appearance of ethane in the gas phase in the early stages of the reaction is evidence for the complete hydrogenation of some acetylene during one residence of the hydrocarbon unit on the surface. The results in section 4.5.3 show that not only is this possible but that the amount of ethane formed via a gas phase ethylene intermediate is small by comparison with the amount formed directly from acetylene. Such a conclusion has also been reached by Guczi et al. (53) who have studied the deuteration of mixtures containing 90% acetylene and 10% [^{14}C]ethylene using palladium black as catalyst. They have observed that although ethane becomes radioactive as the reaction proceeds the main route for ethane formation initially is the one directly from acetylene. These conclusions are in apparent contrast with the findings of McGown et al. (54), who have shown that most of the ethane produced by the hydrogenation of a mixture of acetylene and ethylene comes from the ethylene. However, these latter workers were investigating the hydrogenation of 2% acetylene in ethylene and in the present studies such conditions were only attained near the acceleration point in the reaction. From the results presented in section 4.5.3 and from the work of Guczi et al. (53) it can be concluded that the major factor governing selectivity in the acetylene hydrogenation reaction is the ability or otherwise of the metal to catalyse the direct hydrogenation of acetylene to ethane.

In a recent paper on the hydrogenation of acetylene over silica-supported rhodium, iridium and palladium, Al-Ammar and Webb(72) have proposed two mechanisms to explain the direct acetylene-ethane interconversion.

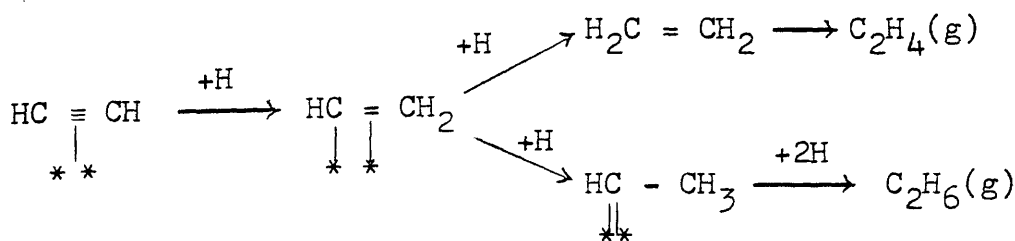
Mechanism 1

It is possible that the hydrogenation of acetylene gives rise to adsorbed ethylene, a constant fraction of which undergoes further hydrogenation rather than desorption as shown below:-



Mechanism 2

The direct route may involve the formation of an α, α -diadsorbed ethylene species, which cannot desorb but must undergo further hydrogenation, as shown below:-



Al-Ammar and Webb(72) conclude that three types of surface hydrogenation sites are present. Type I sites are active for the hydrogenation of acetylene to ethylene; type II sites are active for the direct conversion of acetylene to ethane, but inactive for ethylene hydrogenation; type III

sites are active for ethylene hydrogenation but inactive for acetylene hydrogenation.

In the present work ethylene is observed as the major product up to the acceleration point after which it is hydrogenated to ethane. Also, the main route from acetylene to ethane is via a direct route not involving a gas phase ethylene intermediate. These results are consistent with the existence of type I, type II and type III sites on Ni/SiO_2 catalysts.

The observed increase in selectivity when the catalyst was pretreated with carbon monoxide (section 4.3.3) may be explained in terms of adsorbed carbon monoxide changing the relative numbers of each of the above types of site. Similar proposals have been made by McGown et al. (54).

Carbon monoxide pretreatment resulted in an increase in catalyst selectivity but led to a deactivation of the catalyst in an absolute sense, the rate of production of ethylene falling to a lesser extent than the rate of ethane formation. It has been observed (72) that the presence of carbon monoxide has no effect on the acetylene adsorbed on the secondary region. Since the acetylene species undergoing hydrogenation are located on this region, it can be concluded that carbon monoxide is not a site-blocking agent for acetylene. Another important variable in the system is hydrogen. The surface metal atoms which are vacant on a steady state catalyst (section 4.3.2) may be the sites for the adsorption and activation of hydrogen. Pre-adsorption of

carbon monoxide would lead to a decrease in the number of these sites available to hydrogen and therefore to a decrease in the rate of hydrogenation.

It has been stated above that the major route to ethane does not involve a gas phase ethylene intermediate. However, after ethylene has been desorbed into the gas phase some can readsorb to form ethane as shown by the radiotracer experiments in section 4.5.3. The hydrogenation of [^{14}C]ethylene proceeds very slowly until almost all of the acetylene has been consumed. Thereafter, in the region of the acceleration point, the [^{14}C]ethane yield increases rapidly.

The yield of [^{14}C]ethane only constitutes a small, but constant, proportion of the total ethane yield at conversions which occur before the acceleration point. Also, the amount of [^{14}C]ethane produced, at any particular conversion up to the acceleration point, is directly proportional to the initial pressure of [^{14}C]ethylene. These observations may be used as evidence that the proportion of the total ethane yield formed via gas phase ethylene does not alter until all the acetylene has been consumed. Similar behaviour has been observed previously with Rh/SiO_2 and Pd/SiO_2 catalysts (72).

It has been shown, for Rh/SiO_2 and Pd/SiO_2 , that the amount of [^{14}C]ethylene which can be adsorbed on the catalyst is the same both in the presence and the absence of acetylene (38). During the added [^{14}C]ethylene experiments (section 4.5.3) the surface count-rate was monitored. It is known from this that [^{14}C]ethylene and acetylene adsorption occur

simultaneously during the reaction. At conversions less than approximately 125% the yield of [^{14}C]ethane increased almost linearly with conversion, indicating that the hydrogenation of [^{14}C]ethylene proceeded independently of the amount of acetylene in the reaction vessel. This is further evidence that there is no competition between ethylene and acetylene for surface sites under acetylene hydrogenation conditions on steady state catalysts.

The slow rate of hydrogenation of [^{14}C]ethylene cannot then be explained in terms of adsorbed acetylene preventing the adsorption of ethylene as suggested previously (17,18,20). There is another variable which must be considered, namely the hydrogen. The observations are consistent with an increase in the availability of hydrogen to ethylene once all the acetylene has reacted. Similar variations in hydrogen availability have been observed in the competitive hydrogenation of cycloalkenes over metal catalysts (82).

The idea of hydrogen availability was investigated by varying the initial hydrogen pressure in the reaction mixture (section 4.6). As the initial pressure of hydrogen was increased the overall rate of reaction increased. For all initial hydrogen pressures used, the selectivity for ethylene formation was initially zero but increased rapidly to a constant value. When the initial hydrogen pressure was 20 torr the selectivity reached a steady value of 0.83 ± 0.02 , whilst with a hydrogen pressure of 37.5 torr, the selectivity was 0.78 ± 0.02 . The effect of further increasing the

hydrogen pressure to 60 torr was much less apparent. The results suggest that when the hydrogen pressure is low the main process is the hydrogenation of acetylene to ethylene and hence the selectivity is high. In subsequent experiments using 37.5, 60 and 100 torr of hydrogen there was an excess of hydrogen over and above the amount required to hydrogenate completely all the initial acetylene to ethane and all the added [^{14}C]ethylene to [^{14}C]ethane. The closeness of the selectivity values therefore suggests that the amounts of acetylene following each possible reaction pathway were similar in each of these experiments. It can be concluded that when the system is hydrogen-deficient the favoured pathway is the hydrogenation of acetylene to ethylene, but when the initial hydrogen pressure is in excess reaction pathways leading to ethane are also possible.

5.4 Formation of n -Butane

Hydrogen availability may also be responsible for the very late appearance of butane in the gas phase. An unsaturated species formed by polymerisation on the surface may be prevented from undergoing hydrogenation and desorption until all the acetylene and most of the ethylene has reacted. Until this time the concentration of surface hydrogen available for the hydrogenation of polymers would be very low.

At completion n -butane constituted approximately 15% of the total product. No other C_4 - or higher hydrocarbons

were observed in agreement with the findings of Guczi et al. (53), although these workers observed the gradual formation of butane throughout the course of the reaction. In an earlier study, using a 1:1 mixture of acetylene and hydrogen over Ni/pumice at 200-250°C, Sheridan(6) observed n-butane, 3-methylpentane and n-hexane as major products and, in addition, small amounts of n-pentane, 2-methylbutane, 3-methylhexane and n-heptane. Investigations of the reaction over alumina-supported platinum (18), palladium (19), rhodium and iridium (20) revealed but-1-ene as the major product with varying amounts of other C₄-products formed. Over rhodium and iridium, no butane was observed.

In the present work the absence of unsaturated C₄-products is probably a consequence of there being an excess of hydrogen in the reaction vessel throughout the reaction.

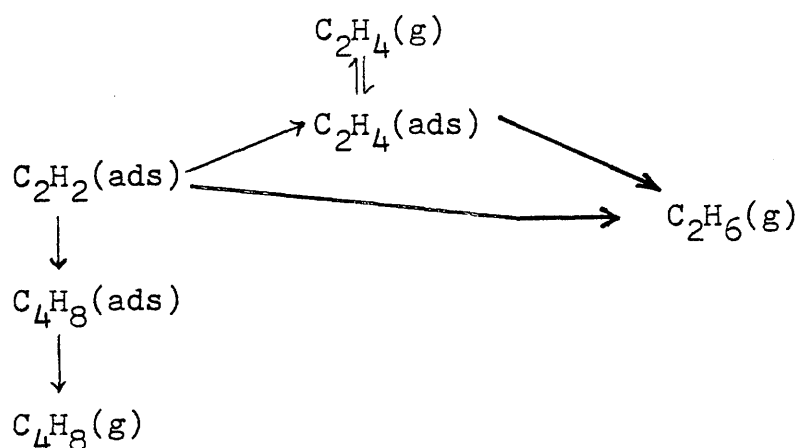
In the experiments described in section 4.5.3, in which small amounts of [¹⁴C]ethylene were added to the reaction mixture, no incorporation of [¹⁴C] into butane was observed. The results are consistent with a mechanism in which butane is formed directly from adsorbed acetylenic species rather than via a gas phase ethylene intermediate. Further evidence for this comes from a study of the hydrogenation of acetylene in excess ethylene over Pd/Al₂O₃ (83) in which but-1-ene, t-but-2-ene, c-but-2-ene and n-butane were all detected. Their experiments were carried out to determine if all the C₄-compounds were produced from two acetylene molecules, two ethylene molecules, or one acetylene molecule and one ethylene

molecule. This was done by carrying out reactions of acetylene in propylene and analysing the products for C_4 -, C_5 - and C_6 -fractions. Only C_4 -compounds were detected, in similar amounts to those found in experiments in excess ethylene. This is further evidence that the C_4 -species are formed from two acetylene molecules.

5.5 General Conclusions

It is envisaged that the hydrogenation of acetylene takes place by a hydrogen transfer mechanism between dissociatively adsorbed C_xH_y species, located on the primary region, and acetylene species adsorbed on the secondary region.

On Ni/SiO_2 it is postulated that the following reaction pathways are possible for acetylene hydrogenation:-



When the system is hydrogen-deficient the favoured pathway is the hydrogenation of acetylene to ethylene, but in the presence of excess hydrogen, pathways leading to ethane are also possible.

It has been found that the main route to the formation of ethane is via a direct route not involving gas phase ethylene and hence the major factor influencing selectivity is the ability, or otherwise, of the catalyst to catalyse the direct route. Butane is formed exclusively from acetylene.

CHAPTER 6

6. MODIFICATION OF SELECTIVITY BY CATALYST PRETREATMENT

The work to be described in this chapter was carried out at ICI (Petrochemicals Division) Research Laboratories. The purpose of the work was to complement the research, described in Chapters 1 - 5, by examining the effect of in situ catalyst pretreatment on selectivity and rate of reaction in the dehydrogenation of cyclohexane over $\text{Pt}/\gamma\text{-Al}_2\text{O}_3$ catalysts. The aim was to find a suitable hydrocarbon pretreatment which would increase the selectivity of the catalyst for cyclohexene production.

6.1 Introduction

In many hydrocarbon reactions catalysed by metals, reaction is accompanied by the build-up of carbonaceous material on the surface of the metal. In industrial processes such as petroleum refining and related petrochemical processes this so-called 'coke' causes a decrease in activity of the catalyst, which is reflected in a drop in the conversion into the product or products of interest. To maintain the production rates within the desired limits the catalyst has to be regenerated from time to time.

Strongly bound surface species, such as those described in the last paragraph, were believed to be simply poisons, but in recent years it has been recognized that carbonaceous

overlayers may stabilize the activity of a catalyst and, in some cases, influence the selectivity for a particular reaction product. Thus, in the dehydrogenation of cyclohexane over a platinum catalyst, Blakely and Somorjai(84) observed that the formation of an adsorbed carbon layer always preceded the desorption of benzene and other olefinic products. Weinberg et al.(85) postulated that the carbonaceous overlayer was the catalytic site for the hydrogenation of ethylene on the Pt(111) surface whilst for the hydrogenation of olefins on metals, Thomson and Webb(26) have proposed that hydrogenation occurs by hydrogen transfer between a dissociatively adsorbed hydrocarbon species $M-C_xH_y$, and an associatively adsorbed unsaturated hydrocarbon. The latter workers also suggested that this dissociatively adsorbed species, C_xH_y , is actually the catalyst and that the metal is only of secondary importance.

These investigations emphasise the importance of carbonaceous overlayers and the need for their characterization. An understanding of their structure and reactivity would permit the chemist to systematically control the type and quantity of surface carbonaceous species to modify the activity of catalysts. The dehydrogenation of cyclohexane was considered a suitable reaction for investigation since, under the reaction conditions used, both benzene and cyclohexene are formed as products. The reaction products which are observed are very dependent upon reaction conditions. Generally, at temperatures less than 300°C, benzene is the

sole product. At higher temperatures production of cyclohexene becomes significant and hydrogenolysis products are sometimes observed. Thus, for example, using Ru-Cu/SiO₂ and Os-Cu/SiO₂ catalysts at 316°C Sinfelt(86) found that the predominant hydrogenolysis product was methane. He suggested that higher carbon-number fragments were formed but that these underwent secondary cracking reactions on the surface rather than desorption, and resulted eventually in the formation of C₁-fragments, which were hydrogenated to methane.

Another interesting feature of the dehydrogenation of cyclohexane is that if cyclohexane is passed over the catalyst in the absence of hydrogen there is a marked loss of activity. In a LEED study using platinum, in the temperature range 27 - 452°C, Blakely and Somorjai(84) observed that, if no hydrogen was introduced into the reaction chamber, no benzene was produced and cyclohexene production was greatly reduced. There was also more carbon residue on the surface than normal. Gryaznov et al. (87) also observed this deactivation phenomenon for the reaction over palladium foil in the temperature range 250 - 322°C. They suggested that hydrogen, both from molecular hydrogen and from the dissociation of cyclohexane molecules, prevented the formation of carbon on the surface.

6.2 Experimental

6.2.1 Catalyst

The catalyst, containing 0.3% w/w platinum supported on γ -alumina, was prepared by dissolving 0.12g platinum acetylacetonate in 50ml Analar benzene, pouring this solution onto the γ -alumina, and allowing to soak for 24 hours. After this time the excess solvent was decanted off and the impregnated alumina dried at 100°C, under a flow of nitrogen, for 90 minutes. The supported salt was calcined at 500°C for 3 hours, ground in a mortar and pestle, and sieved to obtain particles of mesh size 425 - 1000 μ m.

For reactions, the catalyst was mixed with 1g α -alumina (mesh 450 - 1000 μ m) to increase the length of the catalyst bed to approximately 80mm. It was assumed that the α -alumina took no part in the catalytic reaction.

Before use, the catalyst was reduced in situ in a stream of 10% hydrogen in nitrogen (total flow rate 33 cm³ min⁻¹) at 450°C for 2 hours.

6.2.2. Materials

Cyclohexane (B.D.H.) was dried over sodium wire. A vaporiser unit, consisting of a stainless steel tube, i.d. 45mm and length 140mm, was packed with chromosorb P (30 - 50 mesh) saturated with cyclohexane. A flow of nitrogen (17.6 cm³ min⁻¹) upwards through the tube, at room temperature, ensured a constant rate of vaporisation of cyclohexane.

Hydrogen (B.O.C. Ltd.) was purified by passage through a Deoxo unit containing copper(II) oxide supported on magnesium oxide, and then molecular sieves.

Nitrogen (I.C.I.) was dried by passage through molecular sieves.

Ethylene (I.C.I.) was purified by passage through 'Chemiviron' charcoal.

Buta-1,3-diene (Air Products Ltd.) and helium (B.O.C. Special Gases) were used without further purification.

Benzene (Analar) was vaporised using a similar technique to that used for cyclohexane. A 1 metre stainless steel coil, i.d. 45mm, was packed with Chromosorb P (30 - 50 mesh) saturated with benzene. A flow of nitrogen ($1.2 \text{ cm}^3 \text{ min}^{-1}$) through the coil, at room temperature, ensured a constant rate of vaporisation of benzene.

6.2.3 Apparatus

The apparatus consisted of a continuous flow microreactor coupled to a gas chromatography system (figure 6.1). Gas cylinders were connected via lengths of stainless steel tubing to the main line of the continuous flow apparatus. The pressure and flow rates of gaseous reactants could be regulated by use of appropriate valves as shown in figure 6.1. Liquid feeds were vaporised as described in section 6.2.2. Stainless steel tubing was also used to connect the vaporiser units to the main line and pressure and flow rates of vaporised liquid reactants were regulated by use of

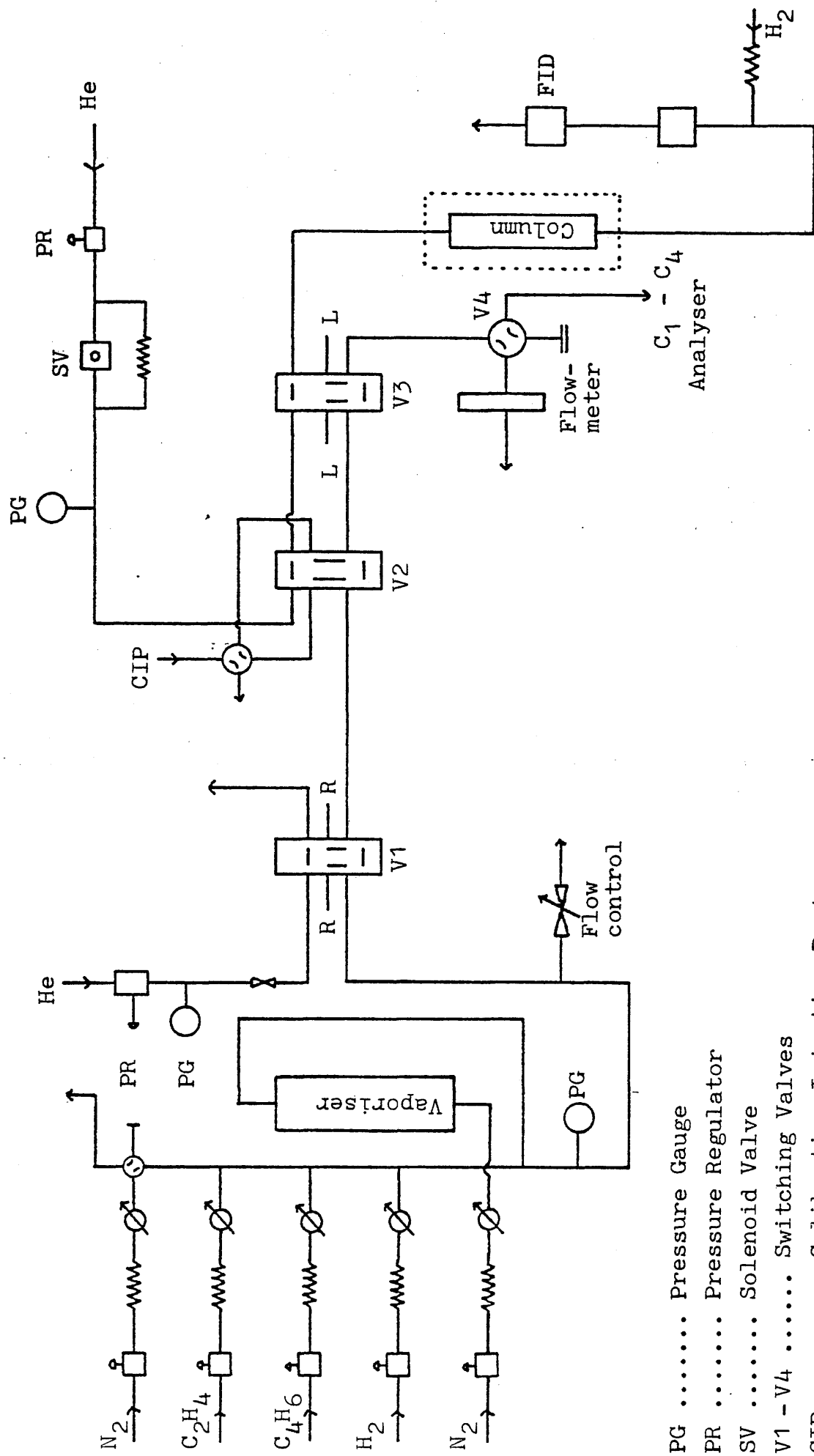


Figure 6.1 Continuous Flow Microreactor

- PG Pressure Gauge
- PR Pressure Regulator
- SV Solenoid Valve
- V1 - V4 Switching Valves
- CIP Calibration Injection Port
- FID Flame Ionisation Detector

appropriate valves as shown in figure 6.1.

The reactor tube, i.d. 3.5mm and length 300mm, was surrounded by a cylindrical brass heating block connected to a West temperature controller and a West programme unit. Reactor temperatures were measured with a thermocouple inserted into the heating block. It was possible to disconnect the reactor tube from the line for cleaning and refilling.

Three Pye Unicam switching valves, V1 - V3, were incorporated into the line. The position of V1 determined whether the reactor tube was being purged with helium, or was 'on-line' for reduction or reaction. V3 allowed products to flow through a sampling loop, whilst, at the same time, the helium flowed through the C₆-chromatography system or, alternatively, with the valve in the other position, helium could flow through the sample loop, carrying a pulse of product mixture into the C₆-chromatograph. V2, used in conjunction with V3, permitted calibration injections to be made. Samples could also be diverted into the C₁ - C₄ chromatography system by turning a Whitey valve, V4.

Cyclohexane, cyclohexene and benzene were separated by passing the product mixture through a 2 metre column of 10% triscyanoethoxypropane on chromosorb P (80 - 100 mesh). The column was operated at 61.5°C using helium (flow rate 85 cm³ min⁻¹) as carrier gas. The signal from the Pye long-reach flame ionisation detector was fed into a Servoscribe chart recorder.

A 2m column of chromosorb 101 was used to separate $C_1 - C_4$ hydrocarbons. It was operated at 100°C using nitrogen as carrier gas. Again a flame ionisation detector was used.

6.2.4 Experimental Procedure

After catalyst reduction the appropriate pressure regulators were adjusted to allow reactant gases to flow through the system. A typical reaction mixture consisted of 2% cyclohexane, 10% hydrogen and 88% nitrogen (which acted as an inert carrier gas). The total flow rate through the catalyst bed was $67\text{ cm}^3\text{ min}^{-1}$. All reactions were carried out at 450°C using 0.05g of 0.3% Pt/ $\gamma\text{-Al}_2\text{O}_3$. At appropriate times the gas sampling valve V3 could be operated to remove samples into the gas chromatography system. Since the system operated under continuous flow conditions, the gases were allowed to flow until sufficient data had been obtained for a particular reaction.

6.3 Results

6.3.1 Standard Experiment

A 0.050g sample of Pt/ Al_2O_3 was reduced at 450°C in a flow of 10% hydrogen in nitrogen (total flow rate $33\text{ cm}^3\text{ min}^{-1}$) for $2\frac{1}{2}$ hours. A reaction mixture, consisting of 2% cyclohexane, 10% hydrogen and 88% nitrogen (total flow rate $67\text{ cm}^3\text{ min}^{-1}$), was allowed to flow over the activated catalyst at 450°C for 25 hours. Samples were analysed by gas

chromatography at regular intervals. The reaction products were predominantly benzene and cyclohexene, although small amounts of $C_1 - C_4$ hydrocarbons were also detected.

Figure 6.2 shows a plot of total conversion against time and selectivity for cyclohexene against time, where selectivity has been defined as

$$\begin{array}{lcl} \text{selectivity for} & & \% \text{ cyclohexene} \\ \text{cyclohexene} & = & \frac{\% \text{ cyclohexene}}{\% \text{ cyclohexene} + \% \text{ benzene}}. \end{array}$$

From the graph it can be seen that initially the total conversion to products was very high but after a period of 25 hours this decayed to ca. 19%. Selectivity for cyclohexene was very low but increased as the total conversion decreased. A plot of selectivity against total conversion is shown in figure 6.3.

6.3.2 Treatment of Results

The experiment described above was found to be reproducible for a freshly reduced sample of catalyst. This experiment was taken as a standard such that comparisons could be made between this and subsequent experiments involving catalyst pretreatment. If a pretreatment caused a decrease in the rate of conversion to products, but the selectivity-conversion relationship was the same as that of the standard experiment, then the pretreatment was merely acting as a poison, probably by decreasing the number of active sites available for the dehydrogenation reaction.

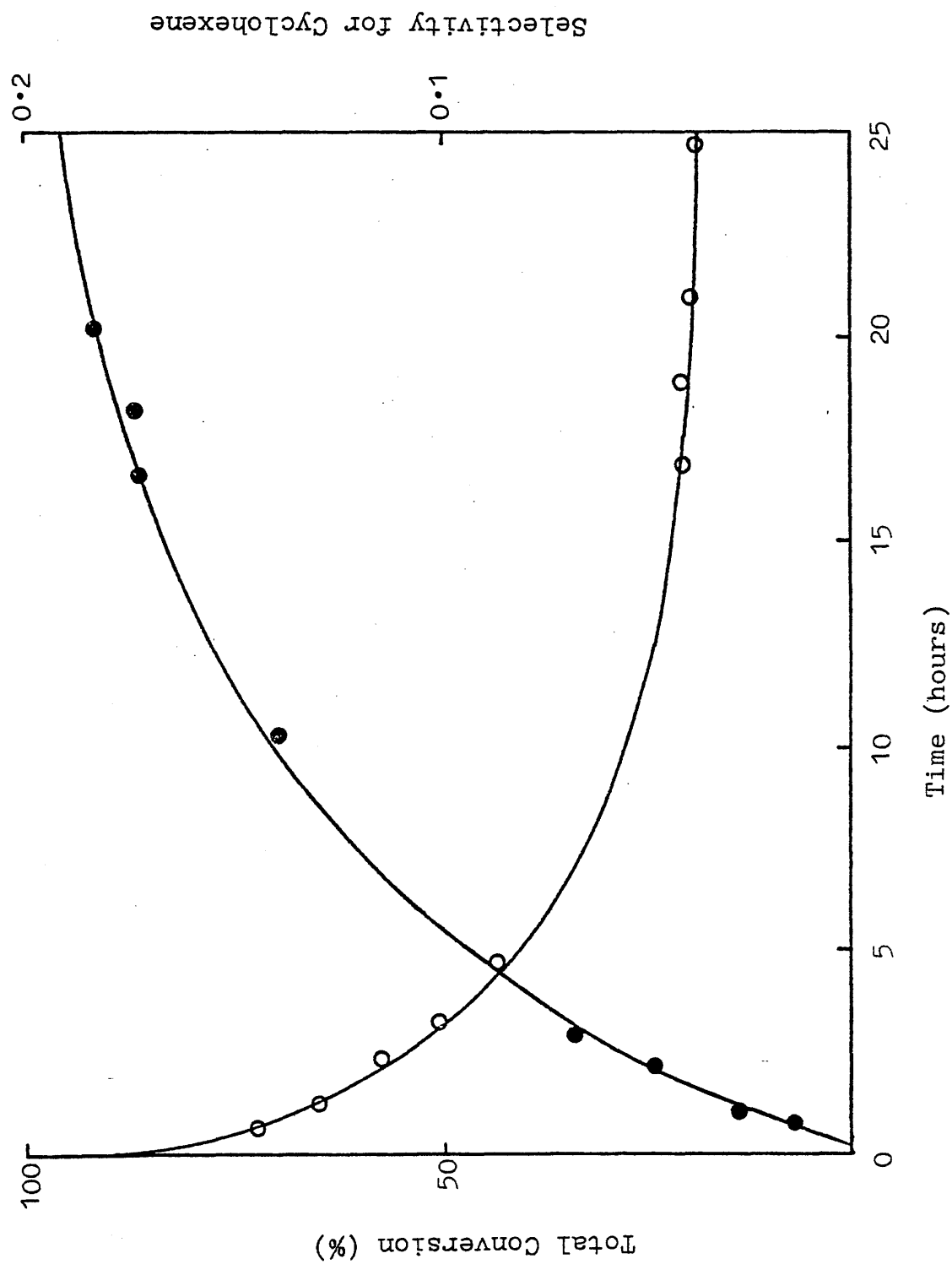


Figure 6.2 Standard Experiment:- % Conversion versus Time and Selectivity versus Time

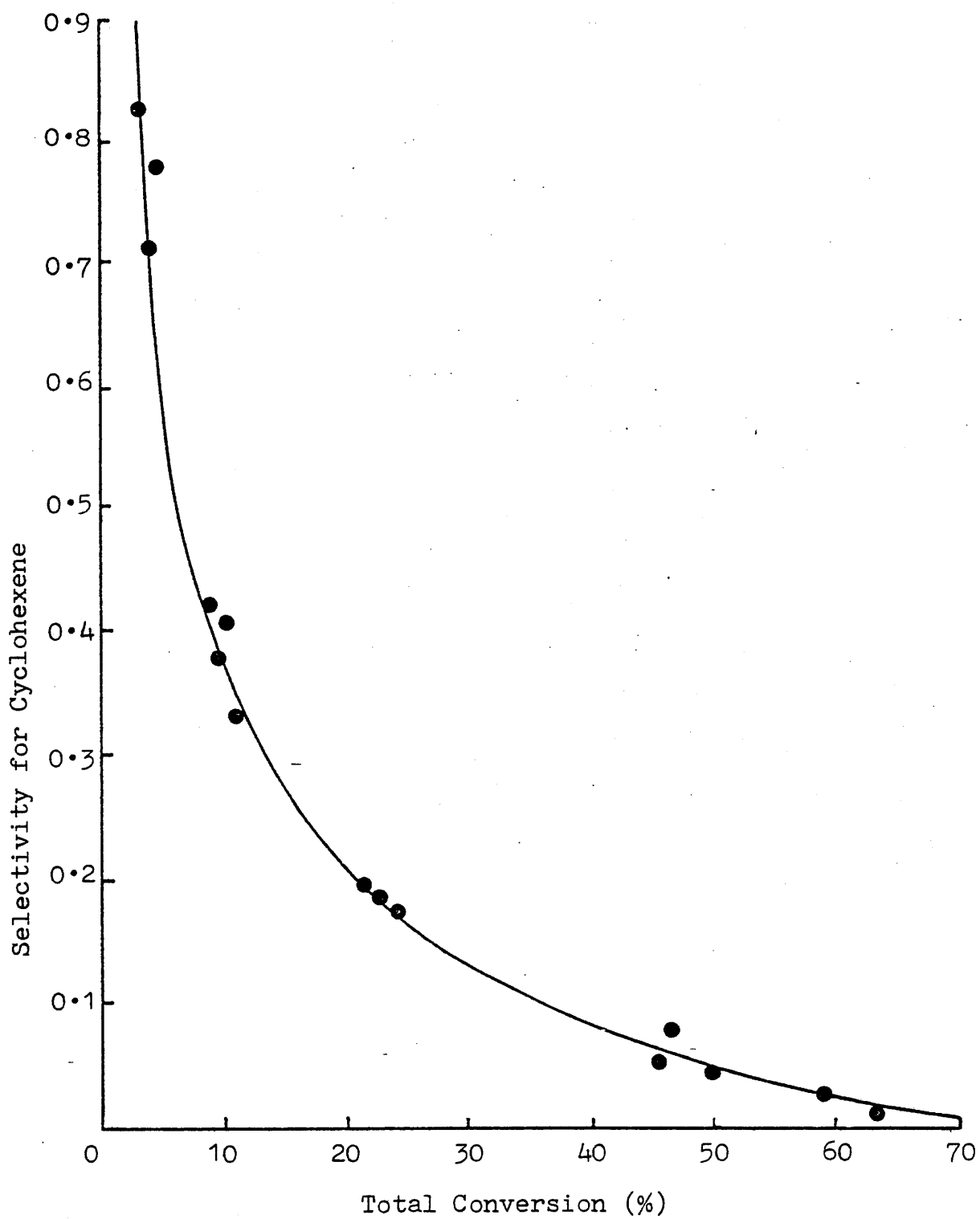


Figure 6.3 Selectivity versus Total Conversion
(Standard Experiment)

If, however, pretreatment caused a change in the selectivity - conversion relationship, the pretreatment was judged to have been successful in influencing the selectivity.

6.3.3 Benzene Pretreatment

0.050g Pt/Al₂O₃ were reduced by the normal procedure. The catalyst was then pretreated with 3.6% benzene in nitrogen (total flow rate 33 cm³ min⁻¹) at 450°C for 1 hour. After this, a dehydrogenation experiment was performed, using a similar procedure to that used for the standard experiment described above.

Figure 6.4 shows that the initial conversion was ca. 57%, lower than in the standard experiment, and this fell to ca. 26% over 1 $\frac{3}{4}$ hours, a faster deactivation than in the standard experiment. Comparison of the selectivity - conversion relationship with that of the standard experiment (figure 6.5) shows that the relationship is the same, suggesting that the catalyst has merely been deactivated. This is perhaps not unexpected, since benzene is a product of the dehydrogenation reaction.

6.3.4 Buta-1,3-diene Pretreatment I

0.050g Pt/Al₂O₃ were reduced by the normal procedure. The catalyst was then pretreated with 10% buta-1,3-diene in nitrogen (total flow rate 33 cm³ min⁻¹) at 450°C for 1 $\frac{1}{2}$ hours, before performing a dehydrogenation experiment.

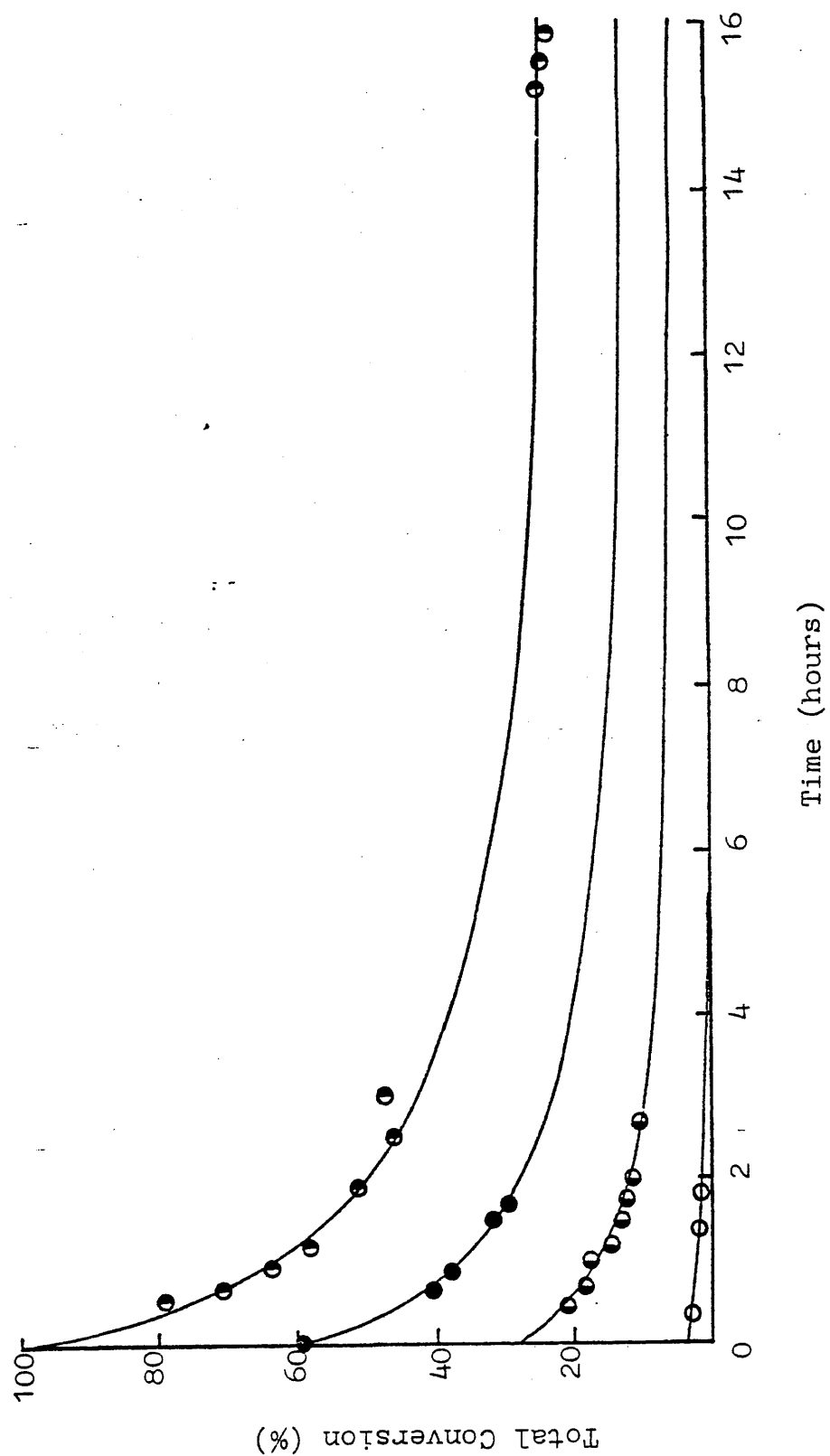


Figure 6.4 Total Conversion versus Time for Standard Experiment (●), Benzene Pretreatment (●) Ethylene Pretreatment (●) and Buta-1,3-diene 10 minute Pretreatment (○).

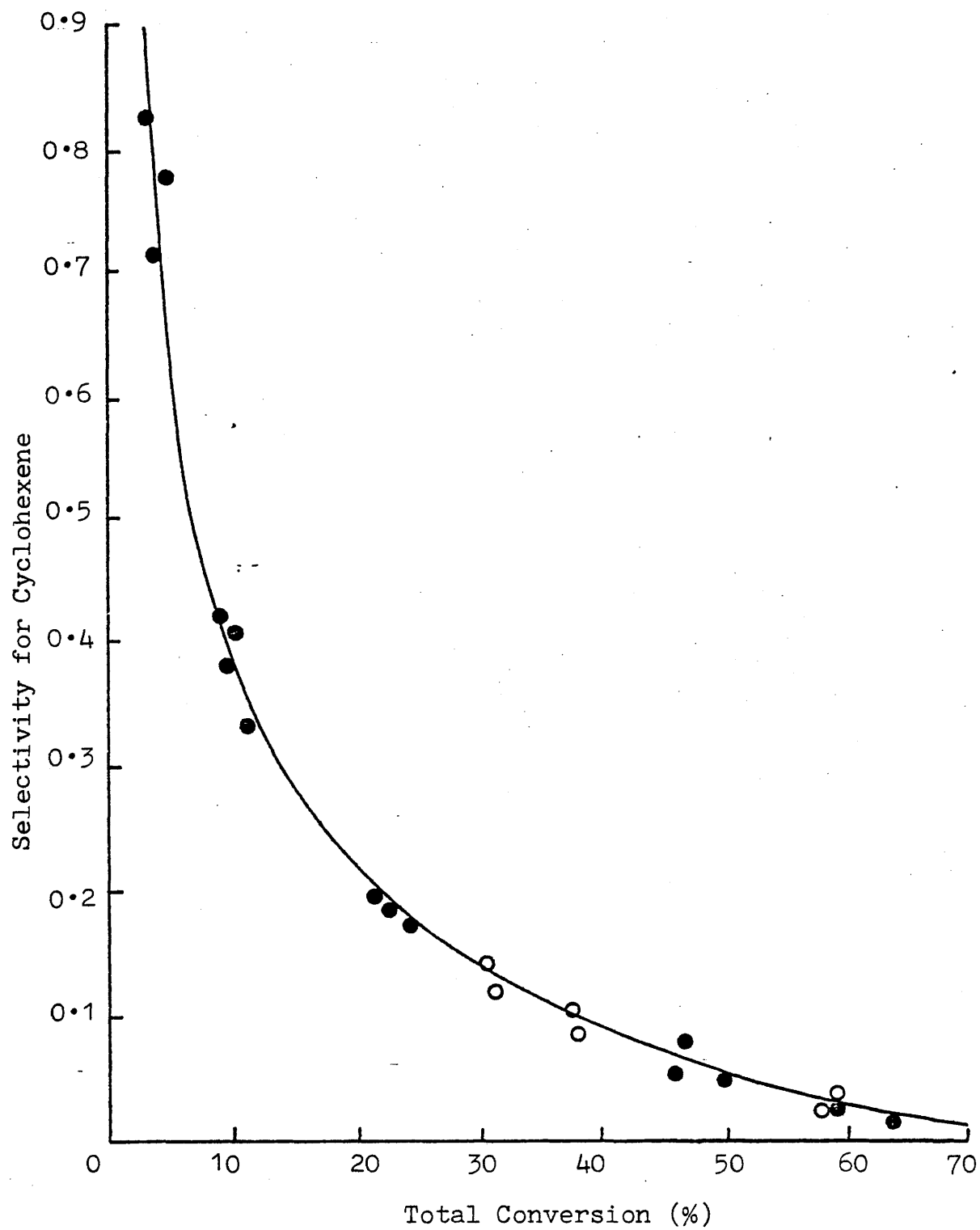


Figure 6.5 Selectivity versus % Conversion for Benzene
Pretreatment Experiment (○) and Standard
Experiment (●).

The percentage conversion was almost negligible and thus accurate calculations of selectivity were impossible. For this reason it was decided to repeat the experiment using a much shorter pretreatment time.

6.3.5 Buta-1,3-diene Pretreatment II

0.050g Pt/Al₂O₃ were reduced by the normal procedure. A pretreatment of 10% buta-1,3-diene in nitrogen (total flow-rate 33 cm³ min⁻¹) at 450°C for 10 minutes was followed by a cyclohexane dehydrogenation experiment.

From figure 6.4 it can be seen that the conversion was slightly higher than that after a 1½ hour pretreatment. However, examination of figure 6.6 indicates that no change has been made in the selectivity - conversion relationship.

6.3.6 Ethylene Pretreatment

0.050g Pt/Al₂O₃ were reduced by the normal procedure. This was followed by treatment in 10% ethylene in nitrogen (total flow rate 33 cm³ min⁻¹) at 450°C for 1½ hours, before a cyclohexane dehydrogenation was performed.

Figure 6.4 shows a graph of % conversion against time. Comparison with the standard experiment shows that the initial conversion was very low and only changes by ca. 4% over 2½ hours. The % conversion was that which would be expected in a standard experiment after 24 hours.

Comparison of the selectivity - conversion relationship with that of the standard experiment (figure 6.7) shows

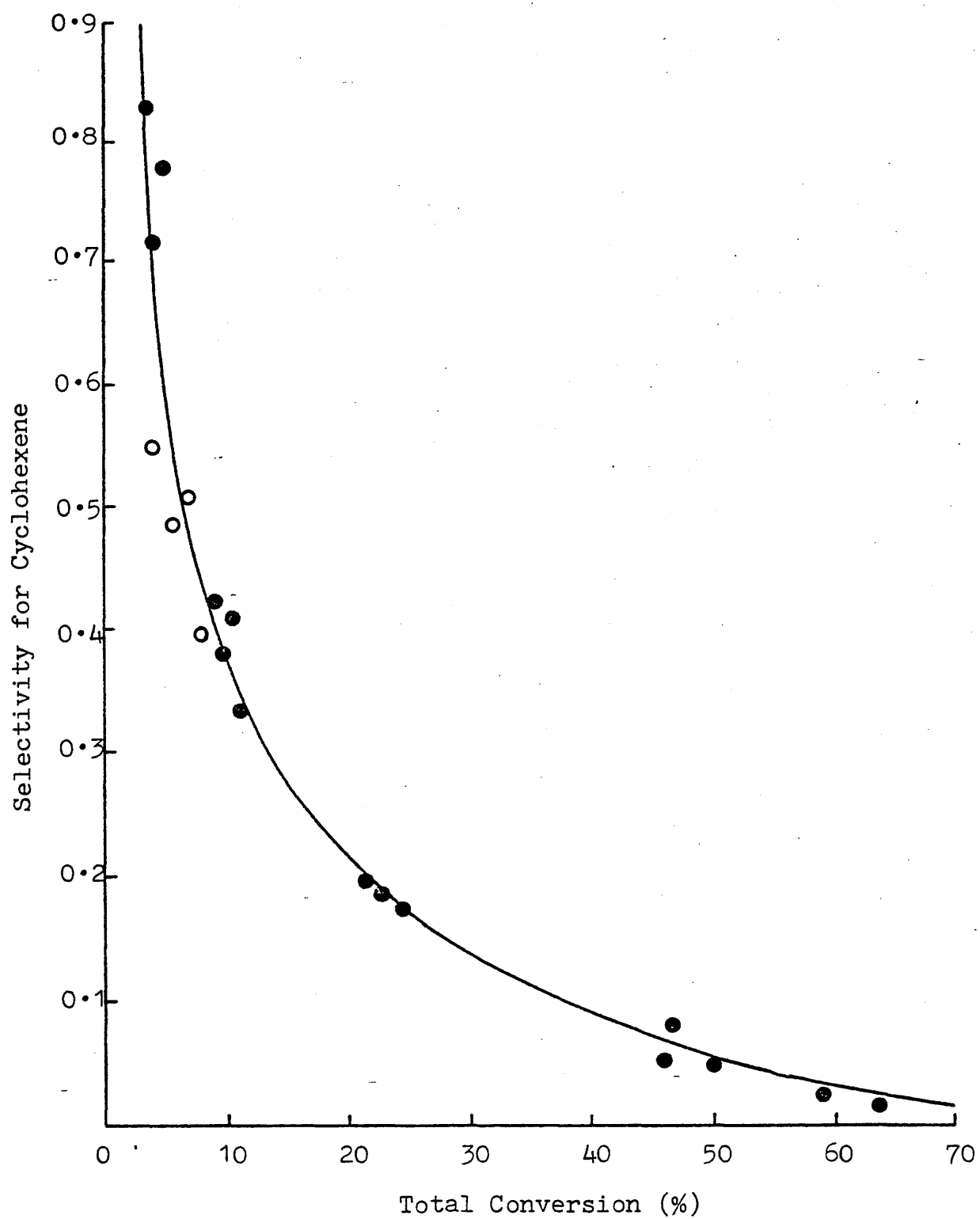


Figure 6.6 Selectivity versus % Conversion for Buta-1,3-diene
10 minute Pretreatment Experiment (○) and
Standard Experiment (●).

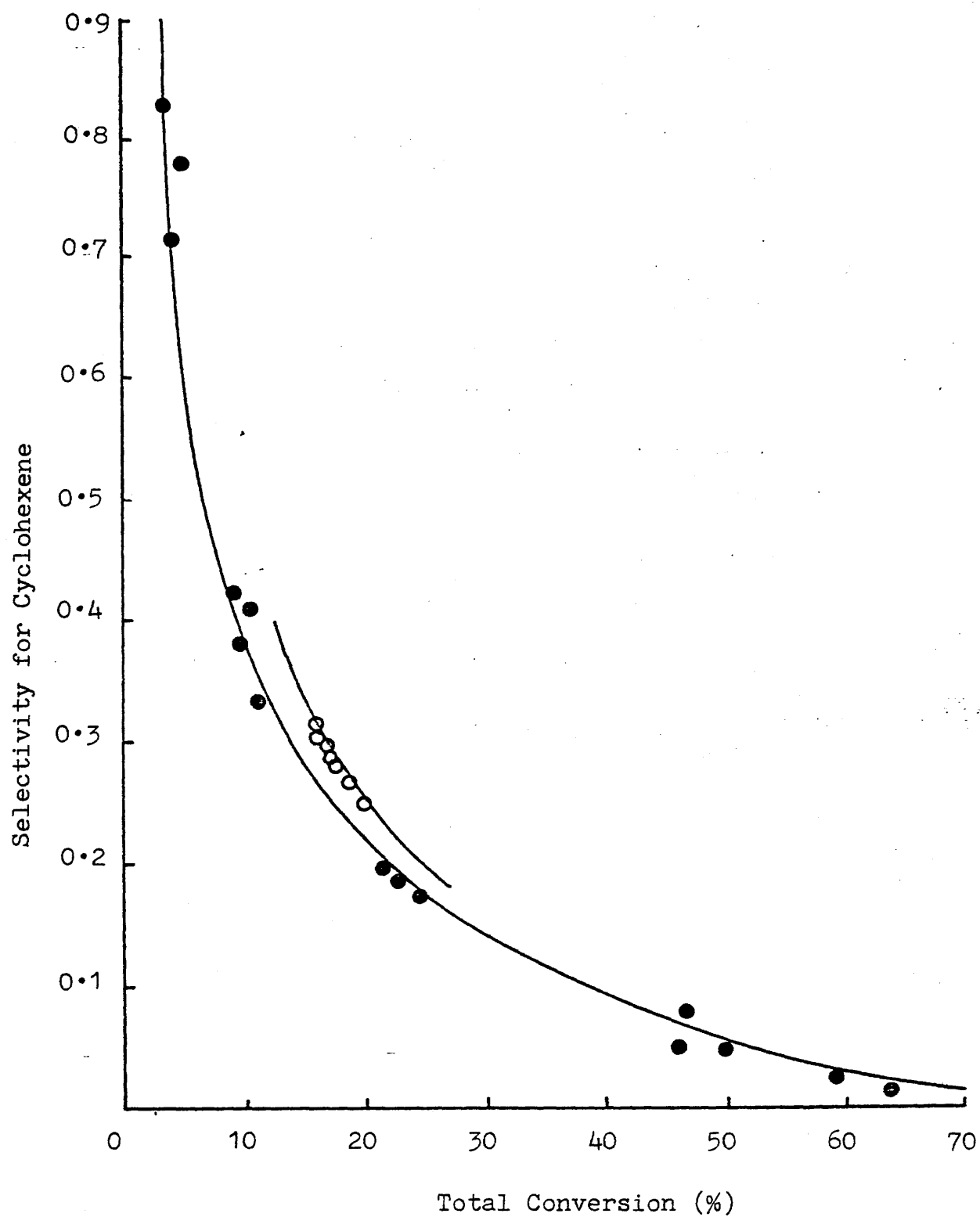


Figure 6.7 Selectivity versus % Conversion for Ethylene
Pretreatment Experiment (○) and Standard
Experiment (●).

that these are different. The results suggest that the ethylene pretreatment has successfully altered the relative amounts of cyclohexene and benzene.

6.4 Discussion

The results of the pretreatment experiments may be summarized as follows:-

- (a) Benzene pretreatment decreases the rate of conversion but does not influence the selectivity for cyclohexene.
- (b) Buta-1,3-diene is very strongly adsorbed on $\text{Pt/Al}_2\text{O}_3$ and almost totally poisons the surface for the dehydrogenation of cyclohexane.
- (c) Ethylene pretreatment causes a decrease in the rate of conversion and an increase in the selectivity for cyclohexene production.

Ethylene was the only substance investigated which caused an increase in selectivity for cyclohexene. However, it functioned in such a way that the catalyst was deactivated in an absolute sense, the relative deactivation of the production of benzene being greatest. It is possible that cyclohexane and cyclohexene adsorb on different types of surface site and ethylene can only compete for cyclohexene sites. Thus, cyclohexane could be dehydrogenated to cyclohexene, but the readsorption and further dehydrogenation of cyclohexene to benzene would be blocked by adsorbed

ethylene. Such a mechanism assumes that the only route to benzene is via a gas phase cyclohexene intermediate.

The reaction pathways for cyclohexane dehydrogenation over Group VIII metals have been elucidated by Tétényi et al. (88). Using 1:1 reaction mixtures of cyclohexane and [^{14}C]cyclohexene it was possible to follow the subsequent incorporation of [^{14}C] into the products. It was found that both cyclohexene and benzene were radioactive, but that the specific activity of benzene was higher than that of cyclohexene. The authors suggested that two pathways of cyclohexane dehydrogenation were operating simultaneously, only one of which involved a cyclohexene intermediate. Their reaction scheme is shown in figure 6.8. It can be seen that cyclohexane forms a monoadsorbed species which dissociates further to form either an α,β - or an α,γ -diadsorbed species. Only the α,β -species can desorb to form cyclohexene, the α,γ -species remains on the surface and dehydrogenates further to form benzene. It is possible that the cyclohexene may readsorb and react further. Thus, the effect of preadsorbed ethylene may be to prevent the readsorption of cyclohexene, or to prevent the formation of an α,γ -diadsorbed species.

Another possible explanation of the mode of action of the ethylene pretreatment is that the surface structure is completely altered by the adsorption of ethylene and this new surface is more selective for the production of cyclohexene. It may be that adsorption and catalysis are

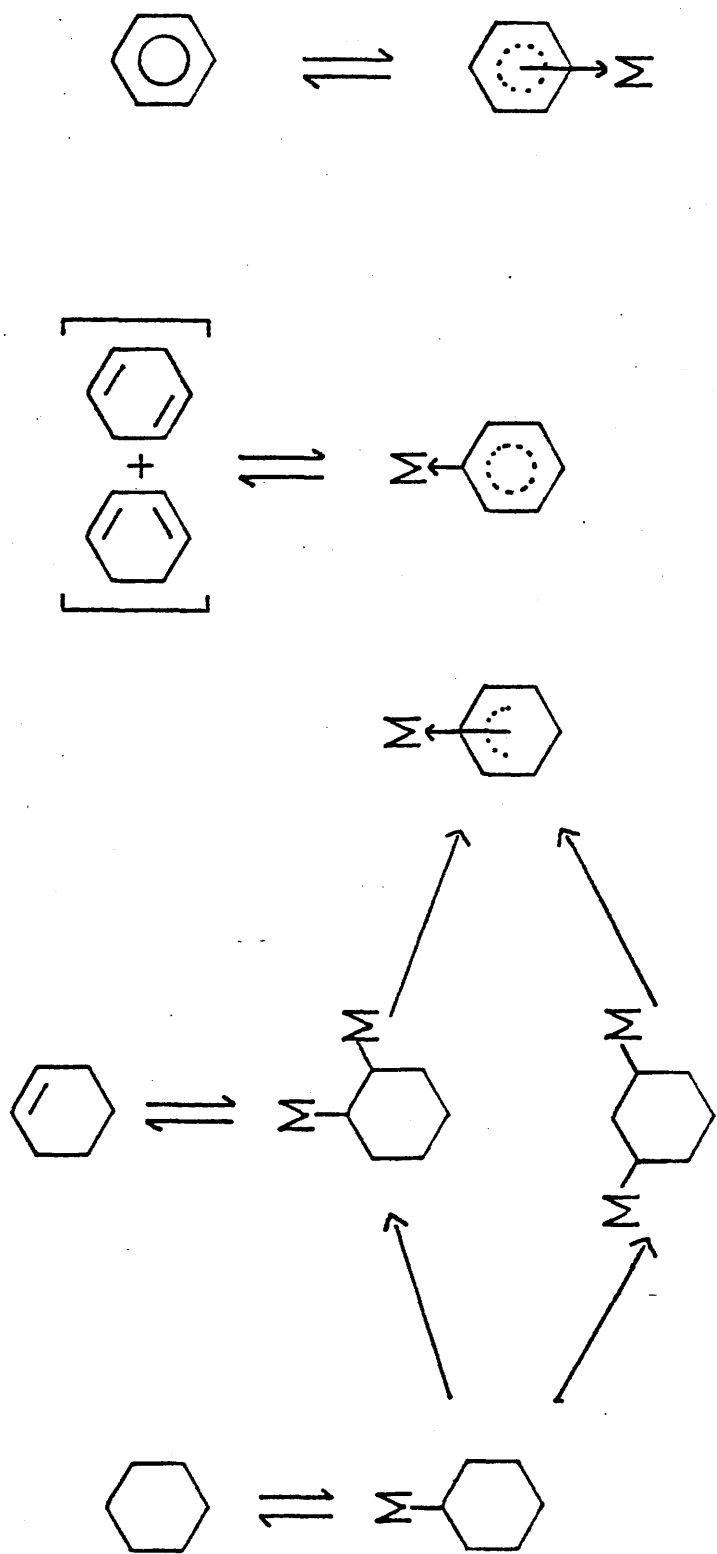


Figure 6.8 Reaction Scheme for Cyclohexene Dehydrogenation

occurring on a carbonaceous overlayer, formed from ethylene, as has been proposed elsewhere for other hydrocarbon reactions (26).

In conclusion, the experiments described in this chapter have led to the discovery of a catalyst pretreatment which enhanced the selective behaviour of platinum for cyclohexene production, although this resulted in an overall deactivation of the catalyst. It would be of interest to investigate other hydrocarbon pretreatments of catalysts, for example the C_6 -compounds hexane, hexene and hexyne, to determine the feasibility of increasing catalyst selectivity without simultaneously incurring a loss in catalyst activity.

REFERENCES

1. H. Davy, Phil. Trans. Roy. Soc., 1817, 107, 77.
2. W. Henry, Phil. Mag., 1825, 65, 269.
Phil. Trans. Roy. Soc., 1824, 114, 266.
3. M. Faraday, Phil. Trans. Roy. Soc., 1834, 124, 55.
4. J.J. Berzelius, Annls. Chim. Phys., 1836, 61, 146.
5. J. Sheridan, J. Chem. Soc., 1944, 373.
6. J. Sheridan, J. Chem. Soc., 1945, 133.
7. J. Sheridan, J. Chem. Soc., 1945, 301.
8. J. Sheridan, J. Chem. Soc., 1945, 305.
9. J. Sheridan, J. Chem. Soc., 1945, 470.
10. J. Sheridan and W.D. Reid, J. Chem. Soc., 1952, 2962.
11. G.C. Bond, J. Chem. Soc., 1958, 3, 2705.
12. G.C. Bond, J. Chem. Soc., 1958, 4, 4288.
13. G.C. Bond and R.S. Mann, J. Chem. Soc., 1958, 4, 4738.
14. G.C. Bond and R.S. Mann, J. Chem. Soc., 1959, 4, 3566.
15. G.C. Bond, D.A. Dowden and N. MacKenzie,
Trans. Faraday Soc., 1958, 54, 1537.
16. G.C. Bond and P.B. Wells, Proc. 2nd Int. Congr.
Catalysis (Paris 1960), p.1159.
17. G.C. Bond, G. Webb, P.B. Wells and J.M. Winterbottom,
J. Catalysis, 1962, 1, 74.
18. G.C. Bond and P.B. Wells, J. Catalysis, 1965, 4, 211.
19. G.C. Bond and P.B. Wells, J. Catalysis, 1966, 5, 65.
20. G.C. Bond and P.B. Wells, J. Catalysis, 1966, 5, 419.

21. G.C. Bond and P.B. Wells, J. Catalysis, 1966, 6, 397.
22. G.C. Bond, G. Webb and P.B. Wells, J. Catalysis, 1968, 12, 157.
23. G.C. Bond and P.B. Wells, Adv. Catalysis, 1963, 15, 91.
24. P.B. Wells, Surface and Defect Properties of Solids (Specialist Periodical Reports, Chemical Society, London, 1972), vol.1, p 236.
25. G. Webb, in Comprehensive Chemical Kinetics, ed., C.H. Bamford and C.F.H. Tipper (Elsevier, Amsterdam, 1978), vol.20, chap.1.
26. S.J. Thomson and G. Webb, J.C.S. Chem. Comm., 1976, 526.
27. S.J. Thomson and J.L. Wishlade, Trans. Faraday Soc., 1962, 58, 1170.
28. D. Cormack, S.J. Thomson and G. Webb, J. Catalysis, 1966, 5, 224.
29. N. Sheppard, Disc. Faraday Soc., 1966, 41, 254.
30. N.R. Avery, J. Catalysis, 1970, 19, 15.
31. H.A. Pearce and N. Sheppard, Surface Sci., 1976, 59, 205.
32. G. Dalmai-Imelik and J. Massardier, Proc. 6th Int. Congr. Catalysis (London, 1976), p.90.
33. A.S. Al-Ammar and G. Webb, J.C.S. Faraday I, 1978, 74, 657.
34. Y. Inoue and I. Yasumori, J. Phys. Chem., 1969, 73, 1618.
35. J. Erkelens and W.J. Wösten, J. Catalysis, 1978, 54, 143.

36. J.E. Demuth, Chem. Phys. Letters, 1977, 45, 12.
37. N. Sheppard and J.W. Ward, J. Catalysis, 1969, 15, 50.
38. A.S. Al-Ammar and G. Webb, J.C.S. Faraday I, 1978, 74, 195.
39. J.U. Reid, S.J. Thomson and G. Webb, J. Catalysis, 1973, 29, 433.
40. S.J. Stephens, J. Phys. Chem., 1959, 63, 188.
41. D.W. McKee, J. Amer. Chem. Soc., 1962, 84, 1109.
42. P.W. Selwood, J. Amer. Chem. Soc., 1961, 83, 2853.
43. R.P. Eischens and W.A. Pliskin, Adv. Catalysis, 1958, 10, 1.
44. I. Horiuti and M. Polanyi, Trans. Faraday Soc., 1934, 30, 1164.
45. J.J. Rooney and G. Webb, J. Catalysis, 1964, 3, 488.
46. J.D. Prentice, A. Lesiunas and N. Sheppard, J.C.S. Chem. Comm., 1976, 76.
47. L.L. Kesmodel, L.H. Dubois and G.A. Somorjai, J. Chem. Phys., 1979, 70, 2180.
48. J.U. Reid, S.J. Thomson and G. Webb, J. Catalysis, 1973, 29, 421.
49. B.E. Gordon, W.R. Erwin, M. Press and R.M. Lemmon, Anal. Chem., 1978, 50, 179.
50. P. Cossee, J. Catalysis, 1964, 3, 80.
51. A. Wheeler, Adv. Catalysis, 1951, 3, 249.
52. H.I. Watermann, C. Boelhouwer and J. Cornelissen, Anal. Chim. Acta., 1958, 18, 395.

53. L. Gucci, R.B. LaPierre, A.H. Weiss and E. Biron,
J. Catalysis, 1979, 60, 83.
54. W.T. McGown, C. Kemball, D.A. Whan and M.S. Scurrrell,
J.C.S. Faraday I, 1977, 73, 632.
55. R.R. Ford, Adv. Catalysis, 1970, 21, 51.
56. N. Sheppard and T.T. Nguyen, Advances in Infrared and
Raman Spectroscopy, 1978, 5, 67.
57. H.M. Powell and R.V.G.Ewens, J. Chem. Soc., 1939, 286.
58. R.K. Sheline and K.S. Pitzer, J. Amer. Chem. Soc.,
1950, 72, 1107.
59. G. Blyholder, J. Phys. Chem., 1964, 68, 2772.
60. G. Blyholder, J. Phys. Chem., 1962, 36, 2036.
61. M. Primet, J.A. Dalmon and G.A. Martin, J. Catalysis,
1977, 46, 25.
62. P. Politzer and S.D. Kasten, J. Phys. Chem., 1976,
80, 385.
63. G. Blyholder, J. Phys. Chem., 1975, 79, 756.
64. J.T. Yates and C.W. Garland, J. Phys. Chem., 1961,
65, 617.
65. R.M. Kroeker, W.C. Kaska and P.K. Hansma, J. Catalysis,
1979, 57, 72.
66. A.C. Yang and C.W. Garland, J. Phys. Chem., 1957,
61, 1504.
67. J. Wojtczak, R. Queau and R. Poilblanc,
J. Catalysis, 1975, 37, 391.
68. A.S. Al-Ammar, Ph.D. Thesis, University of Glasgow,
1977.

69. F. Schmidt-Bleek and F.S. Rowland, Anal. Chem., 1964, 36, 1695.
70. R.B. Bernstein and T.I. Taylor, Science, 1947, 106, 498.
71. Z. Paál and S.J. Thomson, J. Catalysis, 1973, 30, 96.
72. A.S. Al-Ammar and G. Webb, J.C.S. Faraday I, 1979, 75, 1900.
73. N.C. Kuhnen, personal communication.
74. C.E. O'Neil and D.J.C. Yates, J. Phys. Chem., 1961, 65, 901.
75. N.N. Kavtaradze and N.P. Sokolova, Russ. J. Phys. Chem., 1970, 44, 93.
76. M. Primet and N. Sheppard, J. Catalysis, 1976, 41, 258.
77. G. Wedler, H. Papp and G. Schroll, J. Catalysis, 1975, 38, 153.
78. A.M. Horgan and D.A. King in 'Adsorption - Desorption Phenomena', ed. F. Ricca (Academic Press, London 1972), p.329.
79. J.A. Altham and G. Webb, J. Catalysis, 1970, 18, 133.
80. K.C. Campbell and S.J. Thomson, Trans. Faraday Soc., 1959, 55, 306.
81. K.C. Campbell and J. Mooney, J.C.S. Faraday I, 1980, in the press.
82. J.K.A. Clarke and J.J. Rooney, Adv. Catalysis, 1976, 25, 125.

83. W.T. McGown, C. Kemball and D.A. Whan, J. Catalysis, 1978, 51, 173.
84. D.W. Blakely and G.A. Somorjai, J. Catalysis, 1976, 42, 181.
85. W.H. Weinberg, H.A. Deans and R.P. Merrill, Surface Sci., 1974, 41, 312.
86. J.H. Sinfelt, J. Catalysis, 1973, 29, 308.
87. V.M. Gryaznov, L.F. Pavlova, P. Rivera, A. Rosen and É. Khuares, Kinet. Katal., 1971, 12, 1063
(Americal Translation).
88. P. Tétényi, Z. Paál and M. Dobrovolszky, Z. Phys. Chem. Neue Folge, 1976, 102, 267.